**University of Alberta**

# Structural and Functional Studies on Bacterial Elongation Factor G

by

Roxana Nechifor 

A thesis submitted to the Faculty of Graduate Studies and Research
in partial fulfillment of the requirements for the degree of Doctor of Philosophy.

Department of Biochemistry

Edmonton, Alberta
Spring, 2008

*Your file Votre référence*
*ISBN: 978-0-494-45573-9*
*Our file Notre référence*
*ISBN: 978-0-494-45573-9*

## ABSTRACT

The elongation factor G (EF-G) catalyzes fast and accurate translocation of the tRNAs and mRNA connected to them, consuming also GTP in the process. The mechanism of translocation has remained elusive in spite of extensive structural and functional studies.

Our first crosslinking study used a non-specific crosslinker, which showed that at least four ribosomal proteins (S12, L6, L7/L12, and L14) are in close proximity to EF-G when this factor is bound to the ribosome. This was followed by a site specific crosslinking study, which used a library of single cysteine mutants modified with azidophenacyl bromide (AzP), and demonstrated that the following EF-G elements are in close proximity and potentially interacting with the three ribosomal proteins: helix A of the G' subdomain (positions 209 and 231) is in proximity of L7/L12, helix A of domain III (residue 426) is close to S12, while helix A of domain V (amino acids 627 and 637) is located next to L6.

In order to explore further the interaction between EF-G and L7/L12, additional cysteine mutants were created in different structural elements of the G' subdomain and used in AzP crosslinking experiments. As a result, helix B and the N-terminal of helix C of the G' subdomain were also demonstrated to be proximal to L7/L12.

Functional studies on the crosslinking product between EF-G(231C)-AzP and L7/L12 (in the context of the ribosome) revealed that this product is capable of catalyzing multiple rounds of GTP hydrolysis, probably due to the unusual mobility of L7/L12.

In order to test the role of the proposed interaction between helix A of the G' subdomain and L7/L12, three well conserved glutamic acid residues (224, 228, and 231) were mutated to lysines, separately and collectively. The constructed lysine mutants were found to be inhibited in both GTP hydrolysis and translocation assays, as compared to the wildtype protein. Replacement of residues 224 and 228 resulted in severely defective proteins, while 231K was only marginally affected.

All these results taken together shed light on the structural components of the interaction between EF-G and L7/L12, as well as its role in this factor's functions.

## ACKNOWLEDGEMENTS

I would like to start by thanking my supervisor (Dr. Kevin Wilson) for his help in the projects described in this thesis and his support during my PhD program. I am also very grateful for all the patience and advice received from my Committee Members (Dr. Mark Glover and Dr. Andrew MacMillan).

I received a lot of technical help from various past and present members of the Wilson lab (Duane, Mullein, Mark, Melanie, Anne, Nav, Cristina and Boray). I have learned a lot about enzyme kinetics and data interpretation from Dr. Marat Murataliev, who made complicated experiments seem easy, effortless and fun.

Acknowledgement is deserved by the Department of Biochemistry for the scientific, moral, and financial support received during my five and half years spent here, as well as by the Faculty of Medicine, for their financial support.

Lastly, none of this work would have been possible without the unconditional love and patience of my family, who listened to me talking for endless hours about things they had no clue about (nor did they really care to know more about).

## Table of contents

**List of Tables**

## List of figures

## LIST OF ABBREVIATIONS

A = adenosine

AMP = adenosine monophosphate

a.u. = arbitrary units

AzP = 4-azidophenacyl bromide

BABE = (S)-[1-[[Bis(carboxymethyl)amino]methyl]-2-[4-[(2-bromoacetyl) amino] phenylethyl] (carboxymethyl)amino] acetic acid

BP = binding protein

C = cytosine

CTD = C terminal domain

Cryo-EM = cryo-electron microscopy

DSG = disuccinimidyl glutarate

EDTA = ethylenediaminetetraacetic acid

EF = elongation factor

eIF = eukaryotic initiation factor

F site = factor binding site on the ribosome

G = guanosine

GAP = GTP hydrolase activating protein

GdmCl = guanidium chloride

GMPPCP = guanylyl 5'-(β,γ-methylenediphosphonate)

GDP = guanosine diphosphate

GDPNP = guanosine 5′- [β,γ-imido]triphosphate

GEF = guanosine exchange factor

GTP = guanosine triphosphate

IF = initiation factor

IPTG = isopropyl β-D-1-thiogalactopyranoside

IRES = internal ribosome entry site

MANT-nucleotide = 2′/3′-O-(N′-Methylanthraniloyl)-nucleotide

N = any nucleotide

Ni-NTA = nickel-nitrilo triacetic acid

NTD = N terminal domain

p.s.i. = pounds per square inch

Pi = inorganic phosphate

PAGE = polyacrylamide gel electrophoresis

PEAS = *N*-((2-pyridyldithio)ethyl)-4-azidosalicylamide

PDF = peptide deformylase

PDI = protein disulphide isomerase

RF = release factor

r-protein = ribosomal protein

RRF = ribosome recycling factor

rRNA = ribosomal RNA

S = Svedberg unit

SD = Shine-Dalgarno sequence

SDS = sodium dodecyl sulfate

SRL = sarcin-ricin loop

TF = trigger factor

tRNA = transfer RNA

U = uracil

UTR = untranslated region

UV light = ultraviolet light

wt = wild type

# I. PROTEIN SYNTHESIS IN BACTERIA

## I.1. INTRODUCTION

Protein synthesis is accomplished within cells by ribosomes: large ribonucleoprotein complexes, with the role of translating the message coded by the mRNA and assembling the specific amino acids into polypeptide chains.

Starting in the early 1940's, a number of researchers separated ribonucleoprotein containing particles from cells, but the ribosomes were properly visualized only later, during the electron microscopy studies conducted by George Palade and Albert Claude. Initially called Palade's particles, they were identified as containing the majority of the cytoplasmic RNA involved in protein synthesis (for more details see (Spirin, 1999)).

After more than 50 years of research, there is a lot known today about the structure of the ribosomes. Both bacterial and eukaryotic ribosomes are composed of two subunits, which are formed of RNA and proteins. Although the research into the eukayotic protein synthesis is rapidly advancing, the bacterial system continues to remain the best studied one, due to the relative simplicity in material purification and high activity of its translation system *in vitro*. This chapter briefly summarizes the current state of knowledge of the bacterial system, focusing on the fundamental mechanisms of protein synthesis, which are conserved in all domains of life. The following chapters contain the presentations of our own results and potential new directions.

### I.1.1. The bacterial ribosome

The bacterial ribosome (70S) is formed of a large subunit (50S) and a small subunit (30S). S stands for the Svedberg unit, which measures the rate of sedimentation of large particles during ultracentrifugation. 50S is composed of two rRNAs (23S and 5S rRNA), as well as 34 r-proteins, while 30S contains just one rRNA (16S) and 21 r-proteins. The number of r-proteins composing each ribosomal subunit varies between different species, the numbers cited above being valid for *E. coli* ribosomes.

In eukaryotes, there are two types of ribosomes: the cytosolic and the mitochondrial ribosomes. The cytosolic ribosomes (80S) are composed of the small subunit (40S), which contains 18S rRNA and 30-35 r-proteins, and the large subunit (60S), formed of 28S rRNA, 5.8 rRNA, 5S rRNA and 45-50 r-proteins (the number of r-proteins depends on the individual organism). The main characteristic that differentiates

the mitochondrial ribosomes (55S) from the bacterial and cytosolic ones is their high content of r-proteins. Their two ribosomal subunits (39S and 28S) contain smaller rRNAs (16S and 12S rRNA) and approximately 80 r-proteins.

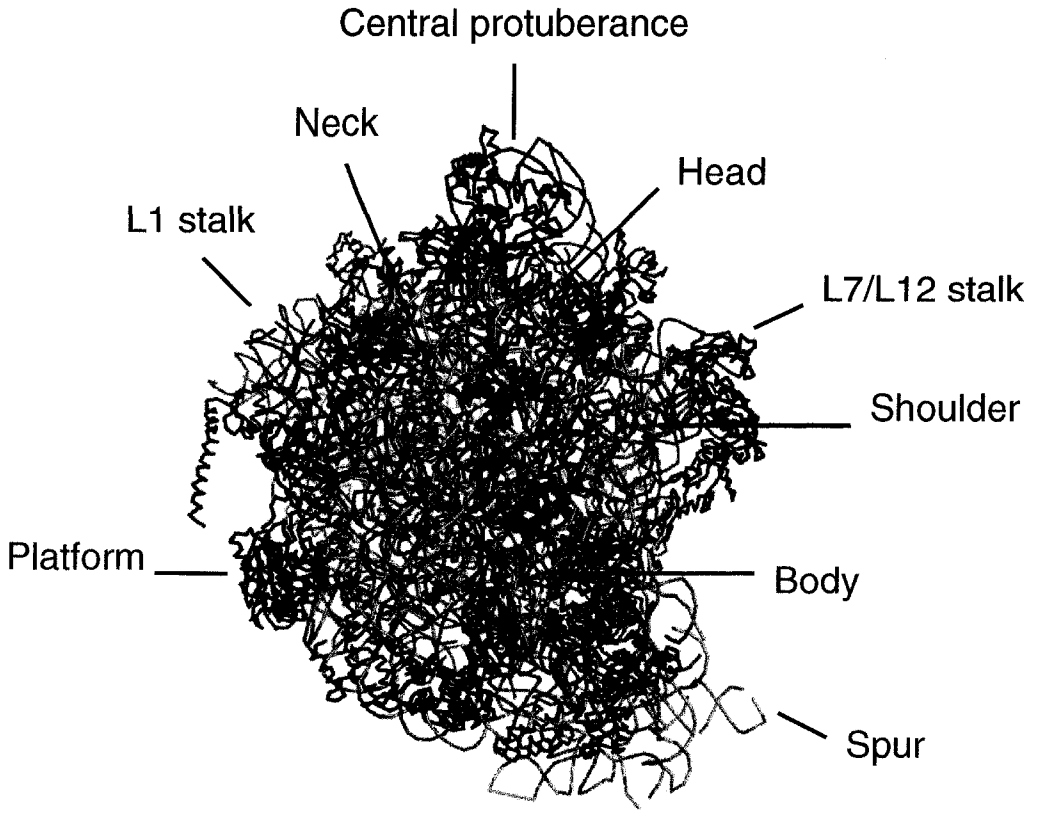


**Fig. I.1. – Cartoon of the structure of the *E. coli* 70S ribosome**. The 50S subunit is depicted in blue, and the 30S subunit is in green. The rRNAs are in lighter colors, while the r-proteins are shown in darker colors. The different regions of the ribosomal subunits are labeled in blue (50S) or dark green (30S). Figure was prepared using PyMOL, PDB 1P6G and 1P85 (Frank and Agrawal, 2000).

The initial lower resolution (~ 25Å) electron microscopy studies defined several structural elements of the ribosomal subunits, as gathered from the shapes of ribosomes. The 50S subunit has a main body and three protuberances, which were named the L7/L12 stalk, the L1 stalk and the central protuberance. The first two stalks were named after one of the main r-proteins in their composition, while the central protuberance received its name according to its position, between the other two stalks. The 30S subunit has more

elements, being organized in six different regions: head, neck, body, platform, shoulder, and spur. (Spirin, 1999) These elements are highlighted on the *E. coli* ribosome cartoon presented in Fig. I.1. Later cryo-EM studies have shown that these structures are mobile in regards to one another, their movements accompanying important functions of the ribosome (e.g. tRNA and mRNA translocation (Valle et al., 2003b)).

The rRNAs form the majority of the interior of the subunits, as well as the inter-subunit bridges, while the r-proteins are mostly situated at the exterior, are smaller in size, and predominately positively charged. The majority of r-proteins have structural roles in the proper folding of the rRNAs, protecting the rRNAs from degradation by ribonucleases, and in preserving the ribosomal structure, while conferring it a certain degree of conformational mobility. A few of the r-proteins have also been identified as having functional roles in protein synthesis, which will be detailed later.

The two ribosomal subunits interact with one another, forming a cavity between them, which provides binding sites for the tRNAs and other protein factors involved in protein synthesis. The subunits are connected by a series of twelve inter-subunit bridges, composed mainly of rRNA elements with contributions also from a few r-proteins (S6, S13, S15, S19 from the 30S subunit, and L2, L5, L14, and L19 from the 50S subunit). Of these twelve bridges, four are composed solely of rRNA elements interactions, three contain a mixture of rRNA-rRNA and rRNA-r-protein interactions, four have only rRNA-r-protein interactions, and only one is formed of the interaction between two r-proteins. The association of the ribosomal subunits is dependent on $Mg^{2+}$ concentration (physiological concentration *in vivo* being approximately 6mM) and some of these bridges can change interacting partners, conferring mobility to the ribosomal structure. (Schuwirth et al., 2005; Yusupov et al., 2001)

### I.1.2 The mRNA

The mRNAs contains the genetic information, which will be translated by ribosomes into proteins. The individual amino acids are encoded by codons, sequences of three mRNA nucleotides. Based on the combinations of the four RNA bases, there are 64 codons, among which 61 code for 20 amino acids, while three (UAG, UAA, and UGA) are nonsense codons, signaling the end of a protein sequence (also called stop codons).

This genetic code is degenerate, most amino acids being encoded by two to six codons, with identical nucleotides in the first two positions and different in the last nucleotide. In the case of the amino acids being encoded by 6 different codons (leucine, serine and arginine), there are also differences in the first and second nucleotides. Two amino acids have just one codon each: methionine (AUG) and tryptophan (UGG). Interestingly, UGA can also function as a sense codon in certain organisms, being interpreted as selenocysteine if it is accompanied by certain structural elements in the mRNA (Chambers et al., 1986; Zinoni et al., 1987).

The mRNA binds to the 30S subunit, crystal structures showing it wrapped around the neck of this subunit and passing through an upstream tunnel, formed between the platform and the head, and a downstream tunnel, formed between the head and the body (Yusupova et al., 2001). Approximately 30 nucleotides of the mRNA interact with the 30S subunit, among which only 8 are exposed in the inter-subunit interface. In order for mRNA binding to occur in this manner, its secondary structural elements have to be disassembled, potentially by the 30S subunit. A recent study has confirmed the previous theoretical hypothesis that the 30S subunit displays intrinsic helicase activity (Takyar et al., 2005). This enzymatic function is localized in the downstream tunnel, between the head and the shoulder regions, where the mRNA was observed to pass through a clamp formed by basic residues belonging to the r-proteins S3, S4, and S5. Mutational studies have shown that S3 and S4 residues play an important role in this helicase processivity (Takyar et al., 2005), the mechanism being probably based on the rotation of the head (where S3 is situated) in regards to the body (the location of S4). Crystal structures also observed a kink between the A and the P site codons of the mRNA, which is necessary in order to allow the proper binding of both A and P site tRNA anticodons. (Yusupova et al., 2001)

### I.1.3. The tRNAs

The tRNAs are a key component in the process of proteins synthesis, bringing to the ribosome the amino acids necessary for the formation of the polypeptide chain. There are 49 different tRNA species in *E. coli*, encoded by approximately 80 genes. Their primary structure contains between 74 and 95 nucleotides, a large number of bases

having modifications. The secondary structure shows the classical "cloverleaf" shape, with five identifiable elements: the anticodon end (pairs with the mRNA codon), the acceptor arm (contains three universally conserved bases CCA at the 3' end), D and T stems, as well as a variable length loop. These elements of the secondary structure fold in an L-shape tertiary structure, with the arms being represented by the anticodon and the acceptor stems, while the D and T arms form the elbow region.

The tRNAs bind in the ribosomal cavity, their anticodon ends making contact with the mRNA nucleotides exposed in the intersubunit cavity. Proper recognition between the codon of the mRNA and the anticodon of the tRNA is the basis for the fidelity of translation, the details of this process being explained in the following subchapters. The binding of tRNAs is also stabilized by extensive interactions with ribosomal elements, three tRNA binding sites (A, P, and E sites) existing in each ribosomal subunit. The names of the tRNA binding sites reflect their functional roles: A site binds the aminoacylated-tRNA, the P site has the highest affinity for the peptidyl-tRNA, while the E (exit) site can only bind the deacylated tRNAs. These binding sites are composed mostly of rRNA elements, but a few r-proteins are also involved as follows: S12, S13 and L16 (A site tRNA), S9, S13, and L5 (P site tRNA), and, S7, L1, and L33 (E site tRNA). Crystal structure of the ribosome in complex with mRNA and three tRNAs occupying the A, P, and E sites revealed that the elbow of A site tRNA and the D stem of the P site tRNA make contact with two different inter-subunit bridges. In the case of the E site tRNA, it is generally believed that it makes only a weak contact (if any) with the mRNA. (Yusupov et al., 2001) Similar with ribosomal subunit association, binding of the tRNAs to the ribosome is also controlled by the $Mg^{2+}$ concentration (Schilling-Bartetzko et al., 1992).

The attachment of the proper amino acid to the 3' end of tRNAs is also a key process in the maintaining the fidelity of translation. This process is catalyzed by aminoacyl-tRNA synthesases, which use the energy released from ATP hydrolysis to accomplish this function. These enzymes belong to two different structural classes, based on the fold of their ATP binding domain: class I (Rossmann fold) and class II (antiparallel β-sheet). Aminoacylation of the tRNA is a multiple step process, each step being catalyzed by the synthetases. First, the amino acid is activated by reaction with

ATP, forming amino acid-AMP and pyrophosphate, reaction easily reversible in the presence of reaction products. The equilibrium of this reaction is altered by the hydrolysis of pyrophosphate by pyrophosphatase. The second step consists of covalent binding of the amino acid to the 3' end adenosine of the tRNA and the release of AMP. Class I synthetases attach the amino acid to the 2'OH of the ribose sugar of the 3' adenine, while class II attaches it to the 3' position. These differences tend to be insignificant functionally, as 2' and 3' isomers exchange readily in solution, until they reach equilibrium. In order for the correct amino acid to be attached to the proper tRNA, these enzymes require good discriminatory capacities between the cognate and non-cognate tRNAs. This is accomplished by specific recognition of both the acceptor arm and the anti-codon stem, in the majority of cases, although there are some enzymes which recognize only one of these two elements. Specific recognition induces a slow conformational change in the enzymatic complex, which is the major structural characteristic of the binding of a cognate tRNA as compared to the binding of a non-cognate tRNA. A final verification step is also believed to exist, at least in the case of some of these synthetases, in which the incorrectly formed aa-tRNA is hydrolyzed by the attack of a water molecule; the free hydroxyl of the ribose of the 3' adenine seems to be playing an important role in this hydrolysis reaction. (for a more detailed review see (McClain, 1993))

## I.2. TRANSLATION

The ribosome has been described as a "macromolecular machine" (Spirin, 2004) that produces proteins from individual amino acids, by using mRNAs as templates, and consuming energy in the process. This complex synthesis is accomplished with the help of additional protein factors.

Each ribosomal subunit has specific roles in protein synthesis: 30S binds mRNA and verifies the correct paring between the codon of the mRNA and the anticodon of the tRNA in the process called decoding, while 50S plays a key role in peptide bond formation. Movement of the tRNAs between different tRNA binding sites together with the mRNA connected to them (translocation) is achieved by a complex interplay between the two subunits.

Conceptually, translation can be divided into three major phases (each comprising a multitude of steps): initiation, elongation and termination.

### I.2.1. Initiation

In bacteria, the initiation of translation comprises the assembly of the initiation complex, which contains the ribosome, the mRNA to be translated and initiator $tRNA^{fMet}$ bound in the ribosomal P site. Three protein factors are involved in the formation of this ribosomal complex, the initiation factors: IF1, IF2, and IF3.

At the start of the initiation, IF1 and IF3 bind to the 30S subunit and act cooperatively in order to maintain the two ribosomal subunits dissociated. IF1, the smallest of the initiation factors, binds over the 30S subunit A site, between helix 44 and the r-protein S12, blocking the association of any elongator tRNA with the 30S subunit. IF1 was also shown to determine conformational changes in helix 44 of 16S rRNA, which probably lead to disruptions in the inter-subunit bridges involving this rRNA helix and may explain its role in subunit dissociation (Carter et al., 2001). IF3 is formed of two domains: the N- and C-terminal domain, connected by an extended and flexible hinge. Its N-terminal domain covers the E site of the 30S subunit, while the C-terminal domain makes direct contact with the anticodon stem loop of the initiator tRNA. Its position sterically blocks several bridges between the 50S and the 30S subunit, explaining its effect on subunit dissociation (Allen et al., 2005). The initial complex formed by the 30S subunit, IF1, and IF3 binds mRNA, initiator $tRNA^{fMet}$ and IF2, in an order that is believed to be random.

The proper recognition of the mRNA by the 30S subunit is very important for the formation of a stable mRNA•30S subunit complex, which in turn leads to efficient protein synthesis. The vast majority of bacterial mRNAs contain the Shine-Dalgarno (SD) sequence in their 5' UTR, sequence defined by a six base consensus sequence (AGGAGG). This is specifically recognized by the anti-SD sequence (CCUCCU) from the 3' of 16S rRNA, located in a cleft between the back of the platform and the head of the 30S subunit. Although it is generally agreed that the main recognition element is represented by the SD sequence, differences in translation efficiency between mRNAs with similar SD sequences may be found in the presence of different secondary structures

of the mRNA (Coleman et al., 1985), which may increase the stability of the mRNA•30S subunit complex in some cases. The r-protein S1 can also facilitate recruitment of the mRNAs to the 30S subunit, being able to specifically recognize a pyrimidine rich region upsteam of the SD sequence of the mRNA (Boni et al., 1991).

The mRNA is "activated" from the initial binding position by the binding of IF2 and the initiator tRNA to the initiation complex. This activation brings the start codon (almost always AUG) into the P site in order to form interactions with the anti-codon of the initiator tRNA.

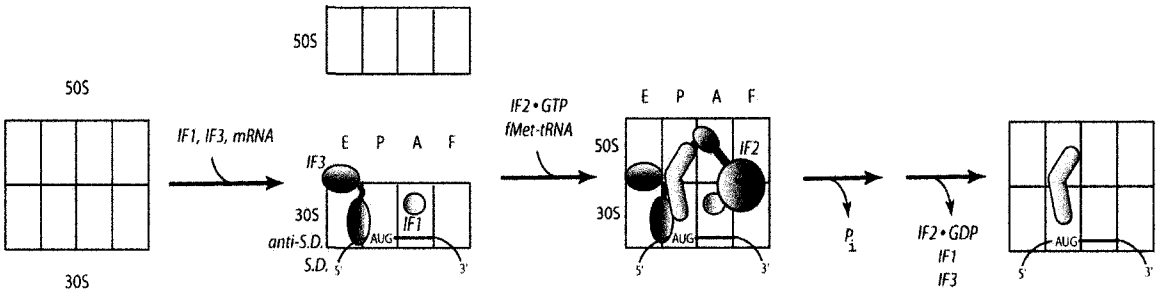


**Fig. I.2. Simplified cartoon of translation initiation.** The small and large ribosomal subunits are shown as grey squares. Initiation factors are in red (IF1), green (IF2), and blue (IF3), and the fMet-tRNA$^{fMet}$ is in light grey. The F site is the factor binding site.

The initiator tRNA carries on its acceptor end a methionine modified by formylation (-CHO) of its amino group, which is only used at the start of the protein synthesis. Inside the mRNA coding sequence, AUG codes for methionine, amino acid delivered to the ribosomal complex by elongator tRNAs. The initiator tRNA is distinguished from the elongator tRNAs by unique structural characteristics. One of the most important ones is the absence of a Watson-Crick base pair between positions 1 and 72 in the acceptor stem, which is the key structural feature for its recognition by the methionyl-tRNA transformylase, the enzyme responsible for methionine formylation. The same structural characteristic prevents recognition by the peptidyl-tRNA hydrolase, hence increasing its life time. Formylation of the methionine seems to be an important element for initiator tRNA recognition by IF2, and it simultaneously prevents binding of the initiator tRNA by EF-Tu (elongation factor which delivers the aminoacylated

elongator tRNAs in the A site). Another unique structural element is the presence of three conserved consecutive GC base pairs in the anticodon stem, which modifies its three dimensional conformation in order to facilitate high affinity P site binding and also serves as a recognition element for IF3. (Laursen et al., 2005)

The initiator tRNA binds to the P site, at first in a codon independent manner. The unique characteristics of fMet-tRNA$^{fMet}$ are recognized by IF2, which binds to the ribosome in complex with GTP, as well as by the C-terminal domain of IF3 (Fig. I.2). Unlike EF-Tu, which forms a complex with aminoacylated elongator tRNAs and GTP in solution, IF2 does not seem to bind the initiator tRNA outside the context of the ribosome. Codon-anticodon interactions between the initiator tRNA and the initiator codon determine a cascade of conformational changes, their main consequence being the dissociation of IF1 and IF3 from the 30S complex, IF2 also being potentially involved in this process. The next steps are represented by association of the 50S subunit to the complex, GTP hydrolysis by IF2 (activated by 50S subunit), IF2 dissociation from the initiation complex and the formation of a complex ready to start the elongation process. The role of GTP hydrolysis by IF2 remains unclear at the moment, this factor being able to accomplish its function(s) in the presence of a non-hydrolyzable GTP analog as well. (For a more detailed review of bacterial initiation see (Laursen et al., 2005))

As compared to bacteria, the eukaryotic initiation is extremely complex, involving at least 12 initiation factors, some of which are multi-protein complexes; it also requires the consumption of both GTP and ATP in the process. The major difference in initiation between bacteria and eukaryotes appears in the recognition of the mRNA and its binding to the 40S subunit steps, which are accomplished with the participation of numerous initiation factors. The eukaryotic mRNAs lack the Shine-Delgarno sequence, their recognition being based on the 5'-terminal cap ($m^7$GpppN) present in the majority of the nuclear transcribed mRNAs. Another structural element of the mRNAs is represented by the 3' poly(A) tail, formed of 50-300 adenosines. This poly(A) tail acts synergistically with the 5'cap in enhancing translation initiation.

Briefly, the mRNAs are recognized through the cap structure by eIF4E and become cyclic during the assembly of a large complex containing the initiation factors eIF4G, eIF4A, eIF4F, eIF4E, eIF4B, and polyA binding protein (PABP). This complex is

loaded onto the 43S complex composed of 40S ribosomal subunit, eIF1, eIF1A, eIF3, and eIF2 ternary complex (eIF2•Met-tRNA$_i^{Met}$•GTP). As is the case with the bacterial analog, the initiator tRNA in eukaryotes is also a methionine tRNA with special structural characteristics which differentiate it from an elongator tRNA. The difference consists of the fact that the methionine is not formylated in eukaryotes.

The next step is represented by *scanning*, in which the small subunit with the initiator tRNA bound to the P site glides along the mRNA looking for the start codon (AUG in the majority of the cases). This process is facilitated by the initiation factors bound to the small ribosomal subunit, eIF4A being a helicase which can disrupt efficiently the secondary/tertiary structures of the mRNA in the presence of eIF4B and eIF4F. After recognition of the initiation codon, the initiation factors are released and the two subunits form a complex with the help of eIF5 and eIF5B•GTP, followed by the final release of these last two elongation factors.

The initiation factors involved in mRNA recognition in eukaryotes are the target of several regulatory systems, which can stop translation initiation using phosphorylation/de-phosphorylation controls under certain conditions for the cell (e.g. stress, mitosis). Although many eIFs have phopsphorylation sites, the best understood mechanism is the hypophosphorylation of eIF4E-BP, which blocks eIF4E and its recognition of the mRNA cap, hence effectively stopping translation initiation of the capped mRNA. (Pestova et al., 2007)

A different mechanism of mRNA translation initiation in eukaryotes was discovered initially for viruses infecting mammalian cells (e.g. hepatitis C, poliovirus). Some of these viruses have the ability to suppress cap-dependent initiation by modifying the initiation factors necessary for cap recognition and hijacking the translation machinery of the cell for the production of viral proteins. These viral mRNAs were found to lack a cap structure and in turn, contain in their 5' UTR, a complex structure of the RNA, called the Internal Ribosome Entry Site (IRES). The function of this structure is to allow mRNA recognition and binding to the 40S subunit using only a subset of the initiation factors, the number of the factors required depending on the specific class of IRES. Further exploration into this field proved that there are also cellular mRNAs which contain IRES, their translation being possible in times where the initiation of all cap

containing mRNAs is inhibited. The function of the proteins coded by these IRES containing mRNA is likely to salvage the eukaryotic cell from the effects of various stressors. (for a more detailed review see (Douda and Sarnow, 2007))

### I.2.2. Elongation cycle

While initiation and termination are individual processes that start and end translation, the elongation cycle comprises the majority of the actual protein synthesis. During the elongation cycle, the polypeptide chain is assembled, one amino acid at a time, until a stop codon is encountered by the ribosome.

Elongation can also be divided conceptually into three steps: binding of the correct aa-tRNA to the A site (Fig. I.3.1-3), peptide bond formation (Fig. I.3.4), and finally translocation of the tRNAs and the mRNA, with the release of the deacylated tRNA from the E site (Fig. I.3.5-6).

The next aa-tRNA is delivered to the A site by elongation factor Tu (EF-Tu). EF-Tu is a G protein (guanosine binding protein), a class of proteins belonging to the larger family of GTPases (proteins with the ability to hydrolyze GTP). Several G proteins are involved in cellular signaling pathways (e.g. heterotrimeric G proteins, Ras), but this class also has members among the ribosomal factors (IF2, EF-Tu, EF-G, and RF3 in bacteria). The G proteins were described as "switch proteins", being in an active state while in complex with GTP, and in an inactive state in complex with GDP. They also share common structural elements, which are not surprisingly situated around the GTP binding region: the nucleoside binding site (residues that interact with guanosine), the P loop (residues that bind the ribose sugar and phosphate groups), switch 1 and 2 (mobile elements that provide interactions mainly for the γ phosphate of GTP and change drastically their conformation upon GTP hydrolysis) (Sprinzl et al., 2000).

The steps of the aminoacyl-tRNA binding to the A site, as well as the kinetics associated with each individual step have been studied in great detail (for a detailed review see (Rodnina et al., 2005)). EF-Tu•GTP recognizes specifically the aminoacylated tRNAs. This tertiary complex (EF-Tu•aa-tRNA•GTP) then associates with the 70S•mRNA•peptidyl-tRNA (P site), the initial binding being codon independent, promoted by the interaction between EF-Tu and the ribosome. It is believed that the

association of the ternary complex with the ribosome is not a random event, but it is at least partially due to the recruitment of EF-Tu by the r-protein L7/L12 (Diaconu et al., 2005). During this initial binding, the tRNA interacts with the A site of the 30S subunit with its anti-codon stem, while the acceptor stem is still bound to EF-Tu (Fig. I.3.2).

Codon-anticodon interactions are monitored by the 30S subunit in a process known as decoding. Decoding is an essential step of translation, but the simple codon-anticodon interactions are not enough to explain the high accuracy of protein synthesis ($10^{-3}$ – $10^{-4}$ error rate *in vivo* (Loftfield and Vanderjagt, 1972)). The proper codon-anticodon interactions were identified by crystallographic studies to induce conformational changes in the 30S subunit, one of the most important ones involving ribosomal bases A1492, A1493 and G530, part of the 30S subunit A site. A1493 flips out from its previous position and engages in interactions with the first nucleotide pair of the codon-anticodon interaction. A similar movement is undergone by the ribosomal base A1492, while G530 changes from a *syn* to an *anti* conformation. Both A1492 and G530 monitor the proper geometry of the second codon-anticodon nucleotide pair. The third base pair is not monitored by ribosomal elements as closely, explaining the possibility of the wobble paring at this position. (Ogle et al., 2001) The local conformational changes of the A site propagate to global conformational changes of the 30S subunit, crystal structures revealing movements of the shoulder and head regions, which form the "closed conformation" of the 30S subunit. (Ogle et al., 2002)

The proper codon-anticodon interaction also determines activation of GTP hydrolysis in EF-Tu, probably by conformational changes in the structure of domain I (the G domain) of EF-Tu. After Pi release, EF-Tu•GDP dissociates from the ribosomal complex. The mechanism of the GTP hydrolysis activation in EF-Tu is still unclear, but the conformational changes responsible for it seem to be propagated through the body of the tRNA, only an intact tRNA being able to transmit the proper signals (Piepenburg et al., 2000). Activation of the GTP hydrolysis in EF-Tu is another step that differentiates the cognate from near-cognate tRNAs, being significantly faster in the case of cognate tRNAs (Gromadski and Rodnina, 2004a). The GTP hydrolysis mechanism itself is not well understood in the case of EF-Tu, but it is generally believed that it involves a rearrangement of the G domain, and the stabilization of the transition state by the GTPase

activation region of ribosome. The current hypothesis regarding the potentially catalytical residues involved in this process, as well as the necessary conformational changes undergone by different elements of domain I of EF-Tu will be described in a further section.

The aminoacyl-tRNA is released from EF-Tu during or shortly after the GTP hydrolysis. After EF-Tu•GDP dissociation, the tRNA is left to *accommodate*, a process consisting of complex rotation and translation movements, which bring the acceptor end of the tRNA in the 50S subunit A site, more than 70Å from its original position (Fig. I.3.3). The near-cognate tRNAs that have survived the preceding steps up to accommodation will have slower kinetics of accommodation at this point as well as less stable binding to the ribosomal complex, being rejected by the ribosome. (Gromadski and Rodnina, 2004a)

EF-Tu•GDP is a very stable complex, its spontaneous dissociation *in vivo* being very slow. Hence, similar to the majority of the G proteins, EF-Tu requires a nucleotide exchange factor called EF-Ts. EF-Ts specifically binds EF-Tu•GDP, contacting domains I and III of EF-Tu and inducing conformational changes, which have as the consequence the dissociation of GDP, followed by GTP binding, and EF-Ts dissociation from EF-Tu•GTP complex.

After accommodation of the A site tRNA, the new peptide bond is rapidly formed by the nucleophilic attack of the amino acid from the A site on the ester bond between the peptide and the peptidyl-tRNA. The reaction rate is augmented by $10^7$ fold on the ribosome compared to the rate of reaction when the reactants are free in solution. The long standing belief that the ribosome is a ribozyme was confirmed by crystal structures showing that the peptidyl-transferase center contains only rRNA (Nissen et al., 2000). In spite of extensive studies, the exact catalytic mechanism of peptide bond formation is not mp;list_uids=9600930 </url></related-

roposed that N3 of A2451 acts both as a catalytic group (general base), extracting a proton from the amino moiety of the amino acid, as well as a stabilizer of the oxyanion of the tetrahedral intermediate (Nissen et al., 2000). More recent experiments deny any direct catalytic involvement of A2451. A water molecule which is positioned by A2602 and U2584 forms hydrogen bonds with the oxyanion of the tetrahedral intermediate, while the 2'OH of the A76 of the P site tRNA is believed to be the element aiding the

believed to be the element aiding the nucleophilic attack, raising the possibility of substrate-assisted catalysis (Schmeing et al., 2005). In light of recent findings, more studies are needed in order to fully elucidate the catalytic moiety of the peptide bond formation reaction, as well as the functional roles of universally conserved bases situated in close proximity to the reactants in the peptidyl-transferase center. For a more detailed review regarding the mechanism of peptide bond formation see (Rodnina et al., 2007).

The nascent peptide passes through the so called "exit tunnel" of the 50S subunit. This tunnel is formed mostly by rRNA, but some r-proteins also contribute to this structure. Among these, the r-proteins L4 and L22 protrude in the lumen at the narrowest point, potentially acting as a control gate. It is possible that the 50S subunit also acts a chaperone, contributing to the first step in the folding of the nascent peptide by interactions with rRNA and protein elements of the exit tunnel. (Nissen et al., 2000) While still attached to the tRNA and the ribosome, the nascent peptide starts to fold, receiving assistance from chaperones (trigger factor (TF) in bacteria and Hsp70 family: DnaK in bacteria, Ssb1/2 in yeast, Hsc70 in mammals), and chaperonins (TRiC in eukaryotes). TF has peptidyl-prolyl isomerase activity and it has been shown to interact with the nascent peptide and the 50S subunit near the r-proteins L23 and L29. Two other enzymes are believed to modify immediately the nascent peptide chain in bacteria: peptide deformylase, which removes the formyl group of the first methionine and methionine aminopeptidase, which cleaves the first methionine, after deformylation. Recent structural studies suggest that these two enzymes bind concomitantly with TF to the 50S subunit, with PDF on one side of TF and using L22 as its major docking site (Bingel-Erlenmeyer et al., 2008), while methionine aminopeptidase is on the other side of TF, interacting with the r-protein L24 (Addlagatta et al., 2005).

Ssb also associates with the ribosome, but it can bind to the nascent peptide only with the help of RAC (ribosome-associated complex), composed of Zuo and Ssz. DnaK (bacteria), Hsc70 (eukaryotes), and TRiC (eukaryotes) do not seem to interact directly with the ribosome, but they bind to the nascent peptide chain. (Craig et al., 2003)

In eukaryotes, the nascent peptide exported into the endoplasmic reticulum (ER) can interact with a large, preformed complex of ER resident chaperones (BiP, GRP94, CaBP1, protein disulphide isomerase (PDI), ERdj3, ER Hsp40, cyclophilin B, ERp72,

GRP170, UDP-glucosyltransferase, SDF2-L1) (Meunier et al., 2002). There is also a second chaperone system in ER formed of UDP-glucosyltransferase, ERp57, calnexin, calreticulin, and glucosidase II, which is specific for glycoproteins. During the folding/maturation steps, the nascent peptide is also modified cotranslationally, forming disulphide bridges (PDI, ERp57), being glycosylated (oligosaccharyl transferase complex), carboxylated by carboxylases, etc. (Ellgaard and Frickel, 2003)

The next step in the elongation cycle is translocation, the concerted movement of the tRNAs in the ribosomal cavity, together with the mRNA base-paired to them. This process is catalyzed by a five domain G protein called elongation factor G (EF-G). Similar to EF-Tu, the GTP hydrolyzing ability of EF-G is only activated in the context of the ribosome.

Recent studies suggest that the peptide bond formation prepares the ribosomal complex for EF-G recruitment, likely by determining conformational rearrangements between the two ribosomal subunits, which increase the affinity of the ribosomal complex for EF-G•GTP (Zavialov and Ehrenberg, 2003). New reports indicate also a loosening of the 30S subunit grip on the mRNA (Uemura et al., 2007), which probably facilitates the movement of the mRNA during translocation. At the moment, the process of translocation appears to be accomplished in at least two different stages, both being dependent on the presence of EF-G. Firstly, EF-G•GTP binding to the ribosomal complex determines the tRNAs to adopt a hybrid state (Fig. I.3.4), moving to the P, and E site in the 50S subunit, while their anticodons remain bound to the A, and P sites on the 30S subunit (Moazed and Noller, 1989). Cryo-EM studies have detected certain conformational changes of the ribosomal complex which accompany the binding of EF-G•GTP to 70S and may be responsible for the formation of the hybrid state. The L1 stalk, containing the 50S E site, was observed to be in a closer position to the central protuberance, perhaps receiving the E/P hybrid tRNA, and facilitating the transition state. The biggest movement observed in the cryo-EM maps is undertaken by the 30S subunit, which rotates in regard to the 50S subunit, producing the so called "ratcheting motion". The head of the 30S subunit rotates counterclockwise at first relative to the central protuberance of the 50S subunit, rotation possibly due to dissolution and re-formation of three inter-subunit bridges (Frank and Agrawal, 2000).

The second step involves the movement of the tRNAs in the 30S subunit and of the mRNA by one codon, a step which is preceded by the GTP hydrolysis in EF-G (Fig. I.3.5). Cryo-EM maps indicated a second set of movements, which are in the opposite direction to the previously described ones: the L1 stalk moves back to its original position, potentially dragging the E site tRNA and positioning it properly in the E/E state, while the 30S subunit reverts to its original position (Valle et al., 2003b). Recent studies have shown that, in the absence of charged tRNAs, the two ribosomal subunits can ratchet spontaneously, suggesting that these conformational changes are an intrinsic property of the ribosome, which is augmented by the binding of EF-G (Ermolenko et al., 2007a).

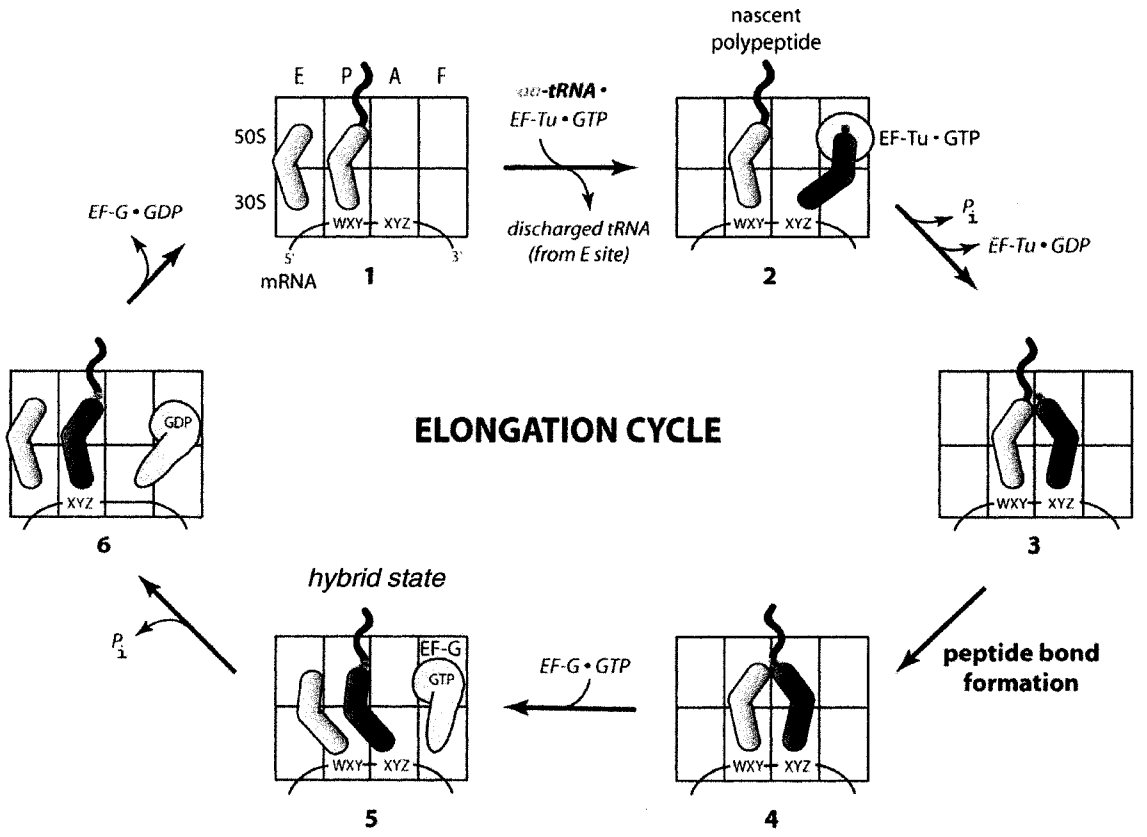


**Fig. I.3 – Current model for the elongation cycle of protein synthesis.** The A site tRNA is colored in blue, and the P and E sites tRNA are in grey. The nascent polypeptide is shown in black. The amino acid attached to the tRNA is a red small sphere, while the mRNA is a dark line. The two elongation factors, EF-G and EF-Tu are represented as orange shapes.

New fluorescent studies suggest that the movement of tRNAs between the two ribosomal subunits may be even more complicated than originally anticipated, the authors identifying a new hybrid state, in which only the deacylated P site tRNA has moved into the P/E position, while the A site tRNA has remained in classical state A/A (Munro et al., 2007).

EF-G•GDP dissociates from the ribosomal complex, leaving it ready for another elongation cycle. Unlike the majority of G proteins, a nucleotide exchange factor has not been identified for EF-G, and this protein has rather similar affinities for both GTP and GDP when it is free in solution (Arai et al., 1975). It is believed that EF-G is able to exchange GDP for GTP *in vivo* due to a 10 fold higher concentration of GTP over GDP. A more recent model attempted to identify the ribosomal complex as the nucleotide exchange factor, trying to prove that EF-G binds to the ribosome in complex with GDP, and that the first step of translocation would be represented by the exchange of GDP for GTP (Zavialov et al., 2005). This model has not gained acceptance in the field, and more recent work questions the experimental data and reinforces the classical model (Wilden et al., 2006).

In spite of the extensive studies cited above, it is still unclear how EF-G is able to accomplish its functions and determine this cascade of conformational changes in the ribosomal complex.

In eukaryotes, EF1A is the homologue of EF-Tu and uses a three subunit protein, EF1B, to facilitate the fast exchange of GDP for GTP. EF2 is the eukaryotic homologue of EF-G. Elongation of already initiated mRNAs can be stopped by phosphorylation of threonine 56 in EF2, which blocks its binding to the ribosome and effectively stops protein synthesis. (for a more details regarding translation elongation control in eukaryotes see (Herbert and Proud, 2007))

### I.2.3. Termination

The elongation cycle ends when a stop codon (UAA, UGA, and UAG) arrives in the A site. These termination codons are specifically recognized by two release factors (RF1 and RF2), both of them being able to detect UAA, while UAG is only sensed by

RF1, and UGA is specific only for RF2 (Fig. I.4). The eukaryotes have only one release factor, which recognizes all three stop codons.

The release factors catalyze the hydrolysis of the ester bond between the nascent peptide and the P site tRNA, but the details of their action mechanism remain largely unknown. Both of them have conserved motifs, which may serve in the catalysis and recognition of stop codons, and they seem to undergo drastic conformational changes upon binding to the ribosome. RF3, the third release factor, is a G protein and binds to terminating ribosomal complexes containing RF1/2, likely in complex with GDP (Fig. I.4). The release of the nascent peptide seems to determine RF3 to exchange GDP for GTP (Fig. I.4IV), switching it to a form with higher affinity for the ribosomal complex, which, in turn, determines the release of RF1/2 from the ribosomal complex (Fig. I.4). This dissociation stimulates GTP hydrolysis in RF3, followed by the dissociation of the RF3•GDP complex (Fig. I.4).

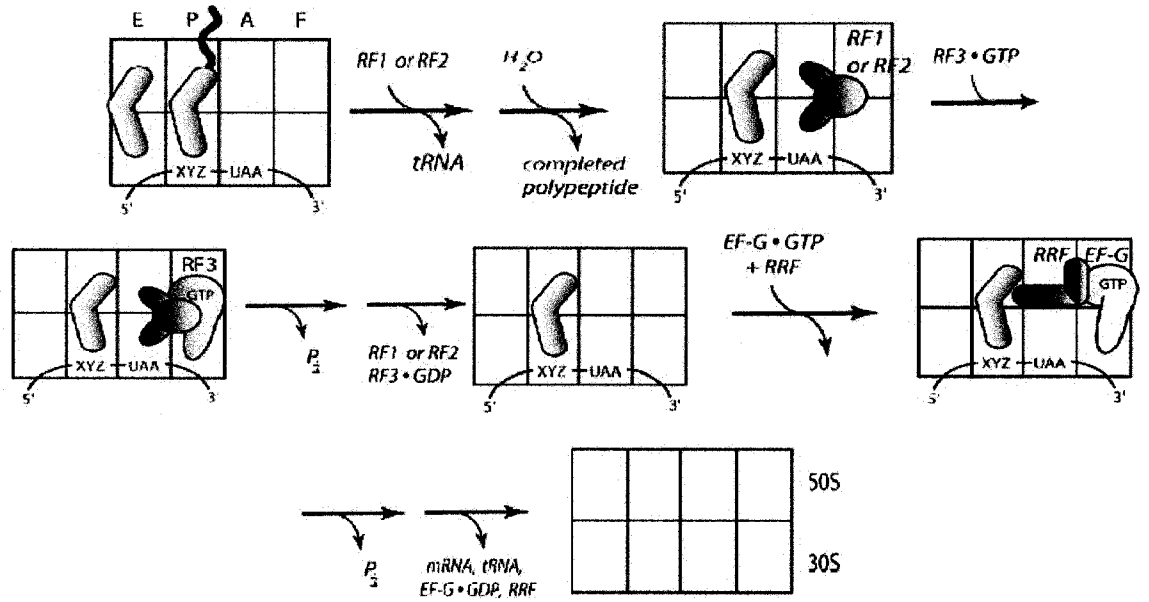


**Fig. I.4 – Multiple steps of the translation termination process.** The ribosomes are depicted as grey squares, the tRNAs are in light grey, RF1/RF2 is shown as a blue shape, RF3 is in magenta, RRF is shown as a cyan L shape, while EF-G is in orange.

The remaining components (mRNA, de-acylated tRNA and ribosomes) are disassembled by the ribosome recycling factor (RRF) and EF-G (Fig. I.4). When RRF structure was initially determined (Selmer et al., 1999), the authors thought this factor resembled closely a tRNA because of its two domains connected by a flexible hinge. This resemblance lead to the hypothesis that this factor may bind in the A site of the post-termination complexes and it may be translocated by EF-G similarly to a tRNA, this translocation having the effect of breaking the two ribosomal subunits (Selmer et al., 1999). Hydroxyl radical probing data (Lancaster et al., 2002), followed by cryo-EM structures (Gao et al., 2005) showed, by contrast, that RRF binds differently to the ribosome than tRNAs, being in contact extensively with 50S subunit and the inter-subunit bridges. The new hypothesis predicts that EF-G produces conformational changes in RRF and the ribosome, which in turn disrupt a critical inter-subunit bridge, facilitating the separation of the two ribosomal subunits. IF3 binds to the newly released 30S and prevents the subunit re-association.

## I.3. ANTIBIOTICS INHIBITING TRANSLATION

After their introduction in clinical use in 1950s, it was believed that antibiotics would lead to the fast control and maybe eradication of all bacterial infections. Unfortunately, bacteria have evolved quite rapidly, adapting to the new environment, helped also partially by the over-prescription of antibiotics, and soon enough physicians started to battle bacterial strains resistant to the most commonly used antibiotics. Today, in spite of huge advancements in the understanding of both antibiotic action mechanisms, as well as the bacterial resistant pathways, we are still facing a continuous race between the creation of new antibiotics and the surfacing of multi-drug resistant hospital bacterial strains.

Protein synthesis in bacteria is one of the most common targets for many classes of antibiotics, with various binding sites and mechanism of action. Because of this, the studies on the bacterial ribosome structure and function have been more important than ever, due to their potential for rational drug design.

### I.3.1. Antibiotics which target the 30S subunit

Aminoglycosides (e.g. gentamicin, tobramicyn, neomycin, and streptomycin) are one of the first class of antibiotics identified to inhibit protein synthesis in bacteria. Initial research into their mechanism showed aminoglycosides to be miscoding agents, inhibiting the proper selection of the cognate tRNA. Further details were revealed by the crystal structures of some of these antibiotics in complex with ribosomes, which identified their binding sites to be at the decoding site in the 30S subunit. The ring of most aminoglycosides structure is inserted within the A site 16S rRNA helix 44, determining local conformational changes, with the consequence of "bulging out" of the universally conserved adenines A1492 and A1493. This conformation mimics the rearrangement determined by the binding of the proper tRNA to the A site and, in turn, allows the acceptance of non-cognate tRNAs by the ribosome. (Francois et al., 2005; Kondo et al., 2006; Ogle et al., 2001)

A particular member of aminoglycosides is streptomycin, which although it produces a similar miscoding effect, was found to have a different mechanism of action. Structural studies have shown streptomycin to bind to helices 18 and 27 of 16S rRNA, as well as to the r-protein S12, producing a rigid structure around the 30S subunit A site: the "ram" state (Carter et al., 2000). From a functional point of view, this conformation stimulates fast GTP hydrolysis in EF-Tu even in the presence on a non-cognate tRNA. At the same time, it slows down the rate of EF-Tu GTP hydrolysis activated by cognate tRNA binding, hence eliminating the difference between the cognate and non-cognate tRNAs (Gromadski and Rodnina, 2004b).

Although a member of this class based on its chemical structure, kasugamycin is, by contrast, not a miscoding agent, but an efficient inhibitor of translation initiation. A recent crystal structure showed its binding site to be between positions -2 and +1 of the mRNA in the initiation complex, inhibiting the association of the initiator tRNA with the ribosomal complex (Schuwirth et al., 2006).

Tetracyclines, another large class of antibiotics, were found to directly inhibit the binding of the A site tRNA to the 30S subunit. Crystal structure of the 30S subunit in complex with tetracycline revealed two functional binding sites for tetracycline: i) the main binding site which overlaps partially with the position of the A site tRNA, and ii) a

second binding site involving helix 27 of the 16S rRNA. Based on this information, the authors believe that the ternary complex is able to associate with the ribosome in spite of the tetracycline being bound to the 30S subunit. After GTP hydrolysis and EF-Tu•GDP dissociation, the tRNAs cannot properly accommodate due to the steric hindrance produced by tetracycline and are ejected from the ribosomal complex. (Brodersen et al., 2000)

### I.3.2. Antibiotics which target the 50S subunit

Several classes of antibiotics act on the 50S ribosomal subunit, binding close to the peptide transfer center. Although binding to proximal or even partially overlapping sites, these classes of antibiotics act through several distinct mechanisms:

- macrolides (e.g. erythroycin, clarithromycin, azitromycin) inhibit protein synthesis by binding at the entrance of the peptide exit tunnel, hence blocking the passage of the nascent peptide (Schlunzen et al., 2001);
- lincosamides (e.g. clindamicyn) bind to the 50S subunit between the A and P sites, inhibiting the association of tRNAs with the ribosomal complex (Schlunzen et al., 2001);
- chloramphenicol interferes with the accommodation of the aminoacyl moiety in the A site (Schlunzen et al., 2001);
- streptogramins consist of a mixture of A and B compounds, which act synergistically in inhibiting protein synthesis in bacteria. Compound A binds in the peptidyl-transferase region and inhibits binding of both A and P site tRNAs, while compound B binds in the peptide exit tunnel, in a site overlapping with macrolides (Harms et al., 2004);
- A new class of antibiotics, oxazolidinones, inhibit protein synthesis by binding in the region of the 50S E site and preventing the formation of a functional initiation complex (Matassova et al., 1999).

Other antibiotics specifically target the elongation factors. In the case of EF-Tu, four classes of antibiotics inhibit its functions by two different mechanisms:

- kirromycin and enalocyxin activate EF-Tu in the absence of the ribosome and inhibit the dissociation of EF-Tu from the ribosomal complex, hence stalling protein synthesis;
- pulvomycin and GE2270 inhibit the formation of the ternary complex by blocking the ability of EF-Tu to bind tRNA. (For a more detailed review see (Parmeggiani and Nissen, 2006)).

EF-G is inhibited by fusidic acid and thiostrepton. Fusidic acid has been identified to bind specifically to an EF-G conformation present only in the post-translocational ribosome complex. Fusidic acid allows EF-G•GTP to bind to the ribosomal complex, hydrolyze GTP and translocate the tRNAs and mRNA, but prevents the dissociation of EF-G•GDP from the ribosomal complex (Bodley et al., 1969). The exact place of fusidic acid binding is uncertain, but based on the position of the majority of the fusidic acid resistant mutants, the working hypothesis at this moment is that fusidic acid binds in a crevice between domains I, III, and V of EF-G (Johanson and Hughes, 1994), probably blocking a conformational change necessary for the dissociation of EF-G from the ribosome. Unlike fusidic acid, thiostrepton binds to the 50S subunit, next to the r-protein L11, but its action mechanism is still the focus of a long-standing controversy in the field. It was suggested that thiostrepton allows EF-G to bind to the ribosome and hydrolyze GTP, but blocks the release of inorganic phosphate and the subsequent conformational changes (Rodnina et al., 1999). A different body of evidence (Cameron et al., 2002), verified also by our own data (Fig. II.5.), argue that thiostrepton inhibits the binding of EF-G to the pre-translocational ribosomal complex, hence preventing translocation of the tRNAs.

Viomycin, another aminoglycoside antibiotic, was proved to inhibit translocation, but it does not seem to act directly on EF-G. Recent data demonstrated this antibiotic to bind next to an important inter-subunit bridge, driving and blocking the tRNAs in a hybrid state, which does not allow translocation to occur (Ermolenko et al., 2007b).

The antibiotics discussed in this chapter are strong inhibitors of protein synthesis in bacteria. The eukaryotic cytosolic ribosomes are mostly protected from their effects due to the differences in rRNA and r-protein sequences between bacteria and eukaryotes, in the case of aminoglycosides and macrolides (Bottger et al., 2001). For tetracyclines,

these compounds do not reach high enough levels in the eukaryotic cells in order to be inhibitory for the 40S subunit. The mitochondrial ribosomes, on the other hand, are closer in sequence to the bacterial ones, becoming a target for some of the antibiotics (e.g. chloramphenicol).

At the other end of the spectrum, sarcin and ricin are two well studied toxins, which affect both bacterial and eukaryotic cytosolic ribosomes. Sarcin, a fungal toxin, cleaves the rRNA of the large ribosomal subunit between G2661 and A2662 (Wool et al., 1992), while ricin, a plant toxin, removes the base A2660, keeping the phosphate backbone intact (Schindler and Davies, 1977). This region of the ribosome is a universally conserved region, and it was named the sarcin-ricin loop (SRL) because it is the target of these toxins. SRL plays a key role in factor binding to the ribosome, EF-G and EF-Tu being identified by footprinting studies to contact residues A2660 and G2661 (Moazed et al., 1988). After cleavage or modification of SRL, EF-Tu and EF-G are no longer able to associate with the ribosomal complex, halting completely protein synthesis.

### I.4. THE ROLE OF EF-G IN TRANSLOCATION

In one of the earliest studies (Gavrilova et al., 1974), translocation was demonstrated to be an inherit property of the ribosome, 70S ribosomes being able to translocate the tRNAs and mRNA in the absence of EF-G, although extremely slow and requiring special conditions (e.g. certain $Mg^{2+}$ concentration). Interestingly, it was discovered that treating the ribosomes with a cysteine-modifying agent activated the intrinsic activity of the ribosome, although they still translocate slower than in the presence of EF-G (Gavrilova et al., 1974). This phenomenon was believed to be due to the modification of the cysteines in the r-protein S12. A more recent study has shown that S12 is not the only r-protein involved in "factor free" translocation, the ribosome requiring the absence of both S12 and S13 from the structure of 30S subunit for significant spontaneous translocation to occur (Cukras et al., 2003). This observation could be explained by the fact that S12 is making contact with the A site tRNA, while S13 is interacting with the P site tRNA, hence their absence may destabilize the contacts of the tRNAs with the ribosome and facilitate their movement. (Cukras et al., 2003).

In light of all these experiments, one cannot help but ask the question of how does EF-G function in the complex process of translocation. After its purification together with EF-Tu in 1966 (Nishizuka and Lipmann, 1966), EF-G has been the center of multiple studies trying to address its exact role in translocation. Functional experiments have quickly identified it to be able to hydrolyze GTP in the presence of ribosomes, while crystal structures have revealed a five domain protein (Fig. I.5.), with the first domain containing the GTP binding site (AEvarsson et al., 1994; Czworkowski et al., 1994).

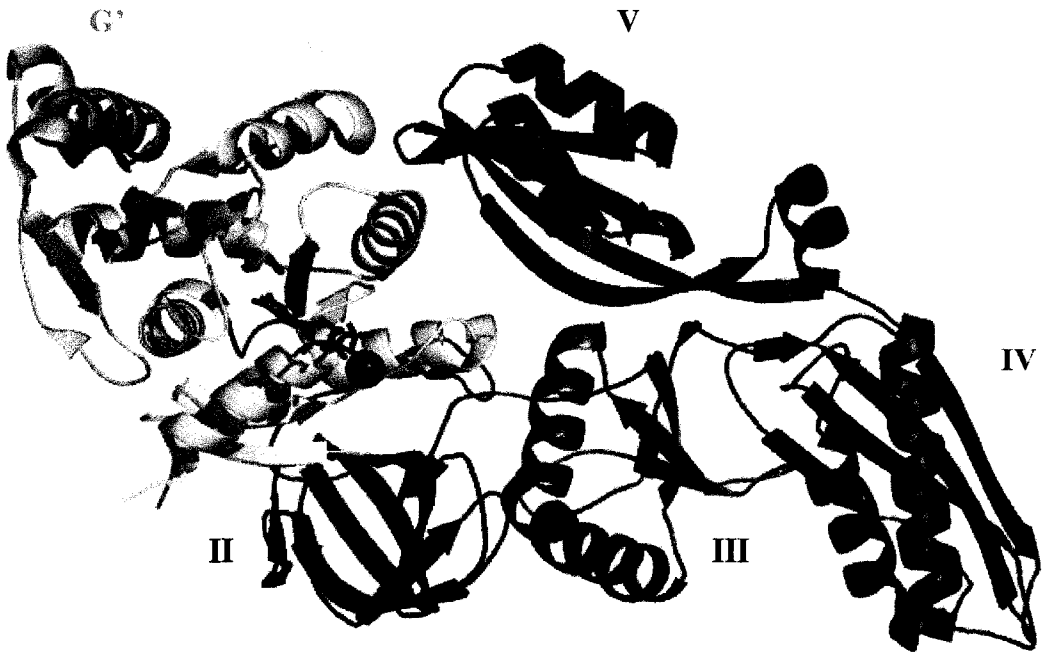


**Fig. I.5. - Cartoon of EF-G structure**. Each domain/subdomain is colored differently. The $Mg^{2+}$ ion is represented as a purple sphere, while the GDP is in blue sticks. Figure was constructed using PyMOL software and it is based on PDB 1FNM. (Laurberg et al., 2000)

The first two domains of EF-G have similar sequences and structures with the first two domains of EF-Tu, with the exception of an insertion into the G domain of EF-G, the G' subdomain. The function of this insertion remained unknown, an initial hypothesis suggesting it may act as an intra-molecular exchange factor for EF-G (AEvarsson et al., 1994), but no experimental proof for such a role was ever obtained. Domain II is a β

barrel domain with mainly structural roles, while domains III-V were determined to be essential for translocation (Martemyanov and Gudkov, 2000; Savelsbergh et al., 2000a).

Interestingly, the structure of EF-G•GDP in solution was noticed to have a similar shape with the structure of the ternary complex formed of EF-Tu, GTP and Phe-tRNA$^{Phe}$, leading to the hypothesis of molecular mimicry (Fig. I.6.) between the tRNA and domains III-V of EF-G (Nissen et al., 1995).

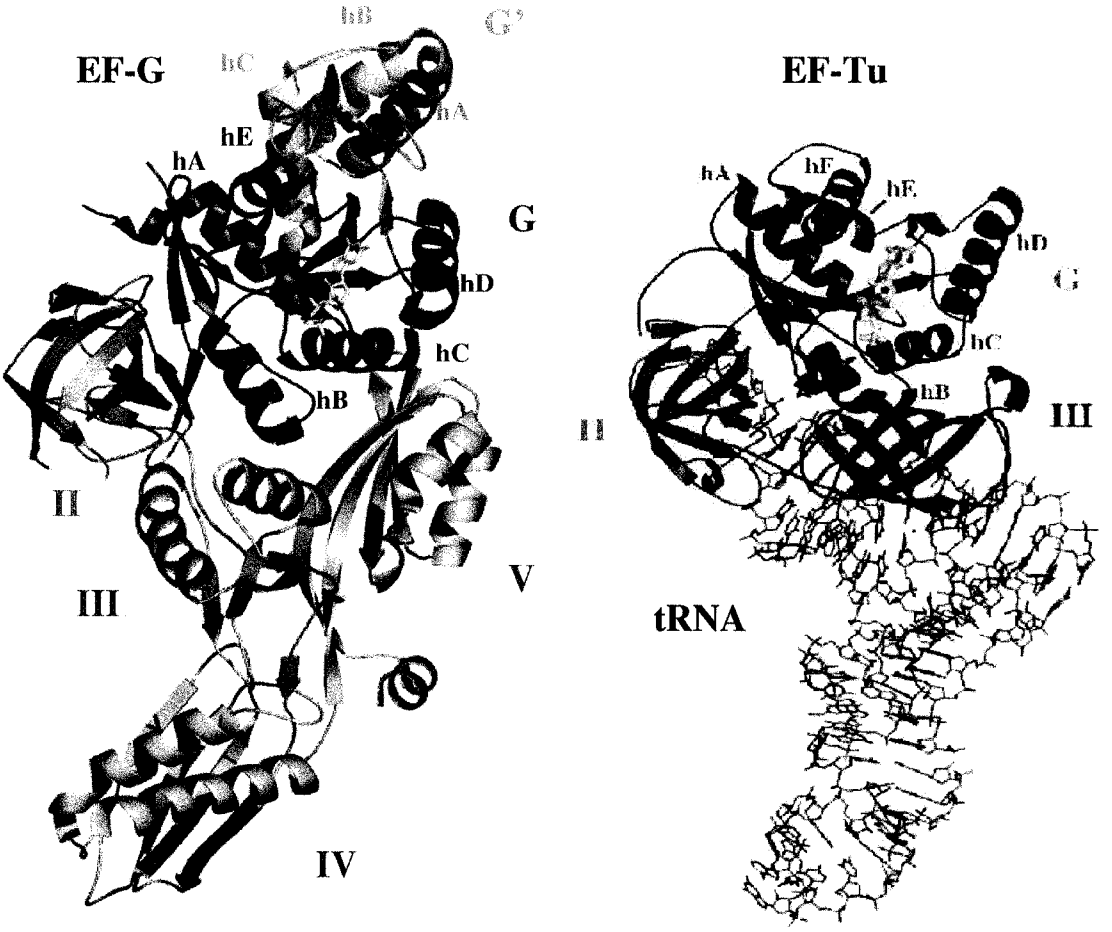


**Fig. I.6. – Cartoon comparing the structures of the ternary complex and EF-G.** The G domains both EF-Tu and EF-G are colored red and domains II are in magenta. Domain III of EF-Tu is represented in cyan, while the G' subdomain of EF-G is in orange. The backbone of tRNA bound to the ternary complex is represented by grey sticks and it is positioned similarly to domains III-V of EF-G, also in grey. Figure was prepared using PyMOL, PDB 1FNM (Laurberg et al., 2000) and PDB 1TTT (Nissen et al., 1995).

Biochemical experiments (Wilson and Noller, 1998), followed by several cryo-EM studies (Agrawal et al., 1999; Agrawal et al., 1998; Valle et al., 2003b) have mapped the position of EF-G in the inter-subunit ribosomal cavity, domains I and V of EF-G interacting with the 50S subunit, domains II and III facing the 30S subunit, while domain IV interacts both with the 30S and 50S subunit. Consistent with the mimicry hypothesis, EF-G was found to bind to the ribosomal complex similarly with the ternary complex, domains I and II occupying an overlapping site (F site) with the first two domains of EF-Tu, while domains III-V of EF-G make similar interactions with the ribosome as the tRNA bound to EF-Tu (Valle et al., 2003a; Valle et al., 2003b).

Research into the translocation mechanism have led to a long standing model hypothesizing that the ribosomal complex switches between a "locked" state, in which the tRNAs are stably bound to their sites, and an "unlocked" state, in which the tRNAs are able to move between sites. Although the ribosome can switch between these two states by itself, only EF-G catalyzes fast translocation of the tRNAs and mRNA, probably by determining conformational changes which "unlock" the ribosomal complex. The effect of EF-G on the ribosomal complex is potentially similar to the effect produced by removing the r-proteins S12 and S13 from the structure of the 30S subunit (Cukras et al., 2003), but the exact details are unknown. Cryo-EM maps of different ribosomal complexes have provided important clues regarding conformational changes of the ribosomal complex during translocation. Their main finding was represented by the ratcheting motion between the two ribosomal subunits, accompanied by the movements of the L1 stalk and the widening of the mRNA tunnel. From the cryo-EM data (Valle et al., 2003b), it seems that the binding of EF-G to the ribosomal complex determines changes in the inter-subunit bridge contacts, with the consequence of forming the hybrid state, in which the tRNAs move in regards to the 50S subunit, but not in the 30S subunit. After GTP hydrolysis by EF-G, the tRNAs and mRNA translocate also in regards to the 30S subunit, the cryo-EM maps observing the reversed motion between the two ribosomal subunits. (Valle et al., 2003b)

One of the regions showing large conformational changes during translocation is represented by the contact area between the head of the 30S subunit and the protuberance of the 50S subunit. At least three inter-subunit bridges from this region change contacts,

three r-proteins (S13, S19 and L5) being involved in this conformational change. EF-G is hypothesized to act as a "wedge", which is inserted in the neck region of the 30S subunit, and causes the rotation of the head and spur of the 30S subunit in regards to the 50S subunit. The axis of this rotation is represented by 16S rRNA helix44 of the 30S subunit, to which EF-G is seen to directly interact with and determine its movement towards the P site. This conformational change in helix 44 is probably helped also by the interaction of domain III of EF-G with the r-protein S12, which in turn contacts helix 44 (Valle et al., 2003b).

The ribosomal complex undergoes complex conformational changes during translocation, some of which were described above. In the same time, EF-G is also believed to change conformations upon binding to the ribosome and during translocation. This was initially suggested by an early study, which showed that fusidic acid is only able to bind to the post-translocational conformation of EF-G (Bodley et al., 1969), but not to free EF-G in solution or in the pre-translocation ribosomal complex. The first description of the conformation of EF-G bound to the ribosome was provided by cryo-EM studies, which showed an extended conformation of this factor on the ribosome as compared to the crystal structure of EF-G (in solution) (AEvarsson et al., 1994; Czworkowski et al., 1994). In order to obtain the structure of EF-G bound to the ribosome, the authors have overlapped the crystal structure of EF-G with the density obtained from the cryo-EM maps, and a good fit was attained by keeping the same position of domains I and II, while translating forward and slightly rotating domains III-V (Valle et al., 2003a).

The translation of domains III-V in regards to domains I and II has as a consequence the creation of a relatively large gap between domains I and V of EF-G (Fig. I.7.), disrupting the previous contacts between these two domains seen in the crystal structure. Although met with some skepticism at first, new functional studies have proven that the ability of domain V of EF-G to break away from domain I is important for this factor, a disulphide bridge uniting these two domains blocking EF-G on the ribosome and preventing its recycling (Peske et al., 2000).

When looking at the conformational changes in EF-G between a pre- and post-translocation state, several experiments showed that domain IV of EF-G occludes the A site of the 30S subunit after translocation (Agrawal et al., 1999; Wilson and Noller,

1998), position previously occupied by the A site tRNA in the pre-translocation complex. This position of domain IV of EF-G seems to be essential for the mechanism of translocation, a mutant of EF-G lacking this domain being inactive in translocation (Savelsbergh et al., 2000a). New studies have also discovered that translocation is a reversible process *in vitro* in the absence of EF-G (Shoji et al., 2006), while this reverse process seems to be catalyzed *in vivo* by a G protein named LepA (Qin et al., 2006). Interestingly, LepA is also structurally related to EF-G, containing similar domains G, 2, 3, and 5, while domain 4 differs between the two factors and LepA does not contain a G' subdomain. These discoveries highlight again the importance of the position of domain IV of EF-G in the A site after translocation has occurred.

It is easy to assume that domain IV probably occupies a different position upon EF-G binding to the pre-translocational ribosome complex. Unfortunately, cryo-EM maps could not be resolved well for a pre- and post-translocation complex, due to low occupancy by EF-G in one of their complexes. Their maps seem to detect well only one of the complexes (initially a post-translocation complex (Agrawal et al., 1999), and more recently a pre-translocation complex (Valle et al., 2003b)). Moreover, their best maps resolutions (around 11Å) do not allow an exact description of the changes in contacts between EF-G and different ribosomal elements, nor the identification of all the ribosomal components that EF-G is interacting with, further studies being needed in order to answer these questions.

A long standing question was raised by the role of GTP hydrolysis in EF-G. Initially, it was believed that EF-G behaves as a classical G protein, being active in complex with GTP (switched on), and becoming inactive upon GTP hydrolysis (switched off). In this model, EF-G•GTP binds to the ribosome and catalyzes translocation, followed by GTP hydrolysis and EF-G•GDP dissociation from the ribosomal complex (for more details see (Kaziro, 1978)). In more recent years, detailed kinetic experiments showed that GTP hydrolysis in EF-G actually precedes translocation, changing the previously inferred order of these processes (Rodnina et al., 1997). In light of this new research, it is now believed that EF-G•GTP binds to the pre-translocation ribosomal complex, followed almost immediately by GTP hydrolysis. Pi release seems to be a slower process than GTP hydrolysis, likely needing certain conformation changes in

domain I of EF-G. Translocation of the tRNAs and mRNA follows Pi release and it is probably caused/accompanied by conformational changes in both the ribosomal complex and EF-G. (for a more detailed review of this model see (Rodnina et al., 2000)) Interestingly, a single round of complete translocation can also be obtained in the presence of non-hydrolyzable GTP analogs, but the rate is approximately 50 times slower as compared to the translocation rate in the presence of GTP (Rodnina et al., 1997), suggesting a direct implication of Pi release in the rate of conformational changes leading to translocation.

Another long standing question in the field deals with the mechanism of GTP hydrolysis by EF-G. For a long time it has been known that EF-G, as well as EF-Tu and other G proteins involved in translation, are only capable of GTP hydrolysis when bound to the proper ribosomal complex. Although both EF-G and EF-Tu bind to overlapping sites on the ribosome, there are many differences when it comes to the activation of GTP hydrolysis between them. GTP hydrolysis in EF-Tu is activated when the proper codon-anticodon interaction is achieved, this factor being only slightly more active when bound to 70S ribosomes in the absence of tRNAs. In the case of EF-G, "naked" 70S (lacking mRNA and tRNAs) activate its GTP hydrolysis ability to the same level as the proper pre-translocation ribosomal complex (Rodnina et al., 1997).

Both EF-G and EF-Tu, as well IF2 and RF3, bind with their G domains to the same ribosomal region, raising the hypothesis that the elements situated in their proximity participate in activating GTP hydrolysis. This region, also known as the GTP activating center, is part of the 50S subunit, being composed of the L7/L12 stalk, the r-protein L11 (and the rRNA elements around it), as well as the SRL.

The r-protein L7/L12 was the first element shown to be essential for GTP hydrolysis by both EF-G and EF-Tu. L7/L12 has unique characteristics among the r-proteins, which will be discussed in detail in the following chapters. A lot of studies have tried to address the mechanism by which this unusual protein is activating GTP hydrolysis. An initial hypothesis thought that its functional role is due to a direct interaction with the domain I of EF-G in the ribosomal complex. This idea seemed to be confirmed by a cryo-EM observation of an arch-like structure, which was originally assigned as connecting the C-terminal of L7/L12 and the G' subdomain of EF-G

(Agrawal et al., 1999), but latter assigned to a contact with the r-protein L11 (Agrawal et al., 2001) and is missing in the recent maps showing EF-G bound to different ribosomal complexes (Valle et al., 2003b). L7/L12 itself is rather elusive to structural studies, being absent in all the crystal structures of the ribosome and ribosomal subunits published so far, as well as missing from the recent high resolution cryo-EM maps (Valle et al., 2003b). One tempting idea would be that L7/L12 may act as a GAP, inserting a lysine finger in the active site of translation factors, similar to RhoGAP or RasGAP. A mutational study trying to address this hypothesis showed that the chosen, universally conserved lysine of L7/L12 was not important for activation of GTP hydrolysis in EF-G and EF-Tu (Savelsbergh et al., 2000b). This however does not rule out the possibility that L7/L12 could be acting through a different mechanism, producing or stabilizing a certain conformational of the active site. One study also reported that L7/L12 is able to directly activate GTP hydrolysis in EF-G by interacting in solution, in the absence of the ribosome (Savelsbergh et al., 2000b), but their results could not be reproduced in our laboratory. More recent studies have revealed a role for L7/L12 in the release of inorganic phosphate after GTP hydrolysis. Although in the crystal structure of EF-G, the Pi is in a solvent exposed region, the authors hypothesize that this becomes closed/hydrophobic upon binding to the ribosome, hence requiring L7/L12 in order to induce a conformational change and facilitate its release (Savelsbergh et al., 2005). Another possible role would be that this protein makes the initial contact and acts as a recruitment part for the translation factors (Diaconu et al., 2005). This is also in line with the fact that L7/L12 has been shown to act as a specificity factor, replacement of L10•L7/L12 complex by the eukaryotic counterparts (P0, P1, P2) allowing bacterial ribosomes to use EF2 (the eukaryotic homologue of EF-G), and vice versa (Uchiumi et al., 1999).

Clarifying the exact role of L7/L12 in activating GTP hydrolysis and describing the exact mechanism by which this r-protein is able to accomplish it, has been challenging, partially due to lack of structural information. Not only is the detailed structure of EF-G in complex with the ribosome not known, but we are also lacking structural information regarding the conformational changes in domain I of EF-G determined by GTP hydrolysis. In the case of EF-Tu, crystal structures of two different

complexes showed the factor to adopt a more extended conformation after GTP hydrolysis. Switch 1 in EF-Tu undergoes a drastic change (Fig. I.7.), changing from a two α helixes structure (GTP state) to an α helix, followed by two small β sheets (GDP complex) (Berchtold et al., 1993).

Due to the similarities between the G domains of EF-G and EF-Tu, it was assumed that similar conformational changes are undertaken by the structure of EF-G. In the case of EF-G, the crystal structures have not been as revealing as for EF-Tu. The initial crystal structures of EF-G did not contain the complete structure of domain III (AEvarsson et al., 1994; Czworkowski et al., 1994), which was only later determined for a point mutant of EF-G, which caused a favorable rotation in the structure (Laurberg et al., 2000). Unfortunately, none of the above mentioned studies was able to determine the structure of switch 1 of EF-G, nor the structure of this factor in complex with GTP, only the GDP solution structure being able to be crystallized. Recently, an EF-G homologue was crystallized in complex with GTP, all the structural elements being present this time (Connell et al., 2007).

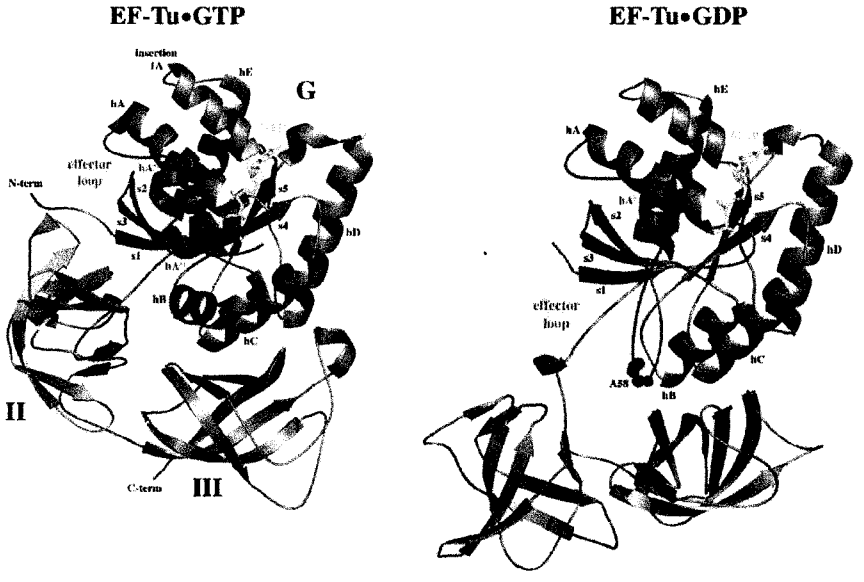


**Fig. I.7. – Comparison between the GTP and GDP crystal structures of EF-Tu.** Switch 1 is colored in cyan. Helix A" of the effector loop from panel A turns into two short beta sheets in panel B, with the residue A58 undergoing the largest movement. Figure was prepared using PyMOL, PDB 1EXM (Berchtold et al., 1993) and PDB 1EFC (Song et al., 1999).

The functional studies on GTP hydrolysis were also difficult due to the unknowns regarding the catalytic mechanism of GTP hydrolysis in EF-G. For EF-Tu, a hypothetical mechanism was designed based on functional and structural studies on EF-Tu, as well as on other G proteins. A water molecule is supposed to attack the γ phosphate with the help of His85, which could stabilize/activate it. This attack would be also facilitated by the movement of Ile61 and Val20 (opening of the hydrophobic barrier) and the stabilization of the position of the γ phosphate by Arg59. The pKa of the His85 could be also affected by the presence of Asp87, which would come in close proximity after the disruption of the previous salt bridge with Arg59. (Sprinzl et al., 2000)

Although EF-G was initially believed to have a similar mechanism, mutating Arg59 did not yield expected results, showing it to be essential for ribosome binding, but not for catalysis (Mohr et al., 2000). It is debatable at this point if the mechanism of GTP hydrolysis is identical in EF-Tu and EF-G, in spite of their structural similarities between their G domains and their similar interactions with the ribosomal complex. A mutation study has attempted to replace the entire switch 1 of EF-G with the sequence from EF-Tu, but the resulting protein was inactive, suggesting that although the sequences may be similar, small differences may have bigger consequences than it was originally anticipated (Kolesnikov and Gudkov, 2002).

To summarize, further studies are needed in order to elucidate the mechanism of translocation, conformational changes induced in EF-G and the ribosomal complex by GTP hydrolysis, as well as the activation of GTP hydrolysis by the ribosomal complex.

## I.5. THESIS OVERVIEW

In order to elucidate further the position of EF-G in the ribosomal cavity and to identify its interaction partners, two different crosslinking techniques were used. Firstly, an arginine specific chemical crosslinker was used to screen the r-proteins situated in close proximity to EF-G when it is bound to two different ribosomal complexes. This study identified several r-proteins, among which S12, L6, L7/L12, and L14 were also confirmed by subsequent immunoblotting experiments. Secondly, a library of single cysteine mutants was employed to determine site specific crosslinks to the previously identified r-proteins. From the 22 EF-G cysteine mutants used in this study, we obtained

five positive crosslinking results: residues 209 and 231 (G' subdomain) crosslinked to the r-protein L7/L12, residues 426 (domain III) crosslinked to the r-protein S12, and residues 627 and 637 (domain V) crosslinked to the r-protein L6. The functional implications of the proximity between different domains of EF-G and these r-proteins are also discussed in detail (Chapter II).

Due to its involvement in activating GTP hydrolysis, further attention was concentrated on the interaction between EF-G and L7/L12. Initially, cysteine probing studies were employed to determine whether or not residues 209 and 231 are protected by L7/L12. Both of this residues were demonstrated to be solvent exposed in both ribosomal complexes attempted, signifying that although they may be close to the interaction surface between EF-G and L7/L12, they are not part of it. Next, we used seven additional cysteine mutants to better define the interaction region. As a result of this new crosslinking study, L7/L12 was proven to also be close to helix B of the G' subdomain and the N-terminus of helix C. (Chapter III).

In order to explore further the mechanism of GTP hydrolysis and the involvement of the r-protein L7/L12, functional mutants were constructed in EF-G by mutating three conserved residues in the G' subdomain: 224, 228, and 231. These EF-G proteins were functionally assessed in steady state and pre-steady state assays, for both GTP hydrolysis and translocation capabilities. These functional results shed more light into the complex mechanism of GTP hydrolysis activation. (Chapter IV)

All these results taken together advance our knowledge of the interactions of EF-G with the r-proteins, shed more light on the details of the interaction between EF-G and the r-protein L7/L12, in particular, as well as on the role of this r-protein in activation of GTP hydrolysis in EF-G.

## I.6. REFERENCES

Addlagatta, A., Quillin, M. L., Omotoso, O., Liu, J. O., and Matthews, B. W. (2005). Identification of an SH3-binding motif in a new class of methionine aminopeptidases from *Mycobacterium tuberculosis* suggests a mode of interaction with the ribosome. Biochemistry *44*, 7166-7174.

AEvarsson, A., Brazhnikov, E., Garber, M., Zheltonosova, J., Chirgadze, Y., al-Karadaghi, S., Svensson, L. A., and Liljas, A. (1994). Three-dimensional structure of the

ribosomal translocase: elongation factor G from *Thermus thermophilus*. EMBO J *13*, 3669-3677.

Agrawal, R. K., Heagle, A. B., Penczek, P., Grassucci, R. A., and Frank, J. (1999). EF-G-dependent GTP hydrolysis induces translocation accompanied by large conformational changes in the 70S ribosome. Nat Struct Biol *6*, 643-647.

Agrawal, R. K., Linde, J., Sengupta, J., Nierhaus, K. H., and Frank, J. (2001). Localization of L11 protein on the ribosome and elucidation of its involvement in EF-G-dependent translocation. J Mol Biol *311*, 777-787.

Agrawal, R. K., Penczek, P., Grassucci, R. A., and Frank, J. (1998). Visualization of elongation factor G on the *Escherichia coli* 70S ribosome: the mechanism of translocation. Proc Natl Acad Sci U S A *95*, 6134-6138.

Allen, G. S., Zavialov, A., Gursky, R., Ehrenberg, M., and Frank, J. (2005). The cryo-EM structure of a translation initiation complex from *Escherichia coli*. Cell *121*, 703-712.

Arai, N., Arai, K., and Kaziro, Y. (1975). Formation of a binary complex between elongation factor G and guanine nucleotides. J Biochem (Tokyo) *78*, 243-246.

Berchtold, H., Reshetnikova, L., Reiser, C. O., Schirmer, N. K., Sprinzl, M., and Hilgenfeld, R. (1993). Crystal structure of active elongation factor Tu reveals major domain rearrangements. Nature *365*, 126-132.

Bingel-Erlenmeyer, R., Kohler, R., Kramer, G., Sandikci, A., Antolic, S., Maier, T., Schaffitzel, C., Wiedmann, B., Bukau, B., and Ban, N. (2008). A peptide deformylase-ribosome complex reveals mechanism of nascent chain processing. Nature *452*, 108-111.

Bodley, J. W., Zieve, F. J., Lin, L., and Zieve, S. T. (1969). Formation of the ribosome-G factor-GDP complex in the presence of fusidic acid. Biochem Biophys Res Commun *37*, 437-443.

Boni, I. V., Isaeva, D. M., Musychenko, M. L., and Tzareva, N. V. (1991). Ribosome-messenger recognition: mRNA target sites for ribosomal protein S1. Nucleic Acids Res *19*, 155-162.

Bottger, E. C., Springer, B., Prammananan, T., Kidan, Y., and Sander, P. (2001). Structural basis for selectivity and toxicity of ribosomal antibiotics. EMBO Rep *2*, 318-323.

Brodersen, D. E., Clemons, W. M., Jr., Carter, A. P., Morgan-Warren, R. J., Wimberly, B. T., and Ramakrishnan, V. (2000). The structural basis for the action of the antibiotics tetracycline, pactamycin, and hygromycin B on the 30S ribosomal subunit. Cell *103*, 1143-1154.

Cameron, D. M., Thompson, J., March, P. E., and Dahlberg, A. E. (2002). Initiation factor IF2, thiostrepton and micrococcin prevent the binding of elongation factor G to the *Escherichia coli* ribosome. J Mol Biol *319*, 27-35.

Carter, A. P., Clemons, W. M., Brodersen, D. E., Morgan-Warren, R. J., Wimberly, B. T., and Ramakrishnan, V. (2000). Functional insights from the structure of the 30S ribosomal subunit and its interactions with antibiotics. Nature *407*, 340-348.

Carter, A. P., Clemons, W. M., Jr., Brodersen, D. E., Morgan-Warren, R. J., Hartsch, T., Wimberly, B. T., and Ramakrishnan, V. (2001). Crystal structure of an initiation factor bound to the 30S ribosomal subunit. Science *291*, 498-501.

Chambers, I., Frampton, J., Goldfarb, P., Affara, N., McBain, W., and Harrison, P. R. (1986). The structure of the mouse glutathione peroxidase gene: the selenocysteine in the active site is encoded by the 'termination' codon, TGA. EMBO J *5*, 1221-1227.

Coleman, J., Inouye, M., and Nakamura, K. (1985). Mutations upstream of the ribosome-binding site affect translational efficiency. J Mol Biol *181*, 139-143.

Connell, S. R., Takemoto, C., Wilson, D. N., Wang, H., Murayama, K., Terada, T., Shirouzu, M., Rost, M., Schuler, M., Giesebrecht, J., *et al.* (2007). Structural basis for interaction of the ribosome with the switch regions of GTP-bound elongation factors. Mol Cell *25*, 751-764.

Craig, E. A., Eisenman, H. C., and Hundley, H. A. (2003). Ribosome-tethered molecular chaperones: the first line of defense against protein misfolding? Curr Opin Microbiol *6*, 157-162.

Cukras, A. R., Southworth, D. R., Brunelle, J. L., Culver, G. M., and Green, R. (2003). Ribosomal proteins S12 and S13 function as control elements for translocation of the mRNA:tRNA complex. Mol Cell *12*, 321-328.

Czworkowski, J., Wang, J., Steitz, T. A., and Moore, P. B. (1994). The crystal structure of elongation factor G complexed with GDP, at 2.7Å resolution. EMBO J *13*, 3661-3668.

Diaconu, M., Kothe, U., Schlunzen, F., Fischer, N., Harms, J. M., Tonevitsky, A. G., Stark, H., Rodnina, M. V., and Wahl, M. C. (2005). Structural basis for the function of the ribosomal L7/12 stalk in factor binding and GTPase activation. Cell *121*, 991-1004.

Douda, J. A., and Sarnow, P. (2007). Translation Initiation by Viral Internal Ribosome Entry Sites, In Translational Control in Biology and Medicine, M. B. Mathews, N. Sonenberg, and J. W. B. Hershey, eds. (New York: John Inglis), pp. 934.

Ellgaard, L., and Frickel, E. M. (2003). Calnexin, calreticulin, and ERp57: teammates in glycoprotein folding. Cell Biochem Biophys *39*, 223-247.

Ermolenko, D. N., Majumdar, Z. K., Hickerson, R. P., Spiegel, P. C., Clegg, R. M., and Noller, H. F. (2007a). Observation of intersubunit movement of the ribosome in solution using FRET. J Mol Biol *370*, 530-540.

Ermolenko, D. N., Spiegel, P. C., Majumdar, Z. K., Hickerson, R. P., Clegg, R. M., and Noller, H. F. (2007b). The antibiotic viomycin traps the ribosome in an intermediate state of translocation. Nat Struct Mol Biol *14*, 493-497.

Francois, B., Russell, R. J., Murray, J. B., Aboul-ela, F., Masquida, B., Vicens, Q., and Westhof, E. (2005). Crystal structures of complexes between aminoglycosides and decoding A site oligonucleotides: role of the number of rings and positive charges in the specific binding leading to miscoding. Nucleic Acids Res *33*, 5677-5690.

Frank, J., and Agrawal, R. K. (2000). A ratchet-like inter-subunit reorganization of the ribosome during translocation. Nature *406*, 318-322.

Gao, N., Zavialov, A. V., Li, W., Sengupta, J., Valle, M., Gursky, R. P., Ehrenberg, M., and Frank, J. (2005). Mechanism for the disassembly of the posttermination complex inferred from cryo-EM studies. Mol Cell *18*, 663-674.

Gavrilova, L. P., Koteliansky, V. E., and Spirin, A. S. (1974). Ribosomal protein S12 and 'non-enzymatic' translocation. FEBS Lett *45*, 324-328.

Gromadski, K. B., and Rodnina, M. V. (2004a). Kinetic determinants of high-fidelity tRNA discrimination on the ribosome. Mol Cell *13*, 191-200.

Gromadski, K. B., and Rodnina, M. V. (2004b). Streptomycin interferes with conformational coupling between codon recognition and GTPase activation on the ribosome. Nat Struct Mol Biol *11*, 316-322.

Harms, J. M., Schlunzen, F., Fucini, P., Bartels, H., and Yonath, A. (2004). Alterations at the peptidyl transferase centre of the ribosome induced by the synergistic action of the streptogramins dalfopristin and quinupristin. BMC Biol *2*, 4.

Herbert, T. P., and Proud, C. G. (2007). Regulation of Translation Elongation and the Cotranslational protein Targeting Pathways, In Translational Control in Biology and Medicine, M. B. Mathews, N. Sonenberg, and J. W. B. Hershey, eds. (New York: John Inglis), pp. 934.

Johanson, U., and Hughes, D. (1994). Fusidic acid-resistant mutants define three regions in elongation factor G of *Salmonella typhimurium*. Gene *143*, 55-59.

Kaziro, Y. (1978). The role of guanosine 5'-triphosphate in polypeptide chain elongation. Biochim Biophys Acta *505*, 95-127.

Kolesnikov, A., and Gudkov, A. (2002). Elongation factor G with effector loop from elongation factor Tu is inactive in translocation. FEBS Lett *514*, 67-69.

Kondo, J., Francois, B., Russell, R. J., Murray, J. B., and Westhof, E. (2006). Crystal structure of the bacterial ribosomal decoding site complexed with amikacin containing the gamma-amino-alpha-hydroxybutyryl (haba) group. Biochimie *88*, 1027-1031.

Lancaster, L., Kiel, M. C., Kaji, A., and Noller, H. F. (2002). Orientation of ribosome recycling factor in the ribosome from directed hydroxyl radical probing. Cell *111*, 129-140.

Laurberg, M., Kristensen, O., Martemyanov, K., Gudkov, A. T., Nagaev, I., Hughes, D., and Liljas, A. (2000). Structure of a mutant EF-G reveals domain III and possibly the fusidic acid binding site. J Mol Biol *303*, 593-603.

Laursen, B. S., Sorensen, H. P., Mortensen, K. K., and Sperling-Petersen, H. U. (2005). Initiation of protein synthesis in bacteria. Microbiol Mol Biol Rev *69*, 101-123.

Loftfield, R. B., and Vanderjagt, D. (1972). The frequency of errors in protein biosynthesis. Biochem J *128*, 1353-1356.

Martemyanov, K. A., and Gudkov, A. T. (2000). Domain III of elongation factor G from *Thermus thermophilus* is essential for induction of GTP hydrolysis on the ribosome. J Biol Chem *275*, 35820-35824.

Matassova, N. B., Rodnina, M. V., Endermann, R., Kroll, H. P., Pleiss, U., Wild, H., and Wintermeyer, W. (1999). Ribosomal RNA is the target for oxazolidinones, a novel class of translational inhibitors. RNA *5*, 939-946.

McClain, W. H. (1993). Rules that govern tRNA identity in protein synthesis. J Mol Biol *234*, 257-280.

Meunier, L., Usherwood, Y. K., Chung, K. T., and Hendershot, L. M. (2002). A subset of chaperones and folding enzymes form multiprotein complexes in endoplasmic reticulum to bind nascent proteins. Mol Biol Cell *13*, 4456-4469.

Moazed, D., and Noller, H. F. (1989). Intermediate states in the movement of transfer RNA in the ribosome. Nature *342*, 142-148.

Moazed, D., Robertson, J. M., and Noller, H. F. (1988). Interaction of elongation factors EF-G and EF-Tu with a conserved loop in 23S RNA. Nature *334*, 362-364.

Mohr, D., Wintermeyer, W., and Rodnina, M. V. (2000). Arginines 29 and 59 of elongation factor G are important for GTP hydrolysis or translocation on the ribosome. EMBO J *19*, 3458-3464.

Munro, J. B., Altman, R. B., O'Connor, N., and Blanchard, S. C. (2007). Identification of two distinct hybrid state intermediates on the ribosome. Mol Cell *25*, 505-517.

Nishizuka, Y., and Lipmann, F. (1966). Comparison of guanosine triphosphate split and polypeptide synthesis with a purified *E. coli* system. Proc Natl Acad Sci U S A *55*, 212-219.

Nissen, P., Hansen, J., Ban, N., Moore, P. B., and Steitz, T. A. (2000). The structural basis of ribosome activity in peptide bond synthesis. Science *289*, 920-930.

Nissen, P., Kjeldgaard, M., Thirup, S., Polekhina, G., Reshetnikova, L., Clark, B. F., and Nyborg, J. (1995). Crystal structure of the ternary complex of Phe-tRNA$^{Phe}$, EF-Tu, and a GTP analog. Science *270*, 1464-1472.

Ogle, J. M., Brodersen, D. E., Clemons, W. M., Jr., Tarry, M. J., Carter, A. P., and Ramakrishnan, V. (2001). Recognition of cognate transfer RNA by the 30S ribosomal subunit. Science *292*, 897-902.

Ogle, J. M., Murphy, F. V., Tarry, M. J., and Ramakrishnan, V. (2002). Selection of tRNA by the ribosome requires a transition from an open to a closed form. Cell *111*, 721-732.

Parmeggiani, A., and Nissen, P. (2006). Elongation factor Tu-targeted antibiotics: four different structures, two mechanisms of action. FEBS Lett *580*, 4576-4581.

Peske, F., Matassova, N. B., Savelsbergh, A., Rodnina, M. V., and Wintermeyer, W. (2000). Conformationally restricted elongation factor G retains GTPase activity but is inactive in translocation on the ribosome. Mol Cell *6*, 501-505.

Pestova, T. V., Lorsch, J. R., and Hellen, C. U. T. (2007). The Mechanism of Translation Initiation in Eukaryotes, In Translational Control in Biology and Medicine, M. B. Mathews, N. Sonenberg, and J. W. B. Hershey, eds. (New York: John Inglis), pp. 934.

Piepenburg, O., Pape, T., Pleiss, J. A., Wintermeyer, W., Uhlenbeck, O. C., and Rodnina, M. V. (2000). Intact aminoacyl-tRNA is required to trigger GTP hydrolysis by elongation factor Tu on the ribosome. Biochemistry *39*, 1734-1738.

Qin, Y., Polacek, N., Vesper, O., Staub, E., Einfeldt, E., Wilson, D. N., and Nierhaus, K. H. (2006). The highly conserved LepA is a ribosomal elongation factor that back-translocates the ribosome. Cell *127*, 721-733.

Rodnina, M. V., Beringer, M., and Wintermeyer, W. (2007). How ribosomes make peptide bonds. Trends Biochem Sci *32*, 20-26.

Rodnina, M. V., Gromadski, K. B., Kothe, U., and Wieden, H. J. (2005). Recognition and selection of tRNA in translation. FEBS Lett *579*, 938-942.

Rodnina, M. V., Savelsbergh, A., Katunin, V. I., and Wintermeyer, W. (1997). Hydrolysis of GTP by elongation factor G drives tRNA movement on the ribosome. Nature *385*, 37-41.

Rodnina, M. V., Savelsbergh, A., Matassova, N. B., Katunin, V. I., Semenkov, Y. P., and Wintermeyer, W. (1999). Thiostrepton inhibits the turnover but not the GTPase of elongation factor G on the ribosome. Proc Natl Acad Sci U S A *96*, 9586-9590.

Rodnina, M. V., Stark, H., Savelsbergh, A., Wieden, H. J., Mohr, D., Matassova, N. B., Peske, F., Daviter, T., Gualerzi, C. O., and Wintermeyer, W. (2000). GTPases mechanisms and functions of translation factors on the ribosome. Biol Chem *381*, 377-387.

Savelsbergh, A., Matassova, N. B., Rodnina, M. V., and Wintermeyer, W. (2000a). Role of domains 4 and 5 in elongation factor G functions on the ribosome. J Mol Biol *300*, 951-961.

Savelsbergh, A., Mohr, D., Kothe, U., Wintermeyer, W., and Rodnina, M. V. (2005). Control of phosphate release from elongation factor G by ribosomal protein L7/12. EMBO J *24*, 4316-4323.

Savelsbergh, A., Mohr, D., Wilden, B., Wintermeyer, W., and Rodnina, M. V. (2000b). Stimulation of the GTPase activity of translation elongation factor G by ribosomal protein L7/12. J Biol Chem *275*, 890-894.

Schilling-Bartetzko, S., Franceschi, F., Sternbach, H., and Nierhaus, K. H. (1992). Apparent association constants of tRNAs for the ribosomal A, P, and E sites. J Biol Chem *267*, 4693-4702.

Schindler, D. G., and Davies, J. E. (1977). Specific cleavage of ribosomal RNA caused by alpha sarcin. Nucleic Acids Res *4*, 1097-1110.

Schlunzen, F., Zarivach, R., Harms, J., Bashan, A., Tocilj, A., Albrecht, R., Yonath, A., and Franceschi, F. (2001). Structural basis for the interaction of antibiotics with the peptidyl transferase centre in eubacteria. Nature *413*, 814-821.

Schmeing, T. M., Huang, K. S., Kitchen, D. E., Strobel, S. A., and Steitz, T. A. (2005). Structural insights into the roles of water and the 2' hydroxyl of the P site tRNA in the peptidyl transferase reaction. Mol Cell *20*, 437-448.

Schuwirth, B. S., Borovinskaya, M. A., Hau, C. W., Zhang, W., Vila-Sanjurjo, A., Holton, J. M., and Cate, J. H. (2005). Structures of the bacterial ribosome at 3.5Å resolution. Science *310*, 827-834.

Schuwirth, B. S., Day, J. M., Hau, C. W., Janssen, G. R., Dahlberg, A. E., Cate, J. H., and Vila-Sanjurjo, A. (2006). Structural analysis of kasugamycin inhibition of translation. Nat Struct Mol Biol *13*, 879-886.

Selmer, M., Al-Karadaghi, S., Hirokawa, G., Kaji, A., and Liljas, A. (1999). Crystal structure of *Thermotoga maritima* ribosome recycling factor: a tRNA mimic. Science *286*, 2349-2352.

Shoji, S., Walker, S. E., and Fredrick, K. (2006). Reverse translocation of tRNA in the ribosome. Mol Cell *24*, 931-942.

Song, H., Parsons, M. R., Rowsell, S., Leonard, G., and Phillips, S. E. (1999). Crystal structure of intact elongation factor EF-Tu from *Escherichia coli* in GDP conformation at 2.05Å resolution. J Mol Biol *285*, 1245-1256.

Spirin, A. (1999). Ribosomes (New York: Kluwer Academic/Plenum).

Spirin, A. S. (2004). The ribosome as an RNA-based molecular machine. RNA Biol *1*, 3-9.

Sprinzl, M., Brock, S., Huang, Y., Milovnik, P., Nanninga, M., Nesper-Brock, M., Rutthard, H., and Szkaradkiewicz, K. (2000). Regulation of GTPases in the bacterial translation machinery. Biol Chem *381*, 367-375.

Takyar, S., Hickerson, R. P., and Noller, H. F. (2005). mRNA helicase activity of the ribosome. Cell *120*, 49-58.

Uchiumi, T., Hori, K., Nomura, T., and Hachimori, A. (1999). Replacement of L7/L12.L10 protein complex in *Escherichia coli* ribosomes with the eukaryotic counterpart changes the specificity of elongation factor binding. J Biol Chem *274*, 27578-27582.

Uemura, S., Dorywalska, M., Lee, T. H., Kim, H. D., Puglisi, J. D., and Chu, S. (2007). Peptide bond formation destabilizes Shine-Dalgarno interaction on the ribosome. Nature *446*, 454-457.

Valle, M., Zavialov, A., Li, W., Stagg, S. M., Sengupta, J., Nielsen, R. C., Nissen, P., Harvey, S. C., Ehrenberg, M., and Frank, J. (2003a). Incorporation of aminoacyl-tRNA into the ribosome as seen by cryo-electron microscopy. Nat Struct Biol *10*, 899-906.

Valle, M., Zavialov, A., Sengupta, J., Rawat, U., Ehrenberg, M., and Frank, J. (2003b). Locking and unlocking of ribosomal motions. Cell *114*, 123-134.

Wilden, B., Savelsbergh, A., Rodnina, M. V., and Wintermeyer, W. (2006). Role and timing of GTP binding and hydrolysis during EF-G-dependent tRNA translocation on the ribosome. Proc Natl Acad Sci U S A *103*, 13670-13675.

Wilson, K. S., and Noller, H. F. (1998). Mapping the position of translational elongation factor EF-G in the ribosome by directed hydroxyl radical probing. Cell *92*, 131-139.

Wool, I. G., Gluck, A., and Endo, Y. (1992). Ribotoxin recognition of ribosomal RNA and a proposal for the mechanism of translocation. Trends Biochem Sci *17*, 266-269.

Yusupov, M. M., Yusupova, G. Z., Baucom, A., Lieberman, K., Earnest, T. N., Cate, J. H., and Noller, H. F. (2001). Crystal structure of the ribosome at 5.5 Å resolution. Science *292*, 883-896.

Yusupova, G. Z., Yusupov, M. M., Cate, J. H., and Noller, H. F. (2001). The path of messenger RNA through the ribosome. Cell *106*, 233-241.

Zavialov, A. V., and Ehrenberg, M. (2003). Peptidyl-tRNA regulates the GTPase activity of translation factors. Cell *114*, 113-122.

Zavialov, A. V., Hauryliuk, V. V., and Ehrenberg, M. (2005). Guanine-nucleotide exchange on ribosome-bound elongation factor G initiates the translocation of tRNAs. J Biol *4*, 9.

Zinoni, F., Birkmann, A., Leinfelder, W., and Bock, A. (1987). Cotranslational insertion of selenocysteine into formate dehydrogenase from *Escherichia coli* directed by a UGA codon. Proc Natl Acad Sci U S A *84*, 3156-3160.

# II. TWO DIFFERENT CROSSLINKING TECHNIQUES IDENTIFY R-PROTEINS SITUATED IN CLOSE PROXIMITY TO EF-G WHEN THIS FACTOR IS BOUND TO THE BACTERIAL RIBOSOME[1]

[1] A version of this chapter was published in Nechifor, R., and Wilson, KS "Crosslinking of translation factor EF-G to proteins of the bacterial ribosome before and after translocation", J Mol Biol, 18 May 2007, 368 (5): 1412-1425.

## II.1. INTRODUCTION

EF-G catalyzes fast and accurate translocation, the process consisting of concerted movement of the tRNAs inside the ribosomal cavity, as well as the mRNA connected to them. This function is accomplished as a close cooperation between EF-G and the ribosome, involving a complex interplay of conformational changes of the two ribosomal subunits, which are activated by EF-G•GTP binding to the ribosomal complex and driven forward by GTP hydrolysis (see Chapter I for further details).

In order to advance further our understanding of the mechanism of translocation, a first and essential step is the identification of the key players involved in this process, namely all the elements participating in the interaction between EF-G and the ribosomal complex. Previous structural studies have tried to address this question, using biochemical and cryo-EM techniques (Agrawal et al., 1999; Agrawal et al., 1998; Valle et al., 2003; Wilson and Nechifor, 2004; Wilson and Noller, 1998).

Initially, biochemical techniques were used to identify the rRNA elements situated close to, and potentially interacting with EF-G in a post-translocation complex. To that end, Fe(II) was tethered to a library of single cysteine EF-G mutants using BABE, a cysteine specific EDTA derivative, followed by trapping the modified EF-G proteins to a post-translocational ribosomal complex, and activation of hydroxyl radicals. The rRNA elements positioned next to each individual cysteine were cleaved by hydroxyl radicals, and the cleavage sites were identified by primer extension (Wilson and Noller, 1998). Some of the conformational differences of the ribosomal complex between a pre- and post-translocation state were also identified using a complementary approach, taking advantage of the hydroxyl radical producing capabilities of Fe(II)-EDTA free in solution. (Wilson and Nechifor, 2004).

EF-G was also visualized on different ribosomal complexes by cryo-EM reconstructions, which used the known crystal structures of EF-G and ribosomal subunits to identify the detected electron densities (Agrawal et al., 1999; Agrawal et al., 1998; Valle et al., 2003). These studies attempted to describe conformational changes both in EF-G and in the ribosome, but the resolution of their structures did not allow the unambiguous identification of the ribosomal elements which interact with EF-G, especially inside the ribosomal cavity where it was more difficult to separate the electron

densities. Another problem encountered was their inability to properly visualize the EF-G electron densities in both pre- and post-translocational states, one of these complexes showing a lower occupancy by EF-G. The identity of the lower occupied complex has also changed between different cryo-EM studies.

An interesting feature of the initial complexes was the visualization of an arc-like structure between domain I of EF-G and the ribosome in a post-translocational complex, which was interpreted as an interaction between L7/L12 and the G' subdomain of EF-G (Agrawal et al., 1999). A later study assigned the same connection to an interaction between the r-protein L11 and the G domain of EF-G (Agrawal et al., 2001), while more recent studies could not identify this connection or a density for the r-protein L7/L12 (Gao et al., 2003; Valle et al., 2003). Due to all these uncertainties, further studies are needed to explore the interaction between EF-G and ribosome.

The translation factors IF3, EF-Tu, EF-G, and RF3 bind to the ribosome in a common area, the F site. This region is particularly rich in r-proteins, some of them playing important functional roles (e.g. L7/L12 in activation of GTP hydrolysis). Hence, we decided to focus our efforts on identifying the interactions between EF-G and r-proteins using crosslinking techniques. Previous crosslinking studies tried to address this question, with various and often times contradictory results (Girshovich et al., 1981; Maassen and Moller, 1974; Maassen and Moller, 1978; Maassen and Moller, 1981; Skold, 1982). Many of the r-proteins identified in these studies are very hard, if not impossible to reconcile with the known structures of the ribosome and EF-G. Another problem worth noting is the fact that the ribosomal complexes used in these studies were not functionally characterized, so the probed state was unknown.

We initially screened all the r-proteins situated in close proximity to EF-G when it is bound to the ribosomal complex by using a non-specific chemical crosslinker. This initial study was followed by a site-specific crosslinking study, which specifically identified the elements of EF-G situated in close proximity to the r-proteins. The crosslinked products were analyzed by mass spectrometry, which identified the r-proteins crosslinked to EF-G. The mass spectrometry identification was later confirmed by immuno-blotting. In our experiments, we tested both a pre and post-translocation

complex, in order to be able to describe any conformational changes undergone by EF-G and/or the ribosome during translocation.

## II.2. RESULTS

Our structural studies are helped by the fact that EF-G can be trapped on the ribosome in a pre-translocation complex, using a non-hydrolyzable GTP analog (GDPNP), and in a post-translocational complex, using the antibiotic fusidic acid and GTP (Wilson and Nechifor, 2004). In the presence of fusidic acid, EF-G•GTP binds to the ribosomal complex, hydrolyzes GTP and translocates the tRNAs and mRNA, but EF-G•GDP cannot dissociate from the ribosomal complex (Bodley et al., 1969).

All our crosslinking reactions were separated by SDS-PAGE and analyzed initially by staining with Coomassie brilliant blue. The crosslinking products of EF-G with any r-protein were identified by comparison with the negative controls, taking advantage also of the fact that EF-G is larger than any r-protein, hence both EF-G and its crosslinking products will separate clearly from the r-proteins.

### II.2.1. Non-site specific chemical crosslinking of EF-G to the r-proteins

For the initial crosslinking screen, we chose disuccinimidyl glutarate (DSG), a lysine specific homo-bifunctional crosslinker. DSG specifically reacts with primary amines at pH higher than 7 through its two succinimydyl ester groups, forming two different carboxamides. As a result, the side chains of two lysine residues will be connected by a covalent link, less than 8Å long (the approximate length of fully extended crosslinker arm – Fig. II.2B). Most of the r-proteins are positively charged and have a large number of lysines, providing the crosslinker with increased number of targets. In spite of being an overall negatively charged protein, EF-G also contains a fair number of lysines (44 in our *E. coli* protein) distributed among all its five domains, the majority of them being solvent exposed.

In order to be able to detect conformational changes during translocation, two different EF-G•70S•mRNA•tRNAs complexes (Fig. II.1.) were assembled: (1) *GDPNP complex*, in which EF-G is trapped on the ribosomal complex by GDPNP; this complex corresponds to a state before the translocation of the mRNA and of the tRNAs in regards

to the 30S subunit has occurred; (2) *fus complex*, in which EF-G is trapped on the ribosomal complex in the GDP state by a combination of fusidic acid and GTP; this complex corresponds to a post-translocation state (Wilson and Nechifor, 2004).

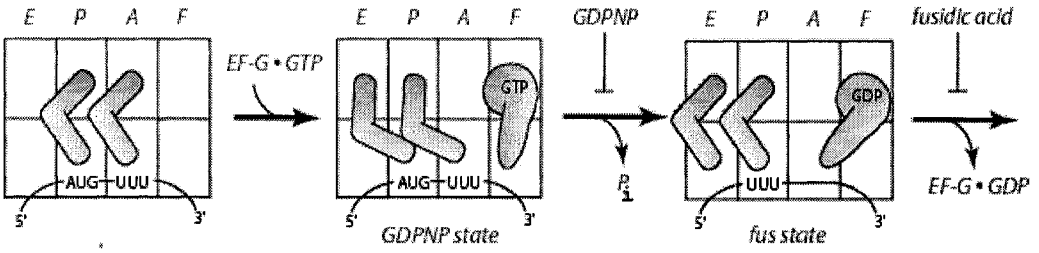


**Fig. II.1. - Cartoon representing the functional states of the EF-G•70S complexes probed in the crosslinking experiments.** Reproduced from (Wilson and Nechifor, 2004).

The functional state of the prepared complexes was tested using the toe-printing method, which monitors the position of the mRNA in regards to the 30S subunit by the extension of a primer annealed to the 3' end of the mRNA (Hartz et al., 1988). The pre-translocation complex is represented by a duplex consisting of two products, corresponding to positions +16 and +17 on the mRNA. The reason for the presence of this duplex is not clear, but it is likely to be due to two different conformations of the ribosomal complex. Upon translocation, the +16 toe-printing product becomes shorter by 3 nucleotides, moving to position +19, and it is easily separated by urea-acrylamide gels (Joseph and Noller, 1998). As seen in Fig. II.2A, the control ribosomal complex, lacking EF-G, is in a pre-translocational state and it does not exhibit any significant spontaneous translocation in the time frame of the experiment. The GDPNP complex is mostly in a pre-translocation state, with only a small fraction being able to achieve full translocation, while the fus complex has translocated almost to completion.

After assembling of the GDPNP and fus complexes, crosslinking was started by the addition of excess DSG, followed by separation of the reaction products on SDS-PAGE (Fig. II.2C). Staining of the gels revealed six bands migrating slower than EF-Gwt full length in the GDPNP and fus complexes treated with DSG (lanes 6 and 8). As compared to the controls (lanes 1-6, 7), the first five bands were dependent on the presence of both ribosomal complexes and DSG. The sixth band in these lanes, migrating just above EF-

Gwt, appears to be similar with a band present in the crosslinking sample containing only EF-G (lane 4), suggesting it to be an internal EF-G crosslink, which probably alters the gel mobility of the full length protein. The uncrosslinked r-proteins (55 in *E. coli* ribosomes) are not separated by the 6% SDS-PAGE used in this experiment, migrating together with the dye front as a strong band at the bottom of the gel (lanes 1-2 and 5-8).

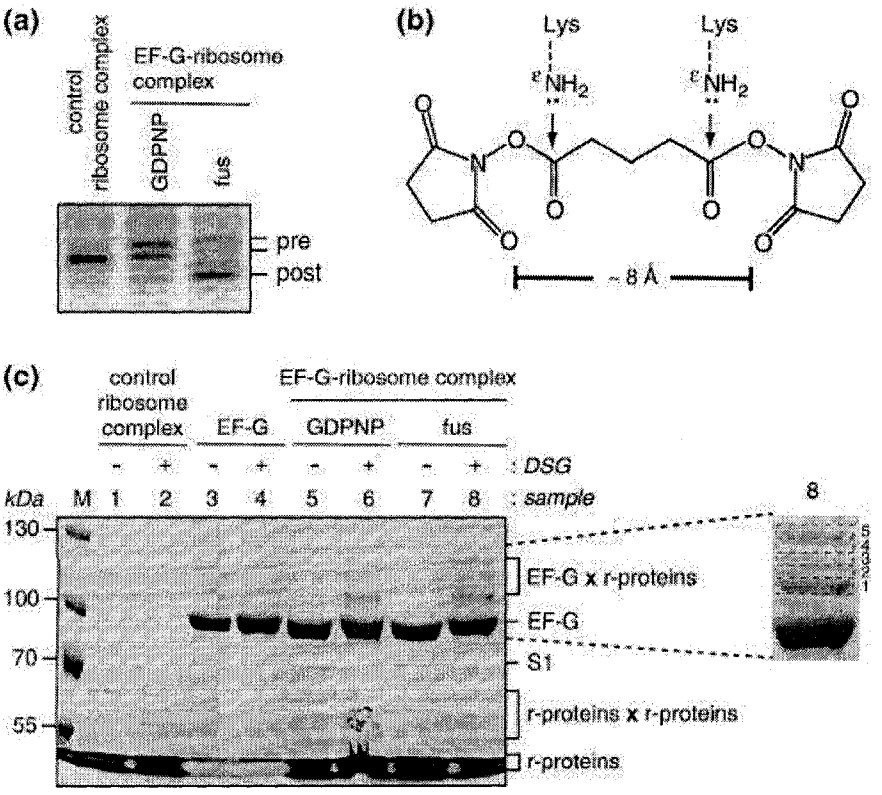


**Fig. II.2. - DSG-mediated crosslinking of EF-G bound to ribosome complexes in pre- and post-translocational states.** *A.* The translocation state of ribosome complexes as monitored by the toe-printing method. The control ribosome complex contained 70S•mRNA•$tRNA^{fMet}$(P site)•$tRNA^{Phe}$(A site). The GDPNP and fus complexes contain the control ribosome complex, with the addition of EF-G and either GDPNP (GDPNP complex) or GTP, and fusidic acid (fus complex). *B.* Structure of the DSG crosslinking agent. *C.* Coomassie brilliant blue stained 6% SDS-PAGE separating the DSG crosslinking reactions and their respective negative controls. The enlargement of sample 8 indicates the crosslinking bands (#1-5), which were submitted for mass spectrometry analysis. Crosslinks formed between proteins are denoted by **x**. M stands for molecular weight marker. S1 refers to r-protein S1. Reproduced from (Nechifor and Wilson, 2007)

There are also additional bands migrating between EF-Gwt full length and the r-proteins. The slower migrating one was identified as the r-protein S1, which is present in sub-stoichiometric amount in our ribosome preparation due to its weaker association with the ribosomes, hence its loss during ribosome purification. The other bands were assigned to unidentified contaminants of our ribosome preparation, based on their presence also in the non-treated ribosome sample (lane 1). The DSG treated ribosomal complexes also show a characteristic set of bands, which seem to be dependent on the presence of DSG and independent on the presence of EF-G, being consistent with crosslinks between r-proteins. (Fig. II.2.)

The five bands highlighted in lane 8 were individually cut from a similar gel to the one presented in Fig. II.2C and submitted for in-gel trypsin digestion and mass spectrometry analysis. Each gel slice yielded a mixture of peptides belonging to *E. coli* EF-G and r-proteins, confirming that the assigned bands were crosslinked products between EF-G and several r-proteins, as described below. Due to the small size of the identified r-proteins (lower than 20kDa), it is unlikely that these results are due to crosslinks between r-proteins, which happen to migrate together with some other crosslinking products involving EF-G. In order to test the theoretical possibility that some r-protein crosslinks might migrate in this region of the gel, we analyzed in a similar manner the equivalent region from lane 2. The mass spectrometry analysis did not yield any hits against *E. coli* r-proteins, eliminating the possibility of non-EF-G dependent r-protein contamination.

The mass spectrometry identifications were followed by immunoblotting, using polyclonal antibodies (Stoffler and Wittmann, 1971) raised against the individual r-proteins. The immunoblotting experiments had two main purposes: (1) to verify the mass spectrometry identifications, and (2) to be able to specifically visualize the crosslinked product between EF-G and the individual r-proteins.

**L7/L12** was one of the main crosslinking partners for EF-G, two peptides (residues 86–96, 110–121) being identified by the mass spectrometry analysis in bands 3 and 5. The immunoblotting experiment revealed one major, faster migrating crosslinking specie, as well as three minor, slower migrating species (Fig. II.3.). The anti-L7/L12 antibody also highlighted other bands migrating between uncrosslinked L7/L12 and EF-

G, which are probably crosslinks between monomers/dimers of L7/L12 and/or other r-proteins (i.e. r-protein L10, its known interacting partner).

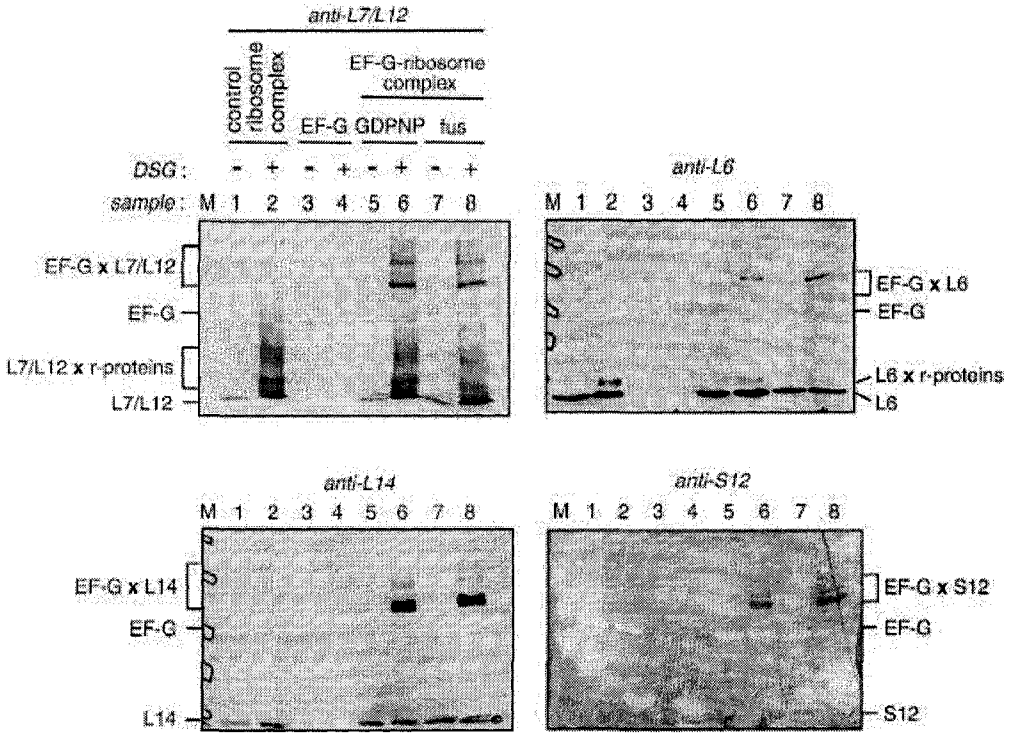


**Fig. II.3. - Immunoblotting analysis of DSG-mediated crosslinking products between EF-G and r-proteins**. Proteins from four gels similar to the one in Fig. I.1C, each containing lanes 1–8, were separately transferred to nitrocellulose membranes and probed individually with antibodies against r-proteins L7/L12, L6, L14 or S12. Reproduced from (Nechifor and Wilson, 2007).

EF-G also crosslinked to **L6**, their crosslinking product being detected in bands 3-5 by sequencing of eight peptides belonging to the r-protein L6 (residues 7–18, 19–27, 36–44, 45–55, 56–69, 70–85, 87–95, 121–139). Immunoblotting visualized one main product (Fig. II.3.). The L6 antibody shows a weak cross-reactivity towards our EF-Gwt protein, clearly highlighting the position of the crosslinked product above the EF-Gwt position. L6 also crosslinked to unidentified r-protein(s), their product migrating just above the dye front.

The r-protein **L14** was identified by mass spectrometry in bands 1-3, two peptides being sequenced (residues 1–17, 71–78). The immunoblotting revealed one main

crosslinking product, as well as two fainter and higher molecular weight products (Fig. II.3.).

A crosslinking product between EF-G and S12 was identified by mass spectrometry analysis in band 4 (peptides 19–30, 37–43), while the immunoblotting showed a main crosslinking product and three fainter and higher molecular weight bands (Fig. II.3.). The S12 immunoblot has a higher than usual background in spite of our attempts to lower it. This was most likely due to a high affinity of this particular antibody for the nitrocellulose membrane. Interestingly, full length EF-G can be visualized as a negative stain on this high background, highlighting again the difference in migration between EF-G full length and the band detected by the antibodies (Fig. II.3.).

The r-proteins S12 and L14 do not appear to crosslink with other r-proteins, while L6 and L7/L12 produced crosslinks involving probably additional r-proteins, but these products were not analyzed further. In the case of r-protein L6, these crosslinked products seemed to be forming more efficiently in the absence of EF-G, and in the GDPNP complex as compared to the fus complex. L7/L12 exhibits a similar pattern of efficiency variations as L6 when it comes to the inter-r-protein crosslinks, but the differences are rather subtle.

The majority of the crosslinking products between EF-G and the r-proteins are represented by more than one band, as visualized by the immunoblotting experiments. The difference in gel migration between the crosslinking products could be attributed to the existence of multiple products as a consequence of crosslinking at different sites of the same proteins. The higher efficiency products likely involve positions that are closer in space and/or have favorable orientations, while the lower efficiency products could covalently link residues that are further apart. In the case of the r-protein L7/L12, there is also the possibility that one molecule of EF-G could crosslink in the same time with a dimer or a tetramer, producing different molecular size crosslinks. Another possibility would be that the antibodies, being polyclonal, recognize more than one r-protein, which is a rather unlikely hypothesis based on their previous characterization (Stoffler and Wittmann, 1971). In order to test the specificity of the antibodies, we separated the r-proteins on a 16.5% SDS-PAGE, followed by individual immunoblotting with the four different antibodies used in the above experiments. The immunoblots show that the

L7/L12, L6, S12 and L14 antibodies recognize only one band among the r-proteins, and that the recognized band migrates around the expected molecular weight for that individual r-protein. (Fig. II.4.) These results prove that the antibodies are specific to the individual r-protein they were raised against, and they do not show any cross-reactivity to other r-proteins under the conditions used in our experiments. At higher r-proteins quantities and longer film exposure times, some other fainter bands appeared (data not shown).

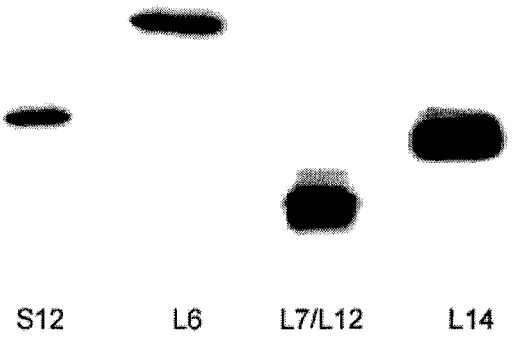


**Fig. II.4. - The polyclonal antibodies recognize only their specific target among the 55 r-proteins of *E. coli* ribosomes.** The image contains 4 individual immunoblots showing r-proteins which were separated on a 16.5% SDS-PAGE, transferred on nitrocellulose membranes and probed individually with the specified antibody.

Mass spectrometry analysis identified also the r-proteins S13 and S19, detected in band 4 (S13) and bands 1-2 and 4 (S19). Unfortunately, we could not procure the antibodies against these particular proteins to further test these crosslinks.

When comparing the DSG crosslinking results between the GDPNP and the fus complex, we could not distinguish any differences in the banding pattern, with the exception of a slight decrease in the intensity of the crosslinking products in the case of GDPNP complex. The subsequent immunoblots have revealed a similar picture, with no qualitative or quantitative differences of the crosslinking bands in the case of L7/L12 and L14. In the case of S12 and L6, there is a slightly higher efficiency of crosslinking in the case of fus complex comparative to the GDPNP complex. These small quantitative differences between the GDPNP and the fus complex could be explained by a slightly

higher stability of the EF-G•70S complex in the presence of fusidic acid and GTP, as was previously observed by us using an ultrafiltration technique (Fig. II.5.).

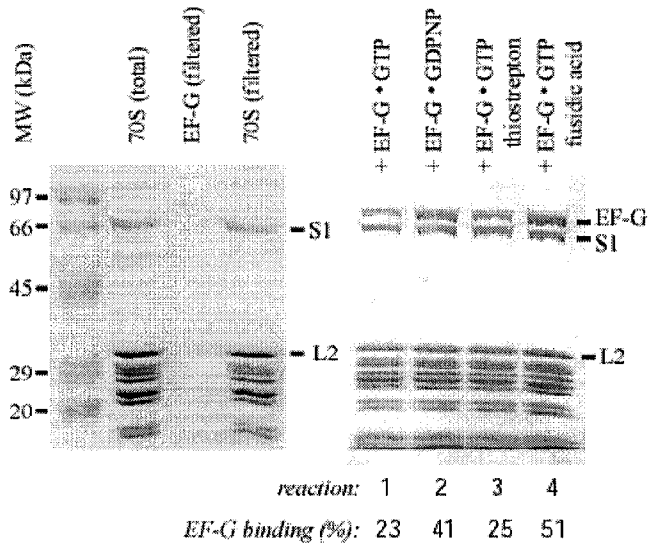


**Fig. II.5. - Stability of EF-G binding to different ribosomal complexes after ultrafiltration**. Preformed EF-G•70S complexes were passed through Millipore filters (exclusion limit 100 kDa), followed by SDS-PAGE separation of the filter retained material. The first panel contains the controls: the molecular weight marker, input ribosomes, EF-G•GTP (retained after filtration), 70S (retained after filtration). The second panel shows the relative binding of EF-G to ribosomes under various conditions (as noted). The numbers below each lane correspond to the densitometry quantification of EF-G retention expressed as percent to the amount of r-protein L2 present in each lane. For further details see the methods section. Reproduced from (Wilson and Nechifor, 2004).

In spite of the richness of information provided by the mass spectrometry and immunoblotting analysis, the DSG crosslinking experiments contain certain limitations. Firstly, our analysis cannot exclude the possibility that some of the identified crosslinked products represent multimeric complexes (i.e. r-proteins crosslinked to EF-G through a second r-protein). Secondly, due to the nature of the crosslinker, the exact location of the crosslinking sites is unknown. In order to be able to answer these questions, a second site-specific crosslinking study was performed.

### II.2.2. Cysteine specific, UV-inducible crosslinking of EF-G to the r-proteins

Our second crosslinking study employed a site-specific crosslinking technique in order to identify the exact elements of EF-G situated in close proximity to the r-proteins revealed by the DSG general screen. Previously constructed single cysteine mutants at 18 different positions on the surface of EF-G (Wilson and Noller, 1998), as well as newly constructed ones (at positions 156, 160, 426, 453, 637) were modified with 4-azidophenacyl bromide (AzP), a hetero-bifunctional crosslinking probe containing photoreactive and thiol-reactive functional groups (Fig. II.6A). The AzP-modified EF-G proteins were individually bound to the ribosome, forming the GDPNP complex or the fus complex. Upon UV irradiation, the azide group of AzP is converted into a short-lived nitrene that inserts itself into covalent bonds less than ~11Å away.

In the previous Fe-BABE probing study (Wilson and Noller, 1998), several cysteine residues (134, 209, 231, 433, 526, 591, and 627) did not produce any rRNA cleavages. At that point, it was hypothesized that these residues may be close to r-proteins, or at the interface between the two ribosomal subunits. Thus, we decided to start the AzP crosslinking experiments by using these particular cysteine mutants.

The first positive crosslinking results were obtained for residue 231C. The crosslinking reactions for this mutant revealed a new band, migrating above EF-G(231C). This new band was dependent on the presence of EF-G(231C), AzP, GDPNP, ribosomal complexes, and UV irradiation (Fig. II.6B), being absent from the negative controls, which lack one of these components. Another important point highlighted by this experiment is that the cysteinless version of EF-G did not produce any crosslinking bands, proving that AzP is specific to cysteine residues under our experimental conditions (Fig. II.6B).

The tentative crosslinking band from a similar gel to the one in Fig. II.6. was submitted for in-gel tryspin digestion and mass spectrometry analysis, yielding 12 peptides from EF-G, as well as 3 peptides belonging to the r-protein L7/L12 (residues 53–60, 86–96, and 110–121). These results argue that a specific crosslink forms between EF-G(231C)-AzP and the r-protein L7/L12 upon UV irradiation.

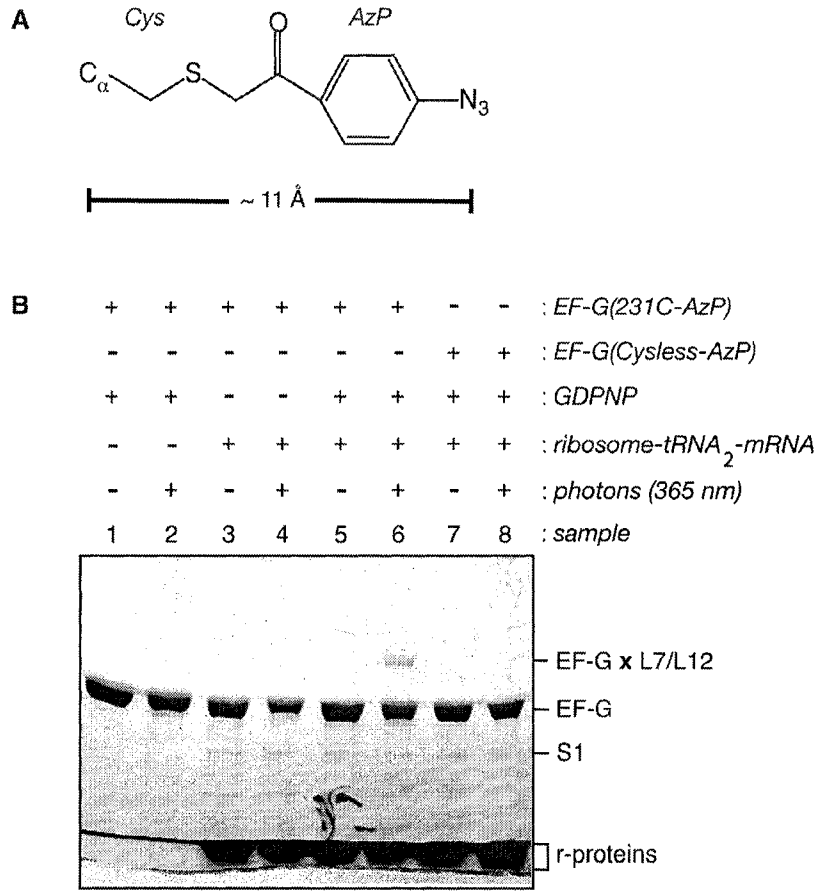


**Fig. II.6. - AzP modified EF-G(231C) specifically crosslinks to r-protein L7/L12.** *A.* Structure of azidophenacyl bromide covalently linked to a cysteine residue. *B.* Analysis of the AzP-crosslinking products using 6% SDS-PAGE stained with Coomassie brilliant blue. S1 refers to r-protein S1. Reproduced from (Nechifor and Wilson, 2007)

The rest of the 20 cysteine residues were tested after AzP modification, yielding four additional crosslinks. In summary, residues 209 and 231, part of the G' subdomain, crosslinked with the r-protein L7/L12, residues 426 of domain III crosslinked with the r-protein S12, while the residues 627 and 637, part of domain V, crosslinked to the r-protein L6. We did not find any crosslinks to L14 and later modeling suggested that none of our cysteine residues had the favorable position/orientation to crosslink to this r-protein.

After this initial scan, we concentrated our attention on the cysteine mutants that gave positive crosslinking results, and assembled full EF-G•ribosomal complexes in two different states: the pre-translocational complex (GDPNP) and the post-translocation complex (fus). The functional states of these complexes containing AzP-modified cysteine mutants were verified by toe-printing. In all five cases, the GDPNP complexes were mostly in the pre-translocation state, while the fus complexes had translocated almost to completion (Fig. II.7.). These results indicated that the addition of the crosslinker group to our cysteine mutants did not interfere with translocation.

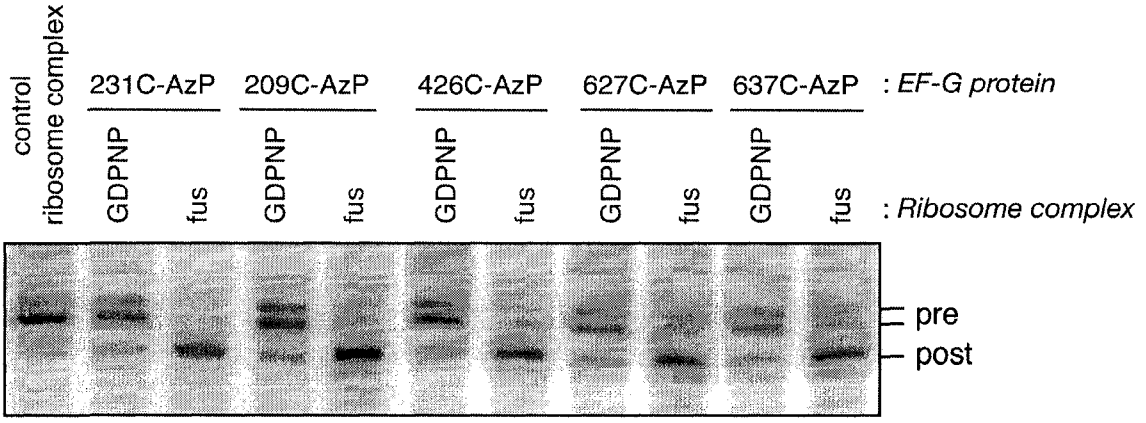


**Fig. II.7. Toe-printing monitoring of the translocation states of AzP-modified EF-G cysteine mutants bound to ribosome complexes.** Control ribosome complex contained mRNA, $tRNA^{fMet}$ in the P site, and $tRNA^{Phe}$ in the A site. GDPNP complexes were derived from control ribosome complex by the addition of AzP-modified EF-G and non-hydrolyzable GTP analog. Fus complexes were formed from control ribosome complex after addition of AzP-modified EF-G, hydrolyzed GTP, and fusidic acid. Reproduced from (Nechifor and Wilson, 2007).

These complexes were then used in crosslinking reactions by activating AzP through UV irradiation. Residues 209 and 231 crosslinked to the r-protein L7/L12 in both the GDPNP and the fus complex as confirmed by immunoblotting. EF-G(231C)-AzP crosslinked to L7/L12 with a higher efficiency as compared to EF-G(209C). (Fig. II.8.)

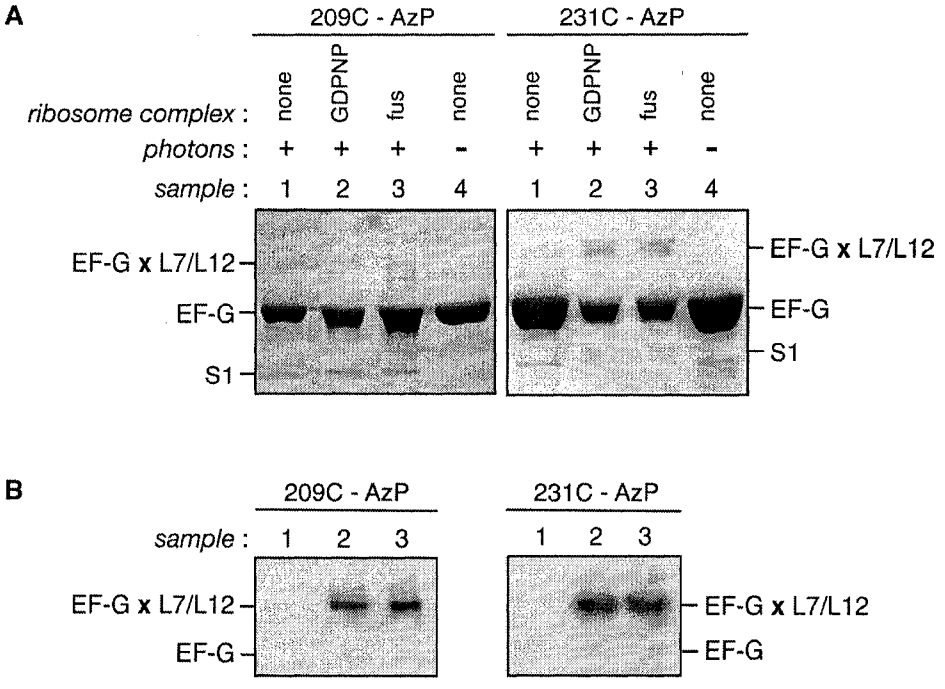


**Fig. II.8. - Site-specific crosslinking of L7/L12 from EF-G residues 209 and 231.** *A.* Gels stained with Coomassie brilliant blue. *B.* Immunoblots probed with anti-L7/L12 antibody. Crosslinked products are denoted by **x**. S1 refers to r-protein S1. Reproduced from (Nechifor and Wilson, 2007)


**Fig. II.9. - The crosslinking product of EF-G(231C)-AzP disappears when L7/L12 depleted 70S are used in the crosslinking reactions.** Reactions 2 and 3 correspond to the GDPNP and fus complexes, respectively. The crosslinking band is marked by **x**.

In our crosslinking reactions, AzP is attached to the EF-G cysteine mutants, so, in theory no multimeric crosslinking product could be formed because the crosslinking reactions should not contain any free AzP. This is in line with the mass spectrometry identifications of only two components in each crosslinking band: EF-G and the respective r-protein. We were able to test further the composition of the crosslinked product in the case of the r-protein L7/L12 because this protein can be stripped from ribosomes by a combination of $NH_4Cl$ and ethanol (see materials and methods for details). To that end, we repeated the AzP-EF-G(231C) crosslinking reactions using L7/L12 depleted ribosomes. This experiment showed that, in the absence of L7/L12, the crosslinking band disappears (Fig. II.9.), confirming again the specificity of our identification and the absence of any additional element in the band assigned to be a crosslinking product between EF-G and L7/L12.

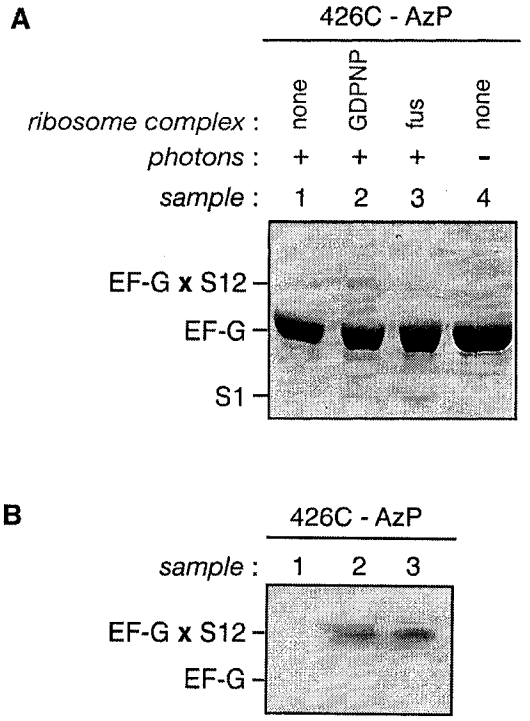


**Fig. II.10. - Site-specific crosslinking of S12 from EF-G residues 426.** *A.* Gels stained with Coomassie brilliant blue. *B.* Immunoblots probed with anti-L7/L12 antibody. Crosslinked products are denoted by **x**. Reproduced from (Nechifor and Wilson, 2007)

The r-protein S12 was crosslinked from residue 426 of domain III of EF-G, as verified by both mass spectrometry analysis and immunoblotting. Similar to the case of L7/L12, this crosslinking was also detected for both the pre and post-translocation states (Fig. II.10.).

Interestingly, the crosslinking experiments using cysteine mutants in domain III highlighted how important the proper orientation of the side chain of the cysteine mutants really is for success of the AzP crosslinking: a neighboring residue (433), part of the same helix, but with the side chain on the opposite site of the helix $A_{III}$ as compared to residue 426 was not able to crosslink to any r-protein (data not shown).

Two residues from domain V (627 and 637) of EF-G crosslinked to the r-protein L6, in both the GDPNP and fus complex (Fig. II.11.). Other residues from domain V (650 and 655), previously positioned next to RNA elements of 23S rRNA, gave multiple, strong intra-molecular crosslinks, but no crosslinks to r-proteins (data not shown), suggesting that they are probably oriented towards other elements of domain V.

As seen in Fig. II.8-11 and Table II.1, there are no significant differences between crosslinks in the GDPNP and fus complexes, with the exception of a qualitative difference for residue 637. These results are consistent with the three EF-G domains undergoing only restricted movements (< 11Å) on the ribosome during the course of translocation, which could also be the cause of cryo-EM failure to visualize detectable differences in conformation of EF-G between the two complexes (Valle et al., 2003). Our crosslinking results do not exclude larger movements of other EF-G domains, such as the tip of domain 4, where no r-protein crosslinking products were detected.

The crosslink between EF-G(637) and the r-protein L6 is consistently more efficient in the GDPNP state than in the fus state (Fig. II.11. and Table II.1). It is possible that the hypothesized interaction between the tail of L6 and helix $A_V$ of EF-G needs to be disrupted in the fus complex, maybe in preparation for EF-G•GDP dissociation from the ribosomal complex, which would explain the lower crosslinking efficiency of EF-G637C in this complex.

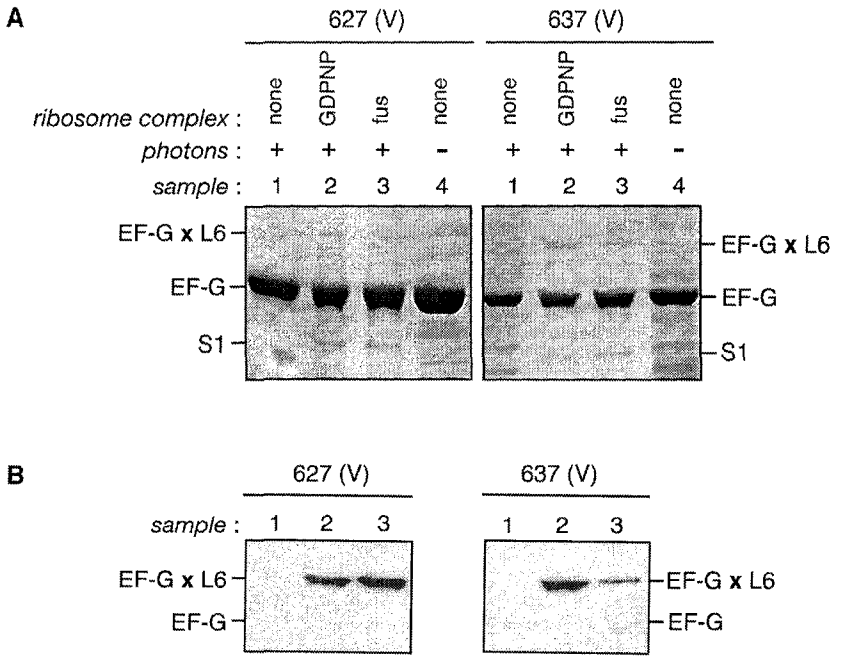


**Fig. II.11. - Site-specific crosslinking of L6 from EF-G residues 627 and 637.** (a) Gels stained with Coomassie brilliant blue. (b) Immunoblots probed with anti-L7/L12 antibody. Crosslinked products are denoted by **x**. Reproduced from (Nechifor and Wilson, 2007).

**Table II.1. The crosslinking efficiencies of AzP modified EF-G cysteine mutants to r-proteins.** Reproduced from (Nechifor and Wilson, 2007)

| EF-G cysteine residue (domain) | Crosslinked r-protein | Crosslinking efficiency (%)[1] | | Crosslinking Ration[2] GDPNP/fus |
|---|---|---|---|---|
| | | GDPNP complex | Fus complex | |
| 209(G') | L7/L12 | 2.9 ±1.6 | 4.2 (±4.1) | 1.1 (±0.6) |
| 231(G') | L7/L12 | 8.3 (±5.1) | 7.1 (±5.9) | 1.3 (±0.2) |
| 426(III) | S12 | 6.9 (±4.7) | 4.1 (±2.4) | 1.7 (±0.8) |
| 627(V) | L6 | 3.6 (±1.6) | 2.7 (±1.1) | 1.4 (±0.5) |
| 637(V) | L6 | 4.8 (±2.6) | 1.3 (±0.7) | **3.9 (±0.9)** |

[1] Reported numbers represent the average crosslinking efficiencies (±standard deviation) determined from three or four independent experiments.

[2] This ratio is the crosslinking efficiency in the GDPNP complex divided by the crosslinking efficiency in the fus complex, and was calculated individually for each experiment. The reported numbers represent the average ratio (±standard deviation).

## II.3. DISCUSSION

We started our crosslinking study by using DSG, a non-specific chemical crosslinker for the purpose of identifying all the r-proteins situated in close proximity to EF-G when this factor is bound to the ribosome in the GDPNP and fus complexes. With the help of mass spectrometry analysis, we identified the r-proteins crosslinked to EF-G, and some of them (S12, L6, L7/L12, L14) were analyzed further using immunoblotting. All the identical r-proteins are positioned in the inter-subunit cavity, very close to the EF-G binding site, so their detection among the crosslinking products is not surprising. They have also been identified previously to crosslink to EF-G (Skold, 1982). The other two r-proteins identified by mass spectrometry, S13 and S19, could not be analyzed further by immunoblotting. S19 was also identified in the same previous study (Skold, 1982), but to our knowledge, this is the first report of a crosslink between S13 and EF-G. S13 and S19 have globular domains situated rather far from the known position of EF-G on the ribosome, but their small tails protrude next to the P site of the 30S subunit. Previous experiments have also shown that the tip of domain IV of EF-G is next to the P site on the 30S subunit in the fus complex (Wilson and Noller, 1998), which would place this domain of EF-G in the vicinity of the tails of S13 and S19, potentially explaining the crosslinking results. Although we tried five different residues from domain IV of EF-G (506, 526, 541, 591, and 700), none of them gave a positive crosslink to any r-proteins (data not shown), so, unfortunately, we could not provide further support to the mass spectrometry detection of the r-proteins S13 and S19 as EF-G crosslinking partners.

A site specific, UV inducible crosslinker (AzP) was used to gather more information about the identity of the EF-G elements situated close to the r-proteins. In this new study, only three of the previously identified r-proteins were found to be close to five of our cysteine residues: L7/L12 is crosslinked from residues 209 and 231, which are on either side of helix $A_{G'}$, S12 is close to cysteine 426, part of helix $A_{III}$, and L6 is in proximity of residues 627 and 637 of helix $A_V$.

When we compare our site-directed crosslinking data with the rRNA Fe-BABE probing experiments, the combined results are striking. Of a total of 22 cysteine mutants in EF-G, 15 have been probed for their proximity to both rRNAs and r-proteins. Ten EF-G residues are proximal to specific elements of either 16S or 23S rRNA, whereas only

three EF-G residues are near r-proteins. Two of the residues tested are not close to either rRNA or r-proteins. None of the cysteine residues was found to be close to both rRNA and r-protein elements. Thus together, these results suggest that almost the entire surface of EF-G is in close proximity to either subunit of the ribosome, being surrounded in majority by rRNA elements rather than r-proteins. (Fig. II.12.)

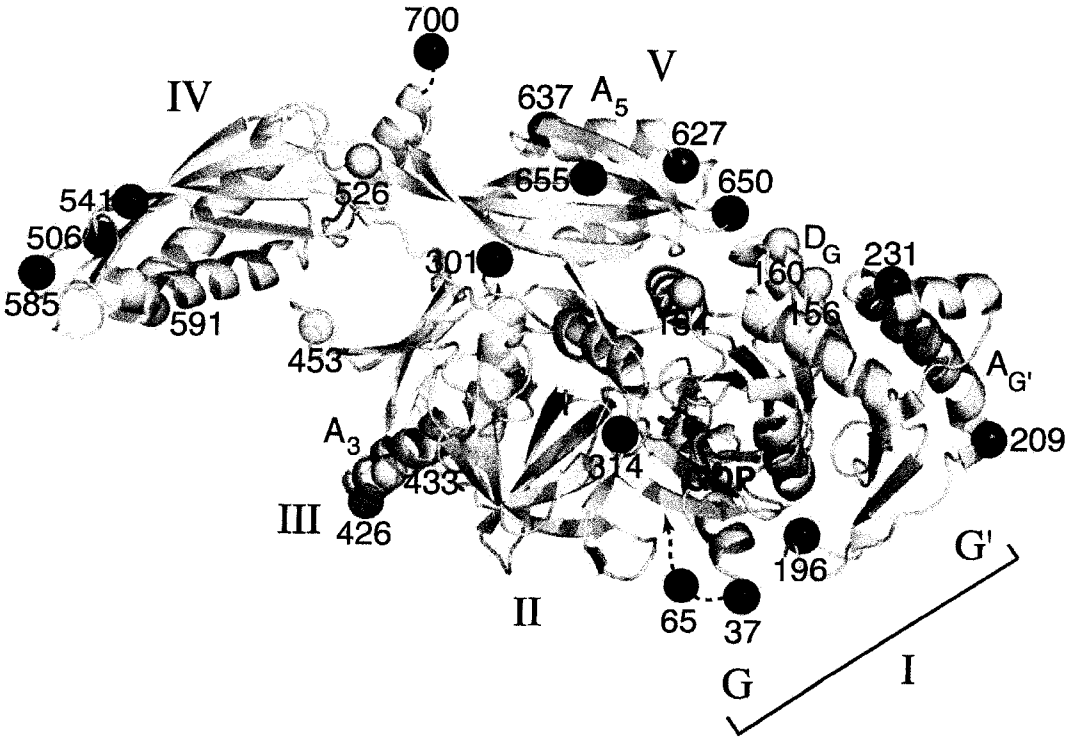


**Fig. II.12. - Positions of single cysteine mutants mapped onto the structure of *T. thermophilus* EF-G-GDP** (Laurberg et al., 2000). Residues mutated to cysteine are indicated by color coded spheres, centered on the α-carbon of the residue: red spheres for residues forming crosslinks to r-proteins, blue spheres for residues targeting various rRNA nucleotides of the ribosome, when modified with FeBABE, and yellow spheres for residues where no ribosomal component (rRNA or r-protein) were identified. Reproduced from (Nechifor and Wilson, 2007).

Using the combined knowledge of the proximities of both rRNA elements and r-proteins, we were able to design a working model for the position of EF-G inside the ribosomal cavity in a post-translocational state. (Fig. II.13.) To construct the model shown here, we superimposed the rigid-body structures of S12, L6, L7/L12 from the *T.*

*thermophilus* 70 S ribosome (PDB 2j00 and 2j01 (Selmer et al., 2006)), and individual domains of EF-G (also from *T. thermophilus*; PDB 1FNM (Laurberg et al., 2000)), onto the cryo-EM coordinates for the EF-G•ribosome complex.

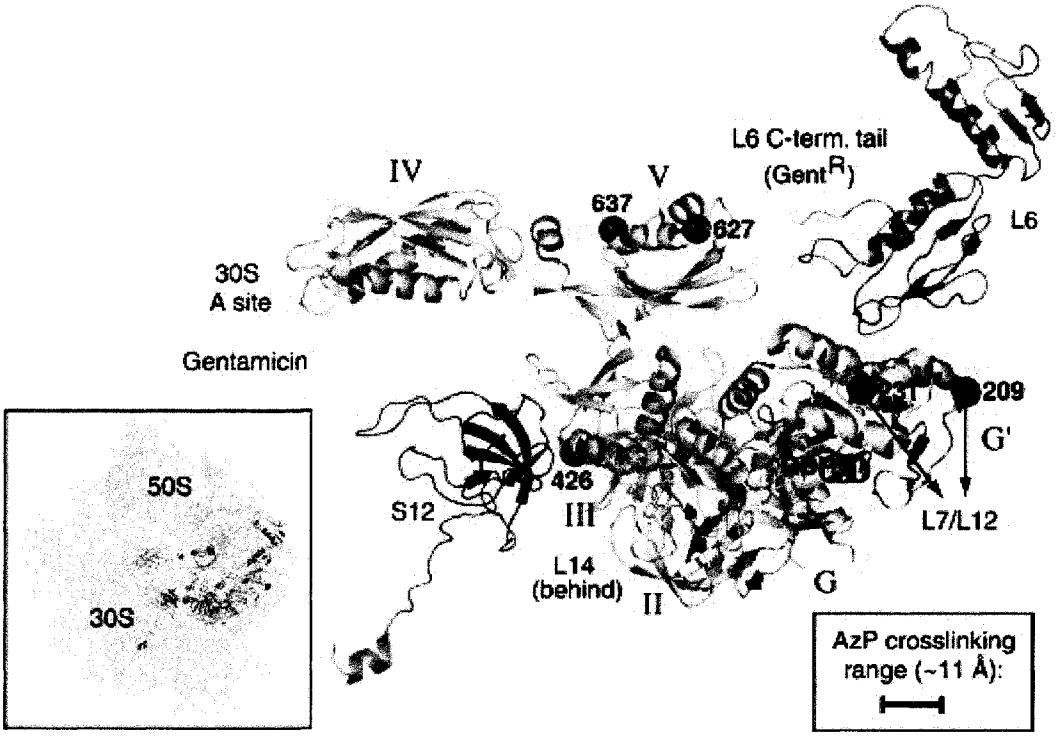


**Fig. II.13. - Structural model of the r-protein components surrounding EF-G, bound to the ribosome in the post-translocational state.** Positions and orientations of EF-G domains are derived from the coordinates of a cryo-EM model of the post-translocational EF-G-ribosome complex from *E. coli* (PDB 1P6G, 1P85, 1PN6, and 1PN7).(Gao et al., 2003; Valle et al., 2003) Relevant r-proteins and EF-G are shown, extracted from the complete model shown in the inset (lower left). AzP-modified cysteine residues, which were crosslinked to S12, L6 or L7/L12, are indicated by red spheres centered on the α-carbon of these residues. Residue numbers refer to *E. coli*. Reproduced from (Nechifor and Wilson, 2007).

Protein L7/12 seems to be an important component both for elongation factors recruitment to the ribosome, as well as for activation of the GTP hydrolysis by these factors once they are bound to the ribosome (Diaconu et al., 2005; Mohr et al., 2002; Savelsbergh et al., 2005). The mechanism appears to involve the activation of inorganic phosphate release by L7/L12 after cleavage of the diphosphate bond (Savelsbergh et al.,

2005). For EF-Tu, a genetic study provided evidence for interactions between helix D of its G domain and the CTD of L7/L12 (Kothe et al., 2004). In the case of EF-G, our crosslinking experiments suggest that L7/L12 interacts with the G' subdomain of EF-G. Domain G of EF-G also contains a helix D, but it is poorly conserved and mostly neutral in charge, as opposed to helix $D_G$ of EF-Tu which is well conserved and negatively charged. Still, we constructed two new cysteine residues in helix $D_G$ of EF-G (156 and 160) and used them for AzP crosslinking. These two AzP-modified proteins did not yield any crosslinking products (data not shown). Based on our crosslinking experiments, we propose that in the case of EF-G, the G' subdomain, not its G domain, interacts with the r-protein L7/L12. Helix $A_{G'}$, which is delimited on either side by residues 209 and 231, is probably part of the interaction surface between EF-G and L7/L12. The CTD of L7/L12 contains a highly conserved patch of positive charged residues, which was proven to be functionally important for both EF-G and EF-Tu (Diaconu et al., 2005; Kothe et al., 2004; Savelsbergh et al., 2005). This positively charged region of L7/L12 is thought to interact with helix $D_G$ of EF-Tu (Kothe et al., 2004), and it also could be part of the interaction surface with EF-G. On the other hand, the G' subdomain of EF-G contains the largest region of negative charge on EF-G, being perfectly capable to provide electrostatic interactions with the positively charged region in the CTD of L7/L12. The differences between the elements of EF-G and the elements in EF-Tu that interact with the same region of L7/L12 could provide a mechanism for the recognition and specific recruitment of these translation factors to the ribosome during protein synthesis.

S12 has long been associated with regulating both the translocation and decoding mechanisms of the ribosome. Chemical modifications of exposed cysteine residues in the globular part of S12 result in ribosomes that can translocate spontaneously, independent of EF-G (Cukras et al., 2003; Gavrilova et al., 1974). Structural studies of the 30S subunit provided a partial explanation for these observations, showing that an extended loop of S12 reaches into the 30S subunit A site, where its P48 residue makes interactions with the codon-anticodon wobble pair (Ogle et al., 2001). Our crosslinking data, suggest that the N-terminal end of helix $A_{III}$ of EF-G contacts the globular part of S12, which is also in agreement with cryo-EM structures (Valle et al., 2003). The functional significance of interactions between the domain III of EF-G and the r-protein S12 is

further supported by the requirement of this EF-G domain for translocation activity (Martemyanov and Gudkov, 2000). It seems possible that the interaction between domain III of EF-G and the r-protein S12 plays a key role in translocation, potentially by affecting the interactions between the bound tRNA and the 30S subunit A site.

Since 627 and 637 are too far away from the globular domain of L6, it seems more likely that the crosslinks are accomplished through the tail of L6, which appears to extend towards domain V of EF-G. From a functional point of view, there is not much known about the r-protein L6. This r-protein has been linked to the decoding mechanism based on the observation that C-terminal truncations of L6 lead to resistance to gentamicin (Buckel et al., 1977; Davies et al., 1998). Like other miscoding antibiotics, gentamicin reduces the fidelity of decoding by binding near the 30S A site and determining 16S rRNA nucleotides A1492, A1493 and G530 to flip out of their helices in order to interact with the codon-anticodon pair even in the absence of proper codon-anticodon base pairing. (Ogle et al., 2001; Vicens and Westhof, 2003) However, the mechanism by which the L6 C-terminal tail could affect the 30S A site, which are separated by ~100 Å and also belong to two different ribosomal subunits, is enigmatic at this moment, but could conceivably act through conformational changes propagated through either EF-Tu or inter-subunit bridges. Interestingly, gentamicin is also a potent inhibitor of EF-G-catalyzed translocation (Cabanas et al., 1978). The proximity between the domain V of EF-G and the r-protein L6, as well as other rRNA elements in this region, could stabilize the extended conformation of EF-G on the ribosome observed by cryoEM (Valle et al., 2003), in which domains I and V are separated by a significant gap.

Analysis of both the GDPNP and the fus complexes, suggests that domains I, III, and V of EF-G undergo only limited movements (< 11Å) in regards to ribosomal elements. The quantitative difference observed for EF-G(637C) may indicate a rotation or translation movement of helix $A_V$ in regards to the r-protein L6.

## II.4. MATERIALS AND METHODS

### II.4.1. Reagents and Buffers

AzP, fusidic acid, GTP, GDPNP, and *E. coli* $tRNA^{fMet}$ and $tRNA^{Phe}$ were purchased from Sigma-Aldrich. DSG was purchased Pierce. Polyclonal IgG antibodies

(Stoffler and Wittmann, 1971) against *E. coli* r-proteins L6, L7/L12, L14 and S12 were a generous gift from Dr. R. Brimacombe (Max Planck Institute). BugBuster was purchase from Novagen, the protease inhibitor cocktail was from Roche Diagnostics, and the Ni-NTA beads were bought from Qiagen. *Buffer 1*: 10mM Tris-HCl pH 8.0, 5% glycerol, 1mM 2-mercaptoethanol. *Buffer 2 (EF-G storage buffer)*: 10mM Tris-HCl pH 8.0, 100mM KCl, 50% glycerol, 3mM DTT. *Buffer 3*: 50mM Hepes-KOH pH 7.7, 70mM $NH_4Cl$, 20mM $MgCl_2$, 1mM DTT. *Buffer 4*: 50mM Tris-HCl pH 7.8, 100mM $NH_4Cl$, 20mM $MgCl_2$. *TBST*: 10mM Tris-HCl pH 8.0, 100mM NaCl, 1‰ Tween. *SDS-PAGE sample buffer*: 30mM Tris-HCl pH 6.8, 1% SDS, 30% glycerol, 10mM DTT, 2.5% bromphenol blue. *Urea sample buffer*: 50mM Tris-HCl pH 8.0, 7.6M urea, 1mM EDTA, 2.5% xylene cyanol, 2.5% bromphenol blue.

### II.4.2. Ribosome purification

Tight coupled 70S ribosomes were prepared after a protocol from (Spedding, 1990), with some modifications. *E. coli* MRE600 cells were grown in LB media until an $A_{600nm}$ of ~ 0.5 and harvested by centrifugation. Bacterial cell pellets were resuspended in lysis buffer (50mM Tris-HCl pH 7.5, 1M $NH_4Cl$, 10mM $MgCl_2$, 0.5mM EDTA, 6mM 2-mercaptoethanol) and passed through a French press at 18,000 p.s.i. The lysed cell solution was than cleared of cellular debris by a short centrifugation (Ti70 rotor, 30,000g, 45 min., 4°C) and the supernatant was submitted to an overnight centrifugation in order to pellet the ribosomes (Ti70 rotor, 112,000g, 14h, 4°C). The obtained crude ribosome pellet was then resuspended in a buffer containing 50mM Tris-HCl pH 7.5, 1M $NH_4Cl$, 6mM $MgCl_2$, and 6mM 2-mercaptoethanol, followed by layering the solution on top of 10-40% sucrose gradients and overnight centrifugation (SW27 rotor, 55,000g, 13h, 4°C). The sucrose gradients were fractionated the next day, the 70S peak was collected, its $MgCl_2$ concentration was adjusted to 10mM and the ribosomes were pelleted again by centrifugation (Ti70 rotor, 72500g, 20h, 4°C). The final ribosome pellet was again resuspended in ribosome storage buffer (50mM Tris-HCl pH 7.5, 100mM $NH_4Cl$, 10mM $MgCl_2$, 1mM DTT) and the final solution was stored as aliquots at -80°C. The 70S concentration was calculated using $1A_{260nm} = 23\mu M$ 70S ribosomes.

### II.4.3. mRNA purification

The mRNA used in these experiments was a fragment of phageT4 gene*32* (138 nt; 54nt upstream, and 81nt downstream, of the AUG codon) inserted between the *Eco*RI and *Bam*HI sites of pUC118 (plasmid construct provided by Rachel Green, Johns Hopkins University). This plasmid was cut with *Bam*HI, followed by *in vitro* transcription using His-tagged bacteriophage T7 RNA polymerase (expression strain provided by Thomas Shrader, Albert Einstein College of Medicine) under the following reaction conditions: 1μg/1μl BamHI-digested plasmid, T7 RNA polymerase (40pmols/pmol DNA), 2mM ATP, 2mM CTP, 2mM GTP, 2mM UTP, 80mM HEPES-KOH pH 7.7, 12mM $MgCl_2$, 4mM DTT, 1mM spermidine for 2h at 37°C. Following transcription, the mRNA was extracted with phenol and chloroform, precipitated with ethanol, and purified from unincorporated NTPs by size exclusion chromatography using a Superdex 200 (10/300) column connected to AKTA purifier (Amersham Biosciences). The peak corresponding to the mRNA was collected, ethanol precipitated and dissolved in $H_2O$. The mRNA concentration was measured using an extinction coefficient of 25 $mg^{-1}$ x ml x $cm^{-1}$. The purity and integrity of the mRNA stock was verified by separation of an aliquot on a 7M Urea-6% polyacrylamide gel and staining with methylene blue.

### II.4.4. EF-G mutagenesis and purification

Our EF-G construct corresponds to the sequence of *E. coli* MRE600 fusA gene inserted in the pET24b+ vector (Novagen), creating pET24-fusA, which expresses a 6 his-tagged version of EF-G. The site-specific crosslinking experiments have taken advantage of previously constructed cysteine mutants (Wilson and Noller, 1998), as well as five newly constructed cysteine mutants at positions 156, 160, 426, 453 and 637, which were individually incorporated into the cysteine-free version of EF-G.

EF-Gwt and the cysteine mutants were expressed in *E. coli* BL21(DE3). Cultures were grown in 0.5L of LB+kanamycin (30μg/ml) at 37°C until $A_{600nm}$ reached 0.7 (approximately 3 h). EF-G synthesis was induced with IPTG (1mM), and cultures were grown for an additional four hours before harvesting by centrifugation. The bacterial cell pellets were resuspended in 5ml/g of cells of BugBuster + Protease Inhibitor Cocktail, incubated for 10 min. at room temperature, followed by centrifugation (Ti50 rotor,

16,500 rpm, 20 minutes, 4 °C) to remove the bacterial cells. The supernatant was applied to a 3ml Ni·NTA agarose column, equilibrated in buffer 1+0.2M KCl. This column was connected to BioRad Biologic LP and washed in the system with 8 column volumes of buffer 1 containing 0.2M KCl, followed by bufer1+1M KCl for another 8 column volumes. EF-G was eluted with imidazole (linear gradient from 20mM to 1000mM imidazole, pH 7.5) and collected in 2 ml fractions. The purity of EF-G fractions was visualized by 10% SDS-PAGE. The purest EF-G fractions were pooled, dialyzed against buffer 2 (EF-G storage buffer), and the purified protein was stored at −80°C. The concentration of EF-G was estimated by the Bradford assay (BioRad reagent) using BSA as a standard. The purity of the EF-G final stock, as assessed by SDS-PAGE, was typically >95%.

### II.4.5. Formation of EF-G•ribosome complexes and chemical crosslinking

In preparation for chemical crosslinking, 70S ribosomes had their buffer exchanged by three consecutive dilutions to 500µl of Buffer 3 and ultrafiltration using Microcons YM-100 (11,000 rpm, 10min., Eppendorf centrifuge). This step was necessary in order to exchange the ribosome storage buffer, because it contains Tris, which is an efficient quencher of the DSG crosslinking reaction (the structure of Tris contains primary amines, which will react with DSG).

EF-Gwt•ribosome complexes were prepared at 37°C in buffer 3 following a multi-step process. Firstly, 70S ribosomes (1µM) were incubated with mRNA (2µM) and uncharged $tRNA^{fMet}$ (2µM) for 15 min. in buffer 3, which allows the initiator tRNA to bind and fully occupy the P site. Next, the uncharged $tRNA^{Phe}$ (2µM) was incubated with the ribosome complex for 30 min. The longer time is necessary due to the slower binding kinetics of the uncharged tRNA to the ribosomal complex A site. At this point, the ribosomal complex contains mRNA and 2 tRNAs bound in the P, and A site, respectively. The complexes were divided in three different tubes and incubated an additional 10 min. after the following additions: (1) *control ribosome complex*, which had only buffer added to it, (2) *GDPNP complex*, formed by addition of EF-Gwt (1µM) and GDPNP (500µM), and (3) *fus complex*, formed by addition of EF-Gwt (1µM), GTP (500µM) and fusidic acid (500µM). The fully formed EF-Gwt•ribosome complexes were

cooled on ice for 10 min., followed by addition of either freshly prepared DSG solution (200μM in DMF) or the same volume of DMF (mock treatment). The crosslinking reactions were allowed to proceed on ice for 5 min. and were stopped by the addition of 50mM Tris-HCl pH 7.5. The reactions were analyzed by SDS-PAGE (6% polyacrylamide in the resolving gel) after mixing with an equal volume of sample buffer and denaturation (90°C, 10 min). The gels were either stained with Coomassie blue or processed for immuno-blotting.

### II.4.6. The modification of EF-G cysteine mutants with AzP

Prior to conjugation with AzP, EF-G proteins had their storage buffer exchanged into 50mM Tris-HCl pH 8.0 and 100mM $NH_4Cl$, by using two consecutive gel filtration spin columns (BioRad). AzP (675μM) was conjugated to EF-G cysteine mutants (200μM) at 4°C, overnight, in the dark. Unreacted AzP was removed from EF-G proteins by dialysis (overnight, at 4°C) against EF-G storage buffer (- DTT). The final EF-G-AzP stock had its concentration re-estimated by the Bradford Assay.

### II.4.7. Formation of EF-G•ribosome complexes and photocrosslinking

AzP-modified EF-G proteins were bound to the ribosome in the GDPNP or fus state as described above with the following modifications. EF-G•ribosome complexes were formed in the dark with ribosomes (1μM), mRNA (2μM), $tRNA^{fMet}$ in the P site (2μM), $tRNA^{Phe}$ in the A site (2μM), AzP-modified EF-G (8μM), and either GDPNP (500μM) or GTP (500μM) and fusidic acid (500μM) in 20μl of buffer 4. Reactions were incubated at 37°C for 15 min, followed by cooling on ice for 5 min. Free EF-G was removed by diluting the samples to 500μl buffer 4 (+20μM fusidic acid for the fus complex) and ultrafiltration by Microcon YM-100 (10,000 rpm, 6min., Eppendorf centrifuge). The reaction volume after ultrafiltration was adjusted back to 20μl with buffer 4. Purified complexes were transferred to a 96-well microtiter plate and irradiated (365nm light, 15 min on ice) with a UV lamp (model UVLS-24, Upland) positioned ~1 cm above the complexes. After irradiation, complexes were mixed with an equal volume of sample buffer, denaturated (90°C, 10 min) and analyzed by SDS-PAGE (6% polyacrylamide in the resolving gel). Crosslinking efficiencies were estimated by

densitometry of Coomassie-stained gels, as a ratio between the crosslinking band and the full length EF-G band.

### II.4.8. Identification of r-proteins crosslinked to EF-G

Putative intermolecular crosslinks between EF-G and r-proteins products were excised from Coomassie-stained gels and submitted to the Institute of Biomolecular Design (University of Alberta) for in gel trypsin digestion and mass spectrometry analysis. To that end, gel slices were de-stained, reduced with DTT, alkylated with iodoacetamide, and digested with trypsin (37°C, 5 hr) through an automated process. The resulting peptides were extracted from the gel with aqueous 2% acetonitrile + 1% formic acid, and resolved by reversed-phase HPLC (C18 capillary column; mobile phase: 0-100% v/v acetonitrile in aqueous 0.2% formic acid). Peptides were analyzed by tandem mass spectroscopy (MS/MS, Q-TOF) and identified using Mascot Daemon software (Matrix Science) to search both the NCBI non-redundant protein sequence database (www.ncbi.nlm.nih.gov) and our specific data based which only contains *E. coli* sequences of r-proteins and EF-G.

### II.4.9. L7/L12 depletion of 70S ribosomes

L7/L12 stripping was done according to an initial protocol developed by (Tokimatsu et al., 1981) and the modifications described in (Mohr et al., 2002). For a larger scale preparation, 450pmols of 70S ribosomes stock were incubated on ice for 10 min. in 450µl of 20mM Tris-HCl, pH 7.5, 0.6M $NH_4Cl$, 20mM $MgCl_2$. After 10 min., 250µL of ice cold 100% ethanol were added and the reaction was incubated on ice for another 10 min. with occasional stirring. At the end of this period, another 250µL of ice cold 100% ethanol was added and the mixture stirred for another 5 min. The ribosomes were pelleted by centrifugation at 14000rpm for 30 min (Eppendorf centrifuge), and then dissolved in 30µl of ribosome storage buffer. The concentration of the L7/L12 stripped ribosomes was re-meassured using their absorbance at 260nm. In order to test the extent of stripping, identical quantities of control and L7/L12 stripped ribosomes were separated on a 16.5% SDS-PAGE and their L7/L12 content was measured by immuno-blotting

using anti-L7/L12 polyclonal ribosomes. The quantity of L7/L12 after the stripping procedure was approximately 2%.

### II.4.10. Immunoblotting

Crosslinking reactions were separated by SDS-PAGE, followed by equilibration of the gels in transfer buffer (25mM Tris base and 192mM glycine) for 30 min. at room temperature with shaking, and proteins transfer to nitrocellulose membranes (400mA, 1h) in the same transfer buffer (Amersham system). After transfer, the membranes were blocked with 10% powder milk in TBST for 1h, incubated overnight with polyclonal antibodies (diluted 1:10,000 in 10% powder milk + TBST) against the candidate r-protein, washed with TBST (6x15 min.), followed by 1h incubation with HRP-conjugated secondary antibodies (Santa Cruz Biotechnology) diluted 1:5,000 in TBST, washed again with TBST (6x15min.) and developed by the chemiluminescence method (ECL kit, GE Healthcare).

### II.4.11. Translocation assays

The translocation state of the EF-G•ribosome complexes was assessed by the toe-printing method. The complexes for toe-printing were specifically assembled to mimic the conditions used in the crosslinking experiments (either for DSG or AzP crosslinking) with the exception that the mRNA had a DNA primer annealed to its 3' end previous to ribosomal complex assembly.

Firstly, the DNA primer (5'-TTT ATC TTC AGA AGA AAA AC-3') was radioactively labeled by 5' phosphorylation using $P^{32}$. The labeling reaction contained 1μM DNA primer, 10% v/v $\gamma P^{32}$-ATP (Perkin Elmer), 0.33U/μl T4 Polynucelotide Kinase (New England Biolabs), in 70mM Tris pH 7.5, 1mM $MgCl_2$, 5mM DTT and was incubated at 37°C for 1h, followed by quenching with 45mM EDTA pH 8.0, phenol and chloroform extractions (in 300mM NaoAc pH 5.4), and ethanol precipitation (10μg of glycogen was used a carrier). The labeled DNA primer (0.5μM) was then annealed to the mRNA (1μM) in 50mM Hepes-KOH pH 7.7, and 100mM $NH_4Cl$ by incubating at 60°C for 3 min, followed by cooling on ice, and adjusting the $MgCl_2$ concentration to the buffer used in the particular ribosome complex. After this step, the ribosomal complexes

were assembled as described for each individual crosslinker, to a final concentration of 1μM. The annealed DNA primer was extended using 0.35U/μl AMV Reverse Transcriptase (Roche Diagnostics) and 220μl each dNTP for 10 min, at 37°C, followed by denaturation in urea sample buffer, and separating on a 6% polyacrylamide – 7M urea gel.

### II.4.12. Ultrafiltration assay for EF-G binding to ribosomes

EF-G (1.5μM) was incubated with vacant 70S ribosomes (1.0μM) in 10μl of buffer 4 at 37 °C for 5 min. in the presence of either GTP or GDPNP (500μM) and/or antibiotics (see Fig. II.5.). After this incubation, all the reactions were diluted to 500μl of buffer 4, and filtered through Millipore filters (100 kDa exclusion limit) by centrifugation (10,000 rpm, 5 min., Eppendorf centrifuge). These filtration membranes allow free EF-G to pass through due its molecular weight of 78,686 Da, which is lower than the exclusion limit of the filters (100,000 Da). The material retained above the filter was separated by SDS-PAGE and stained with Coomassie brilliant blue. Bands corresponding to EF-G bound to the ribosomes and the r-protein L2 were quantified by densitometry (Bio-Rad model GS-800, analyzed with Quantity One software) and the binding efficiency was calculated as the fraction of bound EF-G relative to protein L2 for each lane, being expressed as a percentage in Fig. II.5. The r-protein L2 was chosen as a standard because it is stably bound to 70S, it is present in only one copy and it is well separated from the other r-proteins under these conditions. (Wilson and Nechifor, 2004)

## II.5. CONCLUSIONS

The non-site specific chemical crosslinking experiments identified four r-proteins (L6, L7/L12, L14, and S12) situated in the proximity of EF-G in both a pre- and a post-translocational state. When a site-specific crosslinker was used, five residues, situated in three different domain of EF-G were found to be near three of the previously identified r-proteins: residues 209 and 231 (either side of helix $A_{G'}$) are close to L7/L12, position 426 (helix $A_{III}$) is proximal to S12, while residues 627 and 637 (helix $A_V$) is crosslinked to L6.

## II.6. FUTURE DIRECTIONS

The following chapters will explore further the proposed interaction between the G' subdomain of EF-G and L7/L12. We chose to concentrate our attention on this particular result because of the key involvement of L7/L12 in EF-G functions.

The other potential interactions identified in this study are also worth pursuing in order to understand their functional consequence. EF-G residue 426, situated at the N-terminal end of helix $A_{III}$, lies in a relatively well conserved region with mixed charge characteristics. It is difficult to predict at this point how exactly it interacts with the globular domain of S12. The r-protein S12 appears to be functionally important for translocation, potentially by affecting the stability of A site tRNA binding to the 30S subunit (Cukras et al., 2003; Gavrilova et al., 1974). From this point of view, the interaction between domain III of EF-G and the r-protein S12 could be particularly important in deciphering the mechanism of translocation.

EF-G residues 627 and 637 (helix $A_V$) are part of a negatively charged region, which would be likely to interact with the positively charged tail of L6, which contains the highly conserved sequence KExKKK in bacteria. From the point of view of EF-G, there are two relatively well conserved residues D630 and D634, which may be part of the interaction surface. Mutating them to positively charged residues would probably efficiently disrupt the interaction between EF-G and L6 and may shine some light on the role of this interaction during translocation and maybe the role of L6 in gentamicin resistance. Unfortunately, the previously selected and characterized gentamicin resistant strains containing both the L6 tail deletions could not be obtained, and they are likely completely lost (Buckel et al., 1977; Davies et al., 1998). One could construct new clones, by genetically deleting parts of the L6 tail and testing their sensitivity to gentamicin. Upon reproduction of previous results, ribosomes can be purified from these bacterial strains and their behavior in translocation ca be assessed in both steady and pre-steady state experiments. Another interesting observation is the presence of two very well conserved arginines (R638 and R639) at the C-terminal end of helix $A_V$. These residues could also have important functional roles either by forming an interaction surface with rRNA elements and/or by disrupting the interaction with the L6 tail when it becomes necessary for EF-G to move/dissociate.

Lastly, the possibility of close proximity and potential interactions between EF-G and r-proteins S13 and S19 could give us further insights into the translocation mechanism and it should be tested further. An integrated possible model for translocation may predict that the GTP hydrolysis causes a cascade of conformational changes which are channeled through switch 2 to helix $A_{III}$, being able to re-position domain III and determine further conformational changes in the r-protein S12 and potentially domain IV of EF-G. The interaction between domain III and S12 may change the affinity of A site tRNA for the 30S subunit A site, while domain IV may interact with both S13 and S19, inducing further conformational changes in these proteins, which could lead to decreased affinity of the now de-acylated tRNA for the 30S subunit P site. Another consequence could be changes in the position of the globular domains of both S13 and S19 with dramatic results in inter-subunit bridges, explaining in part the ratcheting motion observed by the cryo-EM studies. The interaction surface between domain V of EF-G and elements of the 50S subunit (23S rRNA and r-protein L6) may stabilize an open EF-G conformation, in which domain V of EF-G breaks away from the G domain, potentially working together with domain III to the re-position the tip of the domain IV next to the 30S subunit P site.

## II.7. REFERENCES

Agrawal, R. K., Heagle, A. B., Penczek, P., Grassucci, R. A., and Frank, J. (1999). EF-G-dependent GTP hydrolysis induces translocation accompanied by large conformational changes in the 70S ribosome. Nat Struct Biol *6*, 643-647.

Agrawal, R. K., Linde, J., Sengupta, J., Nierhaus, K. H., and Frank, J. (2001). Localization of L11 protein on the ribosome and elucidation of its involvement in EF-G-dependent translocation. J Mol Biol *311*, 777-787.

Agrawal, R. K., Penczek, P., Grassucci, R. A., and Frank, J. (1998). Visualization of elongation factor G on the *Escherichia coli* 70S ribosome: the mechanism of translocation. Proc Natl Acad Sci U S A *95*, 6134-6138.

Bodley, J. W., Zieve, F. J., Lin, L., and Zieve, S. T. (1969). Formation of the ribosome-G factor-GDP complex in the presence of fusidic acid. Biochem Biophys Res Commun *37*, 437-443.

Buckel, P., Buchberger, A., Bock, A., and Wittmann, H. G. (1977). Alteration of ribosomal protein L6 in mutants of *Escherichia coli* resistant to gentamicin. Mol Gen Genet *158*, 47-54.

Cabanas, M. J., Vazquez, D., and Modolell, J. (1978). Inhibition of ribosomal translocation by aminoglycoside antibiotics. Biochem Biophys Res Commun *83*, 991-997.

Cukras, A. R., Southworth, D. R., Brunelle, J. L., Culver, G. M., and Green, R. (2003). Ribosomal proteins S12 and S13 function as control elements for translocation of the mRNA:tRNA complex. Mol Cell *12*, 321-328.

Davies, C., Bussiere, D. E., Golden, B. L., Porter, S. J., Ramakrishnan, V., and White, S. W. (1998). Ribosomal proteins S5 and L6: high-resolution crystal structures and roles in protein synthesis and antibiotic resistance. J Mol Biol *279*, 873-888.

Diaconu, M., Kothe, U., Schlunzen, F., Fischer, N., Harms, J. M., Tonevitsky, A. G., Stark, H., Rodnina, M. V., and Wahl, M. C. (2005). Structural basis for the function of the ribosomal L7/12 stalk in factor binding and GTPase activation. Cell *121*, 991-1004.

Gao, H., Sengupta, J., Valle, M., Korostelev, A., Eswar, N., Stagg, S. M., Van Roey, P., Agrawal, R. K., Harvey, S. C., Sali, A., *et al.* (2003). Study of the structural dynamics of the *E. coli* 70S ribosome using real-space refinement. Cell *113*, 789-801.

Gavrilova, L. P., Koteliansky, V. E., and Spirin, A. S. (1974). Ribosomal protein S12 and 'non-enzymatic' translocation. FEBS Lett *45*, 324-328.

Girshovich, A. S., Kurtskhalia, T. V., Ovchinnikov Yu, A., and Vasiliev, V. D. (1981). Localization of the elongation factor G on *Escherichia coli* ribosome. FEBS Lett *130*, 54-59.

Hartz, D., McPheeters, D. S., Traut, R., and Gold, L. (1988). Extension inhibition analysis of translation initiation complexes. Methods Enzymol *164*, 419-425.

Joseph, S., and Noller, H. F. (1998). EF-G-catalyzed translocation of anticodon stem-loop analogs of transfer RNA in the ribosome. EMBO J *17*, 3478-3483.

Kothe, U., Wieden, H. J., Mohr, D., and Rodnina, M. V. (2004). Interaction of helix D of elongation factor Tu with helices 4 and 5 of protein L7/12 on the ribosome. J Mol Biol *336*, 1011-1021.

Laurberg, M., Kristensen, O., Martemyanov, K., Gudkov, A. T., Nagaev, I., Hughes, D., and Liljas, A. (2000). Structure of a mutant EF-G reveals domain III and possibly the fusidic acid binding site. J Mol Biol *303*, 593-603.

Maassen, J. A., and Moller, W. (1974). Identification by photo-affinity labeling of the proteins in *Escherichia coli* ribosomes involved in elongation factor G-dependent GDP binding. Proc Natl Acad Sci U S A *71*, 1277-1280.

Maassen, J. A., and Moller, W. (1978). Elongation factor G-dependent binding of a photoreactive GTP analogue to *Escherichia coli* ribosomes results in labeling of protein L11. J Biol Chem *253*, 2777-2783.

Maassen, J. A., and Moller, W. (1981). Photochemical cross-linking of elongation factor G to 70-S ribosomes from *Escherichia coli* by 4-(6-formyl-3-azidophenoxy)butyrimidate. Eur J Biochem *115*, 279-285.

Martemyanov, K. A., and Gudkov, A. T. (2000). Domain III of elongation factor G from *Thermus thermophilus* is essential for induction of GTP hydrolysis on the ribosome. J Biol Chem *275*, 35820-35824.

Mohr, D., Wintermeyer, W., and Rodnina, M. V. (2002). GTPase activation of elongation factors Tu and G on the ribosome. Biochemistry *41*, 12520-12528.

Nechifor, R., and Wilson, K. S. (2007). Crosslinking of translation factor EF-G to proteins of the bacterial ribosome before and after translocation. J Mol Biol *368*, 1412-1425.

Ogle, J. M., Brodersen, D. E., Clemons, W. M., Jr., Tarry, M. J., Carter, A. P., and Ramakrishnan, V. (2001). Recognition of cognate transfer RNA by the 30S ribosomal subunit. Science *292*, 897-902.

Savelsbergh, A., Mohr, D., Kothe, U., Wintermeyer, W., and Rodnina, M. V. (2005). Control of phosphate release from elongation factor G by ribosomal protein L7/12. EMBO J *24*, 4316-4323.

Selmer, M., Dunham, C. M., Murphy, F. V. t., Weixlbaumer, A., Petry, S., Kelley, A. C., Weir, J. R., and Ramakrishnan, V. (2006). Structure of the 70S ribosome complexed with mRNA and tRNA. Science *313*, 1935-1942.

Skold, S. E. (1982). Chemical cross-linking of elongation factor G to both subunits of the 70-S ribosomes from *Escherichia coli*. Eur J Biochem *127*, 225-229.

Spedding, G. (1990). Isolation and analysis of ribosomes from prokaryotes, eukaryotes, and organelles (Oxford: Oxford University Press).

Stoffler, G., and Wittmann, H. G. (1971). Ribosomal proteins. XXV. Immunological studies on *Escherichia coli* ribosomal proteins. J Mol Biol *62*, 407-409.

Tokimatsu, H., Strycharz, W. A., and Dahlberg, A. E. (1981). Gel electrophoretic studies on ribosomal proteins L7/L12 and the *Escherichia coli* 50 S subunit. J Mol Biol *152*, 397-412.

Valle, M., Zavialov, A., Sengupta, J., Rawat, U., Ehrenberg, M., and Frank, J. (2003). Locking and unlocking of ribosomal motions. Cell *114*, 123-134.

Vicens, Q., and Westhof, E. (2003). Crystal structure of geneticin bound to a bacterial 16S ribosomal RNA A site oligonucleotide. J Mol Biol *326*, 1175-1188.

Wilson, K. S., and Nechifor, R. (2004). Interactions of translational factor EF-G with the bacterial ribosome before and after mRNA translocation. J Mol Biol *337*, 15-30.

Wilson, K. S., and Noller, H. F. (1998). Mapping the position of translational elongation factor EF-G in the ribosome by directed hydroxyl radical probing. Cell *92*, 131-139.

# III. INTERACTION SURFACE BETWEEN SUBDOMAIN G' OF EF-G AND THE RIBOSOMAL PROTEIN L7/L12

## III.1. INTRODUCTION

In our previous crosslinking study (chapter II), EF-G was shown to be in close proximity to the r-protein L7/L12. This r-protein is a major component of the L7/L12 stalk, which contains the r-protein L11, the rRNA region providing binding sites for L11 and L10, as well as a protein complex composed of L10 and several copies of the r-protein L7/L12, the number varying between different bacterial species (e.g. four copies in *E. coli* 70S, 6 copies in *T. maritima* (Diaconu et al., 2005)).

L7/L12 has been the center of multiple studies since it was shown to play a key role in the ribosomal activation of GTP hydrolysis in factors (Hamel et al., 1972). Although believed at first to be two distinct r-proteins due to their slightly different isoelectric point (Moller et al., 1972), L7 has the same primary structure as L12, the only difference being the acetylation of Ser2 in L7. Some studies have shown that the quatity ratio between L7 and L12 varies with different growth conditions (Deusser and Wittmann, 1972; Ramagopal and Subramanian, 1974), but the role for the presence of these two isoforms of the same r-protein on the ribosome is not clear at the moment. The structure of L7/L12 is composed of an N-terminal domain (NTD) and a C-terminal domain (CTD), which are connected by a flexible hinge region (Liljas and Gudkov, 1987). The NTD spontaneously dimerizes and contains the L10 binding site, which interacts with specific sites on helix 8 of L10 (Diaconu et al., 2005). CTD has a globular, α helical structure and it is the part of L7/L12 proven to be essential for activation of GTP hydrolysis in factors. The hinge region (18 amino acids long) connecting the NTD and CTD of L7/L12 can adopt either an α helical structure (compact conformation) or a disordered structure (extended conformation). NMR studies (Bocharov et al., 2004) have solved the structure of L7/L12 dimer in isolation from the rest of the ribosome, showing that there are two major conformations which can be encountered: one monomer in compact structure and the other one in an extended conformation, or both monomers in an extended conformation. Due to space infringements, both monomers cannot be in the compact conformation (Bocharov et al., 2004). Recent cryo-EM studies on ribosomal complexes have suggested that the L7/L12 stalk region of the 50S subunit resembles a molecular octopus, with the NTD of L7/L12 extending in solution away from the

ribosome and its CTD possibly providing the first association points with the translation factors (Diaconu et al., 2005).

L7/L12 sequence is very well conserved among different bacteria, the only variable region being represented by the hinge region. Mutation studies have shown that the sequence of this region and its mobility properties are not important for the function of L7/L12, due to the fact that replacing 7 amino acids of its structure with a chain of 7 proline residues did not modify its activity (Dey et al., 1995). It appears that the most important structural element is the length of the hinge region: eliminating it completely prevents proper association with L10, while deletion of 11 amino acids from its structure allows the L7/L12 mutants to bind in 4 copies to the ribosomal complex, but the reconstituted ribosomes are not active in protein synthesis (Oleinikov et al., 1993b).

Another interesting question is represented by the role of the multiple copies of L7/L12 on the ribosomal complex. Functional studies have shown that protein synthesis is not affected when the CTDs belonging to the same L7/L12 dimer are linked by a covalent bond, indicating that their complete mobility regarding one another is not absolutely required for activity (Oleinikov et al., 1993a). Interestingly, only two L7/L12 CTDs per ribosome (as compared to the normal four) are enough to sustain similar *in vitro* polyphenylalanine synthesis rates as control ribosomes (Oleinikov et al., 1998). Although these *in vitro* studies suggest that not all L7/L12 copies are necessary for protein synthesis, the situation *in vivo* may still require all these copies under certain growth conditions which are not currently identified.

Our previous crosslinking experiments identified L7/L12 to be in close proximity to the G' subdomain of EF-G, and in particular to residues 209 and 231, which flank helix $A_{G'}$. In the current chapter, a more detailed picture of the interaction between the G' subdomain of EF-G and L7/L12 was obtained by additional crosslinking experiments using new cysteine mutants constructed in other structural elements of the G' subdomain. The functional analysis of the crosslinking product between EF-G(231C) and L7/L12 yielded interesting results, with important insights into the extent of the L7/L12 mobility.

## III.2. RESULTS

### III.2.1. Proximity between residues 209 and 231 of the G' subdomain and the r-protein L7/L12

The crosslinking results presented in the previous chapter showed proximity between helix A of G' subdomain and the r-protein L7/L12 and strongly suggested interaction due to the relative short length of the crosslinkers arms (8, and respectively 11Å). EF-G(231C)-AzP had the highest crosslinking efficiency from all our positive crosslinking sites, so it seemed more likely for this position to be part of the interaction surface between EF-G and the r-protein L7/L12. In spite of these arguments, a high crosslinking efficiency does not absolutely prove the existence of an interaction between these two elements, as is the case with the majority of crosslinking techniques. This is especially true in the case of the r-protein L7/L12, which has a very mobile structure and was shown to crosslink to r-proteins situated at a large distance from the L7/L12 stalk region (Traut et al., 1995).

If these cysteine residues (209 and 231) are truly part of the interaction surface, they should be protected by L7/L12 from modification with a cysteine specific probe. We chose to examine the surface accessibility of cysteine residues by using a combination of two cysteine specific probes, iodoacetamide (IA) and NTCB (2-Nitro-5-thiocyanatobenzoic acid), using a protocol (Fig. III.1.) developed by (Silverman and Harbury, 2002). In their method, iodoacetamide specifically reacts with the thiol group of solvent exposed cysteines, while NTCB is used to identify the presence of the iodoacetamide modifications on the denatured polypeptide chain (Fig. III.1.). NTCB reacts specifically with the thiol group of cysteine residues, only if they have not been previously modified by iodoacetamide. In order to eliminate the restrictions imposed by the position of the cysteines in the tertiary fold of the protein, NTCB reaction is started together or just after protein denaturation (Fig. III.1.), and it results in the cyanilation of the protein. These cyanilated products undergoe re-arrangements under alkaline conditions (Fig. III.1.) leading to either a break in the polypeptide chain at the N-terminus of the cysteine residue (which can be separated by SDS-PAGE and detected by staining with Commassie blue) or to a β elimination reaction, which conserves the polypeptide

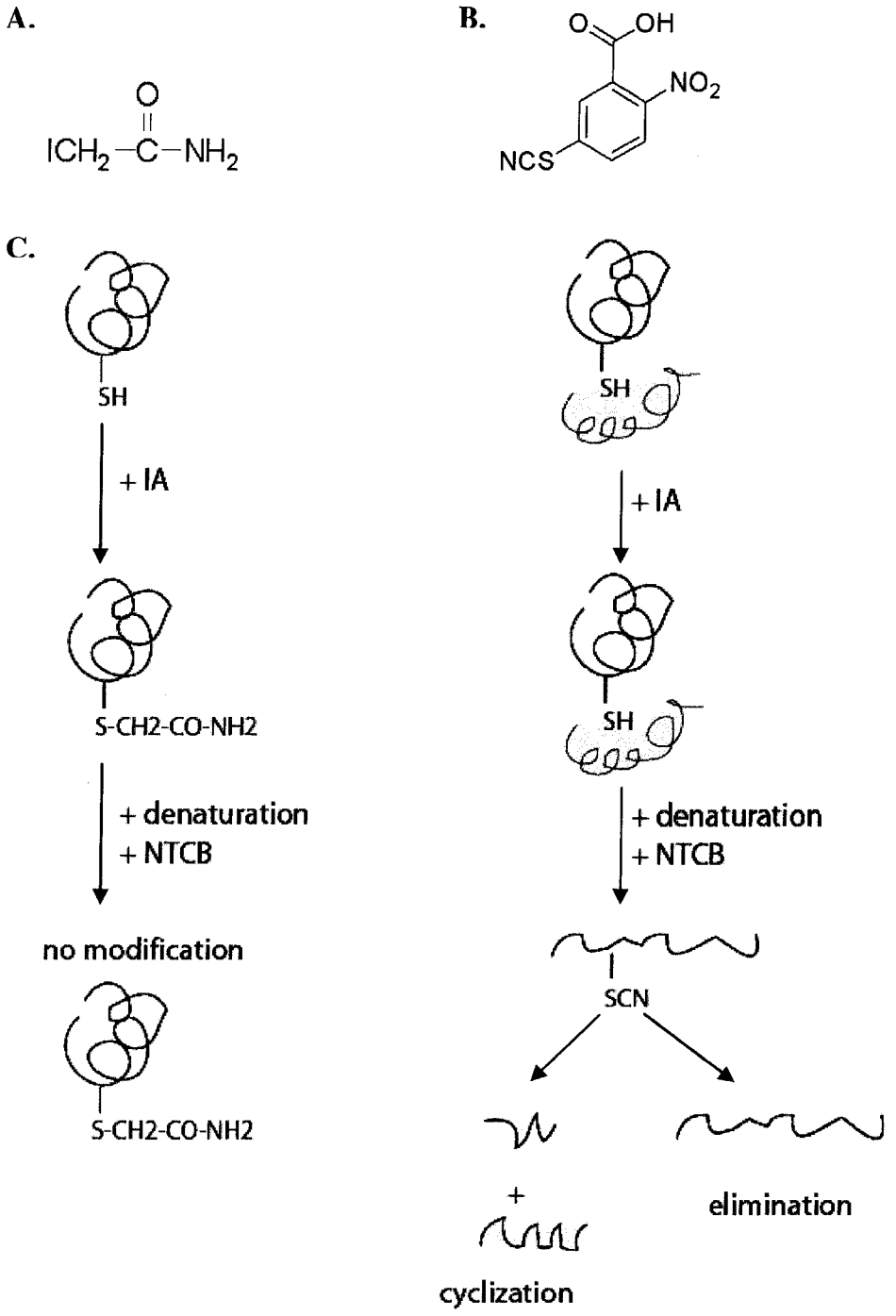


**Fig. III.1 – The method for testing the solvent accessibility of cysteine side chains using iodoacetamide and NTCB.** *A.* The structure of iodoacetamide (IA) (www.sigmaaldrich.com). *B.* The structure of NTCB (www.sigmaaldrich.com). *C.* The steps in the protocol described by (Silverman and Harbury, 2002). On the left side, the cysteine is solvent exposed, while on the right side of this figure the cysteine is buried. The side chain of the cysteine residue is represented by SH. Denaturation of the tested protein is accomplished by GdmCl or SDS, added together with or just before NTCB (see Methods).

chain (not detectable by SDS-PAGE) (Degani and Patchornik, 1974). There is no preference between the cleavage and the elimination reaction, but the addition of ammonium ions is believed to favor the cleavage reaction (Jacobson et al., 1973).

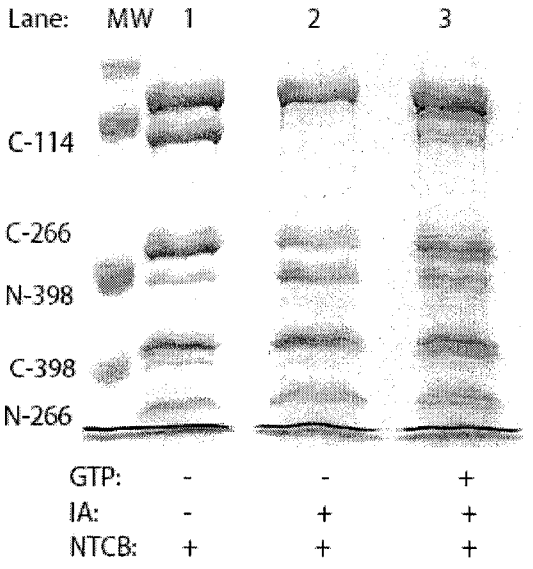


**Fig. III.2. – 7.5% SDS-PAGE stained with Coomassie blue separating the NTCB cleavage fragments of EF-Gwt under different conditions (as labeled).** All reactions were denatured with 7M Guanidium chloride before NTCB treatment. The resultant cleavage fragments were labeled according to the number of the cysteine residue, N indicating an N-terminal fragment, while C represents a C-terminal fragment. The N terminal fragment of cysteine 114 is too small to be separated by this gel and runs together with the dye front. It can be observed using a 10% SDS-PAGE (data not shown).

In order to test this previously developed protocol (Silverman and Harbury, 2002) in our particular system, wildtype EF-G was used to assess the specificity and efficiency of the NCTB cleavage reaction (Fig. III.2.). EF-Gwt contains three naturally occurring cysteines situated in the G domain (C114 and C266) and in domain II (C398). In the absence of iodoacetamide and under denaturing conditions, they all react with NTCB, resulting in cleavage products of different molecular weights, which were easy to separate by SDS-PAGE (Fig. III.2. – lane1). The same experiment was repeated with the cysteineless version of EF-G, no cleavage fragments being observed for this protein (data

not shown). These experiments confirmed that NTCB is specific to cysteines under our experimental conditions and that it can react with all of the naturally occurring cysteines under denaturing conditions.

We also tested the ability of the iodoacetamide to be sensitive to the environment of a particular cysteine residue. To that end, EF-Gwt was incubated briefly with iodoacetamide on ice, the reaction being quenched with a reducing agent, followed by the reaction with NTCB under denaturing conditions. The cleavage reaction was separated on SDS-PAGE (Fig. III.2. - lane 2) and visualized by staining with Commassie blue. Comparing lanes 1 and 2 in Fig III.2., it is clear that after iodoacetamide treatment, cysteine 114 is no longer cleaved by NTCB, while cysteines 266 and 398 continue to be cleaved by NTCB, with a decrease in the cleavage efficiency in the case of cysteine 266. These results are in complete accord with the crystal structure of *T. thermophilus* EF-G (Laurberg et al., 2000), indicating that C114 is solvent exposed, while C398 is buried in domain II, and C266 appears to be partially solvent exposed.

One last test of the IA/NTCB cleavage method was to determine if a cysteine can be protected from iodoacetamide modification by a ligand. C114 is next to the guanosine binding site in EF-G and it has been shown previously to be protected from modification by the presence of GTP bound to EF-G (Marsh et al., 1975). In order to confirm the previous result under our experimental conditions, EF-G•GTP complex was treated with iodoacetamide/NTCB as above and the reaction separated by SDS-PAGE. Upon staining with Commassie blue, the cleavage product of C114 was visible again (Fig. III.2. – lane 3), showing that GTP can protect C114 from iodoacetamide modification, leaving it free to react with NTCB and become cleaved afterwards. In spite of a great excess of GTP over EF-G, the protection obtained was only partial, also in line with the fact that C114 does not directly interact with the guanosine (Laurberg et al., 2000), its protective effect being due most likely to steric hindrance and creation of a hydrophobic pocket.

In order to test the solvent accessibility of residues 209 and 231, these EF-G cysteine mutants were bound to ribosomal complex using either GDPNP or GTP/fusidic acid, followed by a brief reaction with iodoacetamide on ice, denaturation and NTCB reaction. The NTCB products were allowed to re-arrange overnight under alkaline pH conditions and in the presence of ammonium ions, being separated the next day by SDS-

PAGE. Due to the presence of ribosomes in our reactions, the original protocol had to be modified, guanidium chloride not being able to provide proper denaturation of the complexes and it was substituted by SDS and heating (see Materials and Methods).

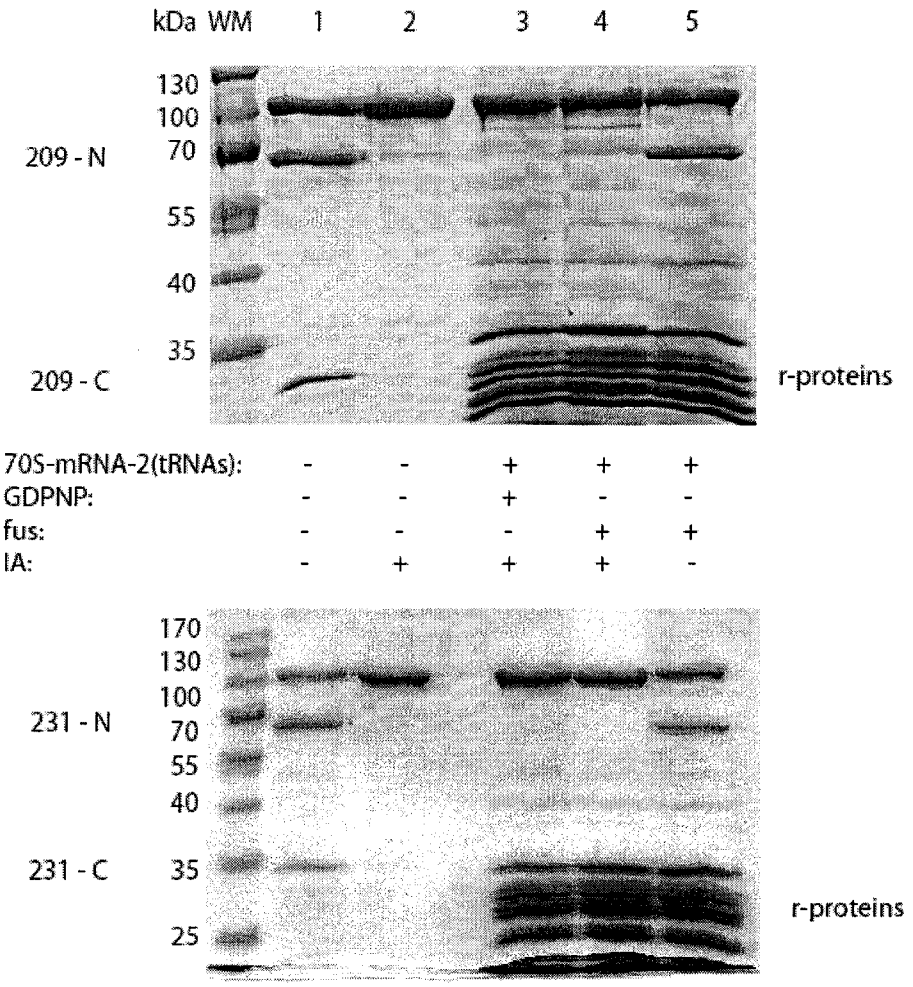


**Fig. III.3. – IA/NTCB probing of the solvent accessibility of EF-G cysteine mutants 209 and 231 under different conditions.** The order of reactions is identical between the two gels shown in this figure. The N-terminal fragment is represented by the number of the cysteine mutant followed by N, while 209-C and 231-C indicate the C terminal fragments.

The NTCB positive cleavage control (Fig. III.3. – lane 1) demonstrates that both EF-G(209C) and EF-G(231C) react well with NTCB under denatured form in solution and in the absence of iodoacetamide, the cleavage efficiency being approximately 50% as

estimated by SDS-PAGE. It is also obvious that both 209 and 231 positions are solvent accessible in the absence of ribosomes, reacting to completion with iodoacetamide (Fig. III.3. - lane 2), as predicted by the crystal structure (Laurberg et al., 2000). The NTCB cleavages of these cysteine mutants proceeded with equivalent efficiency in the presence of ribosomes, although the r-proteins contain additional cysteine targets that may compete for NTCB (Fig. III.3.-lane 5). In the case of EF-G(231C), there are no cleavage bands in the presence of iodoacetamide, in either the GDPNP or the fus complex, demonstrating that in both of these complexes, residues 231 is solvent accessible. Interestingly, EF-G(209C) shows a very faint cleavage band in the GDPNP complex, while the same band becomes reproducibly stronger in the fus complex. The intensity of the 209C cleavage bands were estimated by densitometry measurements, being expressed as a percent of the sum between the intensity of the full length EF-G and the cleaved fragment. These measurements confirmed that, in the case of the fus state, the cleavage efficiency is approximately three times increased as compared to the GDPNP complex.

Although the differences observed are rather subtle, we believe them to reflect the reality of these complexes due to their highly reproducible nature. Our attempts of improving the iodoacetamide probing of these complexes by using lower concentrations of iodoacetamide and shorter incubation times have failed to produce larger differences (data not shown).

The correct assembly of these ribosomal complexes in the presence of EF-G209C and EF-G231C was tested by toe-printing, as previously described (Chapter II). The toe-printing gel confirmed that, for both of these two EF-G cysteine mutants, the GDPNP complex corresponds to a pre-translocational state, while in the fus complex, the vast majority of the complex is in a post-translocational position (data not shown).

In order to test if the differences observed in the case of EF-G209C were due to the presence of the r-protein L7/L12, the ribosomal complexes were assembled using L7/L12 stripped 70S, and the reactions repeated as above (Fig. III.4.). Under these conditions, there is no difference in the very faint cleavage efficiency observed between the GDPNP and the fus complex for both EF-G(209C) and EF-G(231C).

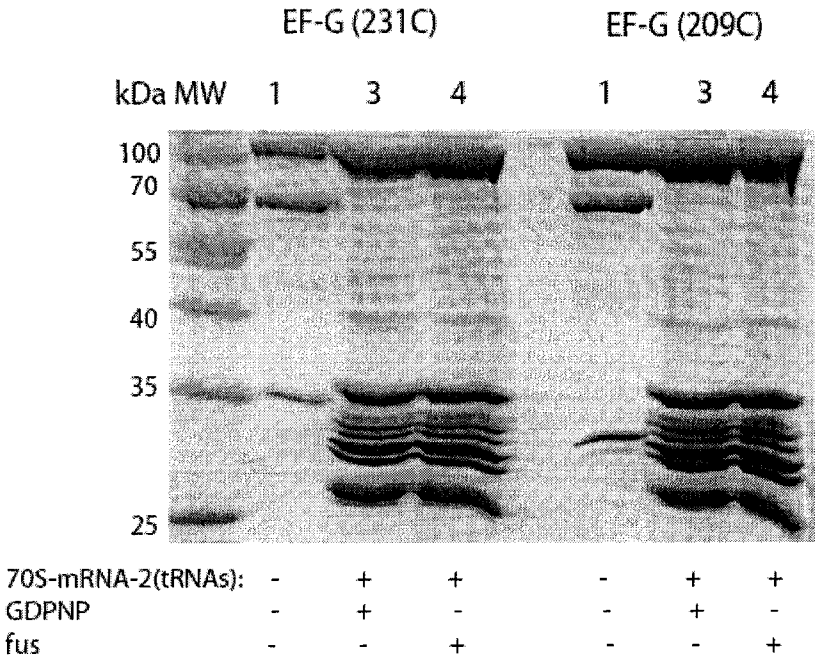


**Fig. III.4. – The IA/NTCB cleavage in the presence of L7/L12 depleted 70S ribosomes.** The lane numbers correspond to the ones in Fig. III.4.

### III.2.2. Identification of the elements of the G' subdomain situated in the vicinity of the r-protein L7/L12

Our initial crosslinking study contained only three cysteine mutants (residues 196, 209 and 231) situated in the G' subdomain. Position 196, part of a loop connecting two β sheets, did not form any crosslinking products with r-proteins, negative result consistent with its previous positioning next to rRNA elements, namely the SRL (Wilson and Noller, 1998). Residues 209 and 231 are situated on either side of helix A of the G' subdomain and they both crosslinked to the r-protein L7/L12, suggesting that helix $A_{G'}$ is part of the interaction surface with the r-protein L7/L12. There are also additional structural elements of the G' subdomain situated in close proximity to helix $A_{G'}$, which could be potentially involved in the interaction with the r-protein L7/L12.

In order to properly define the interaction surface between the G' subdomain of EF-G and the r-protein L7/L12, we constructed seven additional cysteine mutants (175, 203, 221, 234, 241, 246, and 260), by replacing solvent exposed, non-conserved residues of the G' subdomain (Fig. III.5.). These residues were selected so that they cover all the

surface exposed structural elements of the G' subdomain (Fig. III.5.). The newly constructed single cysteine mutants were purified, labeled with AzP and bound to the ribosomal complex in the GDPNP and fus complex as previously described in Chapter II.

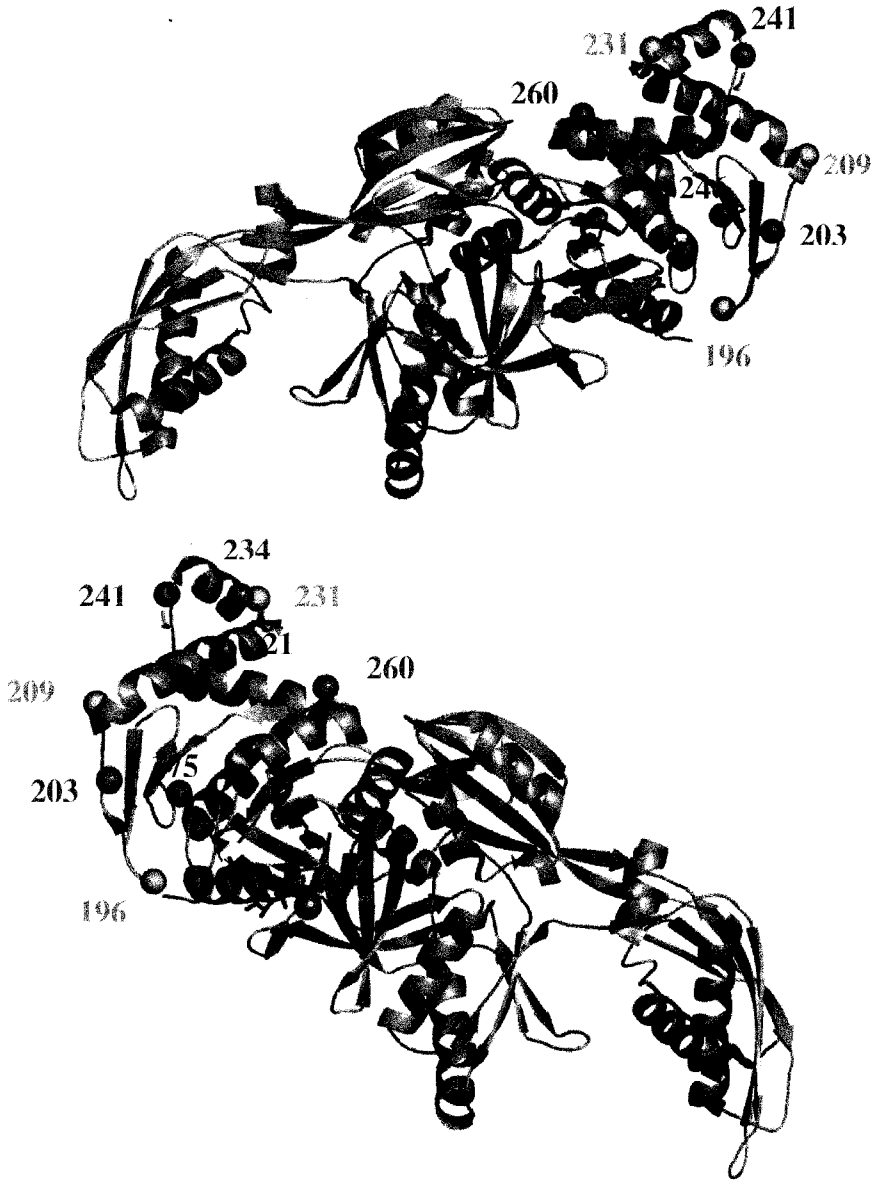


**Fig. III.5. – Cartoon of EF-G showing the position of the cysteine residues used in the crosslinking experiments.** The orange spheres represent the previously constructed cysteine mutants, while the magenta ones indicate the position of the newly created cysteine mutants. The $Mg^{2+}$ ion is represented by a grey sphere and the GDP is in blue sticks. Figure was created using PyMOL (http://pymol.sourceforge.net/) and it is based on pdb 1FNM (Laurberg et al., 2000).

Residues 175 and 203, part of two different loops connecting structural elements of the G' subdomain, as well as residue 260, situated at the C terminus of helix C, did not provide any positive crosslinking products (data not shown). In contrast, when using AzP-modified cysteine mutants at positions 221 (helix A), 234 (N terminal of helix B), 241 (C terminal of helix B), and 246 (N-terminal of helix C), we obtained crosslinking products, migrating slower than the full length EF-G (Fig. III.6. and 7). The observed crosslinks had different efficiencies, residues 234 and 241 producing more intense crosslinking bands than residues 221 and 246. It was also obvious that the crosslinking product involving EF-G(246C) migrated slower in the SDS-PAGE than the rest of the newly obtained crosslinks.

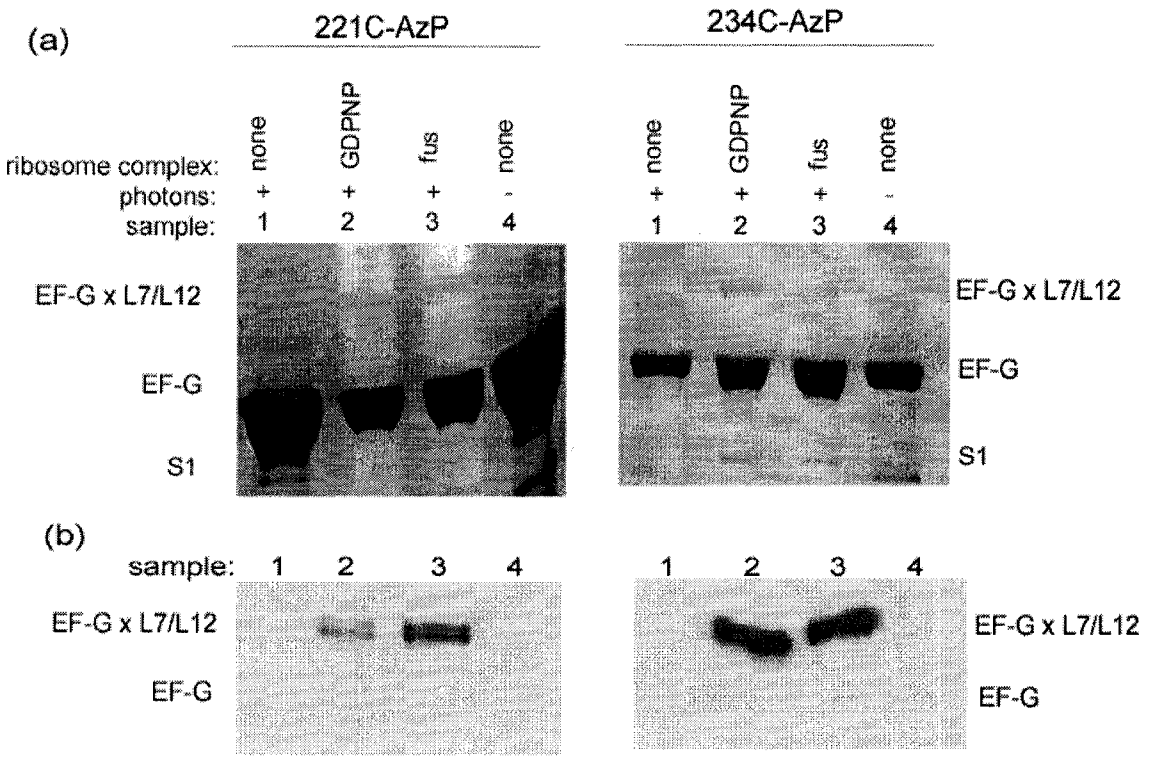


**Fig. III.6. - Site-specific crosslinking of L7/L12 from EF-G residues 221 and 234.** (a) Gels stained with Coomassie brilliant blue. (b) Immunoblots probed with anti-L7/L12 antibody. Crosslinked products are denoted by **x**. *Sample 1*, AzP modified cysteine mutant, protein alone, exposed to UV light. *Sample 2*, AzP modified cysteine mutant bound to the ribosome in the GDPNP state, exposed to UV light. *Sample 3*, AzP modified cysteine mutant, bound to the ribosome in the fus state, exposed to UV light. *Sample 4*, AzP modified cysteine mutant, purified protein alone, without exposure to UV light.

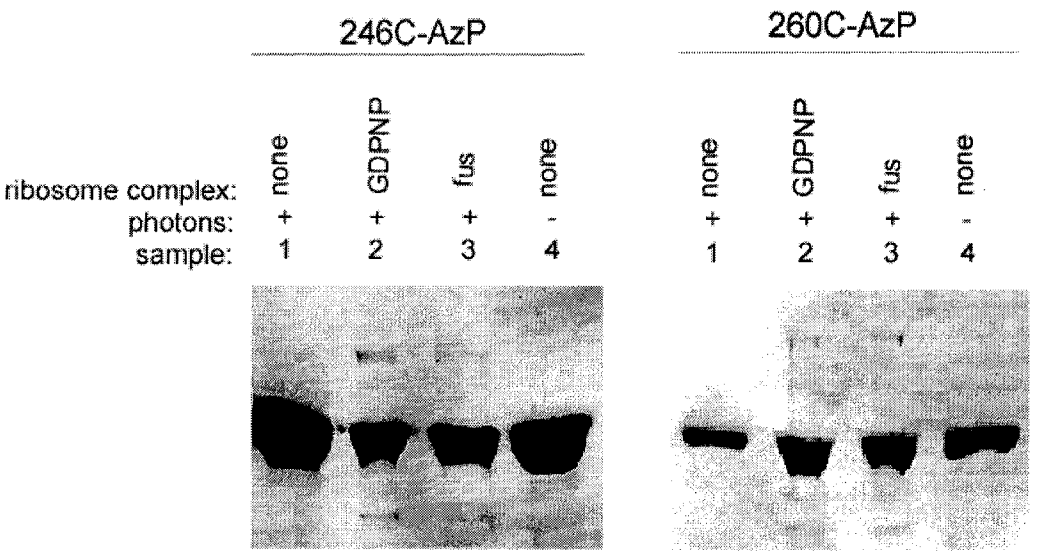


**Fig. III.7. - Site-specific crosslinking of L7/L12 from EF-G residues 241 and 246.** (a) Gels stained with Coomassie brilliant blue. (b) Immunoblots probed with anti-L7/L12 antibody. Crosslinked products are denoted by **x**. Sample numbers correspond to the ones in Fig. III.7.

In order to verify that the new cysteine mutants crosslink also to the r-protein L7/L12, similar crosslinking reactions were separated on SDS-PAGE, processed for immuno-blotting and probed with anti-L7/L12 antibodies. The crosslinking products of all four cysteine mutants (221, 234, 241 and 246) reacted with the anti-L7/L12 antibodies, demonstrating that the crosslinking partner is indeed the r-protein L7/L12 (Fig. III.7. and 8). The anti-L7/L12 antibody was proven previously to recognize only the r-protein L7/L12 under our experimental conditions (Fig. II.4.), in spite of its polyclonal nature.

### III.2.3. Exploring the interaction between EF-G and the r-protein L7/L12 from the perspective of L7/L12

Our crosslinking experiments have mapped the interaction surface between EF-G and the r-protein L7/L12 to elements of G' subdomain. In order to obtain a full understanding of the interaction between EF-G and L7/L12, it is important to describe the interaction surface from the perspective of L7/L12. Based on previous studies, it is likely that the CTD of the L7/L12 contains the region interacting with the G' subdomain due to

the fact that it is essential for activating the GTP hydrolysis. A mutational study on EF-Tu and L7/L12 showed that helices 4 and 5 of the CTD of L7/L12 interact with EF-Tu, using hydrophobic interactions stabilized by salt bridges (Kothe et al., 2004). By analogy, it is possible that the positively charged patch on the helices 4 and 5 of the CTD represents also the interaction partner of the negatively charged surface on the G' subdomain of EF-G.

In order to investigate further the interaction between EF-G and the r-protein L7/L12, we started from a previous observation, in which it was noticed that the r-protein L7/L12 had different protease cleavage profile between different states of the ribosome•EF-G complex (Gudkov and Gongadze, 1984). According to their study, trypsin susceptibility of L7/L12 was very high in a pre-translocation complex (EF-G•GMPPCP•70S), while L7/L12 was resistant to trypsin attack in both the absence of EF-G and in the fus complex (Gudkov and Gongadze, 1984). These changes in protease accessibility were interpreted to represent a conformational change of L7/L12 between the pre- and the post-translocational states.

Our first experiments were aimed at reproducing these results in hope that the cleaved peptide could be separated and analyzed in order to identify the position of this proposed conformational change. Unfortunately, no cleavage of L7/L12 by trypsin could be identified by our immunoblotting experiments in any of the probed complexes: 70S in the absence of EF-G, EF-G•GDPNP•70S, and EF-G•GDP•fusidic acid•70S (data not shown). Interestingly, the same reactions separated by SDS-PAGE after trypsin cleavage revealed a differential cleavage of EF-G between the GDPNP and the fus complex, with EF-G being protected from trypsin attack in the GDPNP state and cleaved by trypsin in the fus complex (Fig. III.8B). The SDS-PAGE in Fig. III.8B shows the 15 min. time point. One obvious difference between these two complexes is the presence of different nucleotides, so we tested trypsin cleavage of EF-G in solution bound to either GTP or GDP, or the absence of nucleotides. As seen in Fig. III.8A, the partial trypsin cleavage of EF-G in solution is not modified by the presence or absence of any nucleotides, so the difference observed in the ribosomal complexes is due most likely to the presence of 70S.

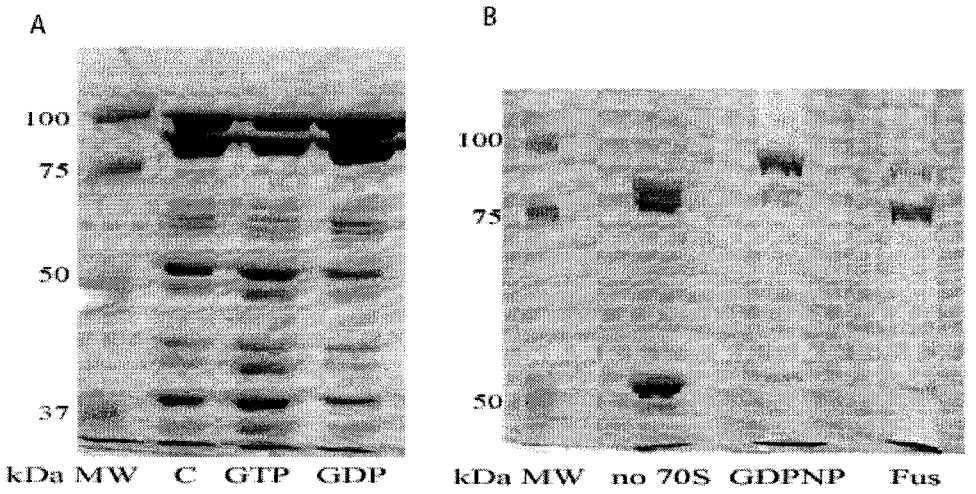


**Fig. III.8. – Trypsin digestion of EF-G under different conditions.** (A) Commassie blue stained 7.5% SDS-PAGE showing the partial trypsin cleavage of EF-G in solution in the presence of either no nucleotide (C), GTP or GDP; (B) Comassie blue stained 6% SDS-PAGE comparing the trypsin cleavage of EF-G free in solution (no 70S) with the cleavage obtained when EF-G is bound to the ribosome (GDPNP and fus complexes).

In order to explore further this difference in trypsin accessibility, we repeated the same experiments with a different protease, protease V8, which has a glutamic and aspartic acid specificity. By using protease V8, there was no difference in EF-G accessibility between the GDPNP and fus complex, both complexes being cleaved at the same rate (data not shown).

Next, we tried to determine if this difference in trypsin accessibility is dependent on the presence of L7/L12. To that end, we repeated the trypsin cleavage experiment using ribosomes stripped of L7/L12 and compared them to the control ribosomes. There was no difference between the complexes assembled with control ribosomes and the ones assembled with L7/L12 depleted ribosomes, when it came to EF-G cleavage by trypsin. The partial protection in the GDPNP state is still present in the absence of L7/L12 from the ribosomal complex (Fig. III.9A).

In order to investigate further the properties of the EF-G fragment produced by trypsin digestion in the fus complex, we used an ultrafiltration technique. The EF-G•70S complexes were assembled and digested with trypsin as before. The trypsin cleavage was stopped by addition of trypsin inhibitor, followed by ultrafiltration of the digested

reactions and separation of the retained products. As seen in Fig. III.9B, the EF-G fragment was retained on top of the filtration membrane, suggesting that it retains the ability to bind to the ribosome.

In order to identify the cleavage site, the EF-G fragment was separated by SDS-PAGE, transferred to a PVDF membrane, and sequenced by Edman degradation. The cleavage site was identified to be in switch 1 of EF-G, between Arg59 and Gly60 (Fig. III.9C), a region of domain G of EF-G believed to change conformations upon GTP hydrolysis.

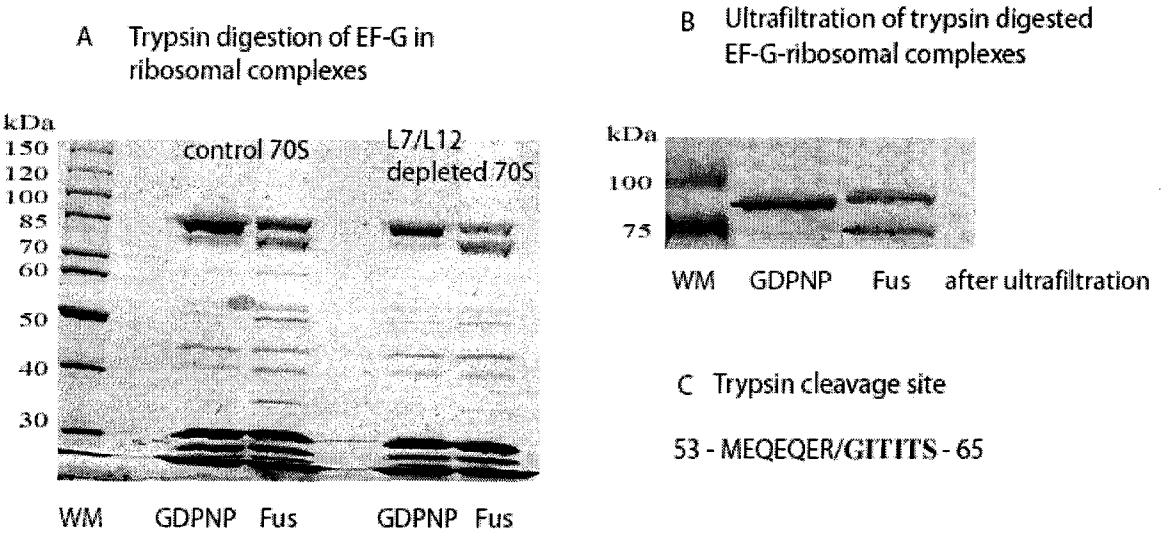


**Fig. III.9. – Tryspin digestion of EF-G in complex with ribosomes.** (A) Trypsin digestion of EF-G in the GDPNP and fus complexes comparing control ribosomes with ribosomes stripped of L7/L12. (B). SDS-PAGE separation of products retained by the ultrafiltration membrane. (C). The trypsin cleavage site as provided by the sequencing of the cleavage fragment by Edman degradation.

In parallel with the previously described experiments, other various techniques were tried in order to determine the region in L7/L12 which interacts with EF-G. These experiments used EF-G(231C), which was our first cysteine mutant to provide a strong crosslink with the r-protein L7/L12. One of the first techniques attempted was the use of hydroxyl radicals to cleave the peptide bonds in L7/L12 closest in space to residue 231C from EF-G. Although originally employed in our lab for cleaving RNA (Wilson and

Nechifor, 2004), this technique has been successfully utilized previously on other protein complexes in order to define their interactions (Miyake et al., 1998). To that end, we used Fe-BABE to modify the side chain of residue 231C, followed by assembly of the EF-G(231C-Fe-BABE)•70S complexes and activation of the hydroxyl radical cleavages by the mixture of ascorbic acid and hydrogen peroxide. Unfortunately, we were not able to find a specific cleavage fragment of L7/L12, which was dependent on the presence of the cysteine residue, FE-BABE, and the cleavage mixture.

We next tried to analyze the crosslinking product between EF-G(231C)-AzP and L7/L12 by mass spectrometry techniques, in order to identify the peptide of L7/L12 which participates in the crosslinking product. Several different experiments were attempted in collaboration with the Institute of Biomolecular Design and the laboratory of Dr. Li (Department of Chemistry). The majority of the work was focused on the identification of the crosslinked peptides by trying a variety of procedures: different proteases to digest the crosslinked products, protease cleavage in normal and $O^{18}$ labeled water, identification of the crosslinked peptides based on the different charge properties compared to the non-crosslinked peptides and based on the predicted molecular weight, and electro-elution of the crosslinked product from the gels. Unfortunately, in spite of the large amount of work invested in this project, the crosslinked peptides could not be identified by mass spectrometry.

### III.2.4. Functional activity of EF-G•L7/L12 crosslinked product

A covalent link between the G' subdomain of EF-G and L7/L12 may affect the dynamic interactions of EF-G with the ribosome. In order to explore the functional properties of the crosslinking product between EF-G(231C)-AzP and the r-protein L7/L12, we tested it in the GTP hydrolysis assay. In our crosslinking samples, the majority of EF-G is still in uncrosslinked form, so in order to focus on the functional activity of only the crosslink, the uncrosslinked EF-G had to be removed using two high salt washes, followed by another two washes, which exchange the high salt with the GTP hydrolysis buffer (see Methods). The vast majority of the uncrosslinked EF-G is removed by this procedure, leaving a mixture of the EF-G crosslinked to ribosomes and uncrosslinked ribosomes (Fig. III.10A). Several controls were formed and purified from

full length EF-G in an identical manner: a crosslinking sample without UV activation of AzP (reaction 3), a sample with unmodified EF-G(231C) exposed to UV irradiation (reaction 4) and a sample that had no EF-G added to it, but was exposed to UV irradiation (reaction 5). All the controls that contained EF-G had the same amount of EF-G remaining after the washes, independent of the presence of AzP and UV irradiation (Fig. III.10A). The crosslinked sample and all the above described controls were tested for GTP hydrolysis (Fig. III.10B). Reactions 3 and 4 show a small amount of GTP hydrolysis, which is due to the traces of EF-G present in the samples, while reaction 2 has a strong GTP hydrolysis activity, superior to either controls tested. Reaction 2 contains EF-G(231C-AzP) attached to 70S ribosomes through a covalent link with L7/L12, as well as, an excess of free 70S ribosomes. Based on the crosslinking efficiency, we have estimated that only approximately 15% of all the ribosomes in reaction 2 contain EF-G, up to a maximum of 0.3 pmols of crosslinked product per GTP hydrolysis reaction. The observed GTP hydrolysis rate in reaction 2 is only possible when the crosslinked product between EF-G and L7/L12 goes through multiple rounds of GTP hydrolysis (Fig. III.10B).

We have purified in a similar manner the crosslinked product between EF-G(426C-AzP) and S12 (Fig. III.10C). In this case, the crosslinked product (reaction 2) shows a GTP hydrolysis activity no different than that of its negative controls (reaction 3-5) (Fig. III.10D).

In order to confirm the extent of activity of AzP modified cysteine mutants in GTP hydrolysis, sample 6 was also introduced. This sample contained approximately the same amount of EF-G (estimated by densitometry) as the remaining material in the crosslinking reactions after the ultrafiltration washes, and it shows that both of these modified cysteine residues are capable of multiple rounds GTP hydrolysis. (Fig. III.10B and D)

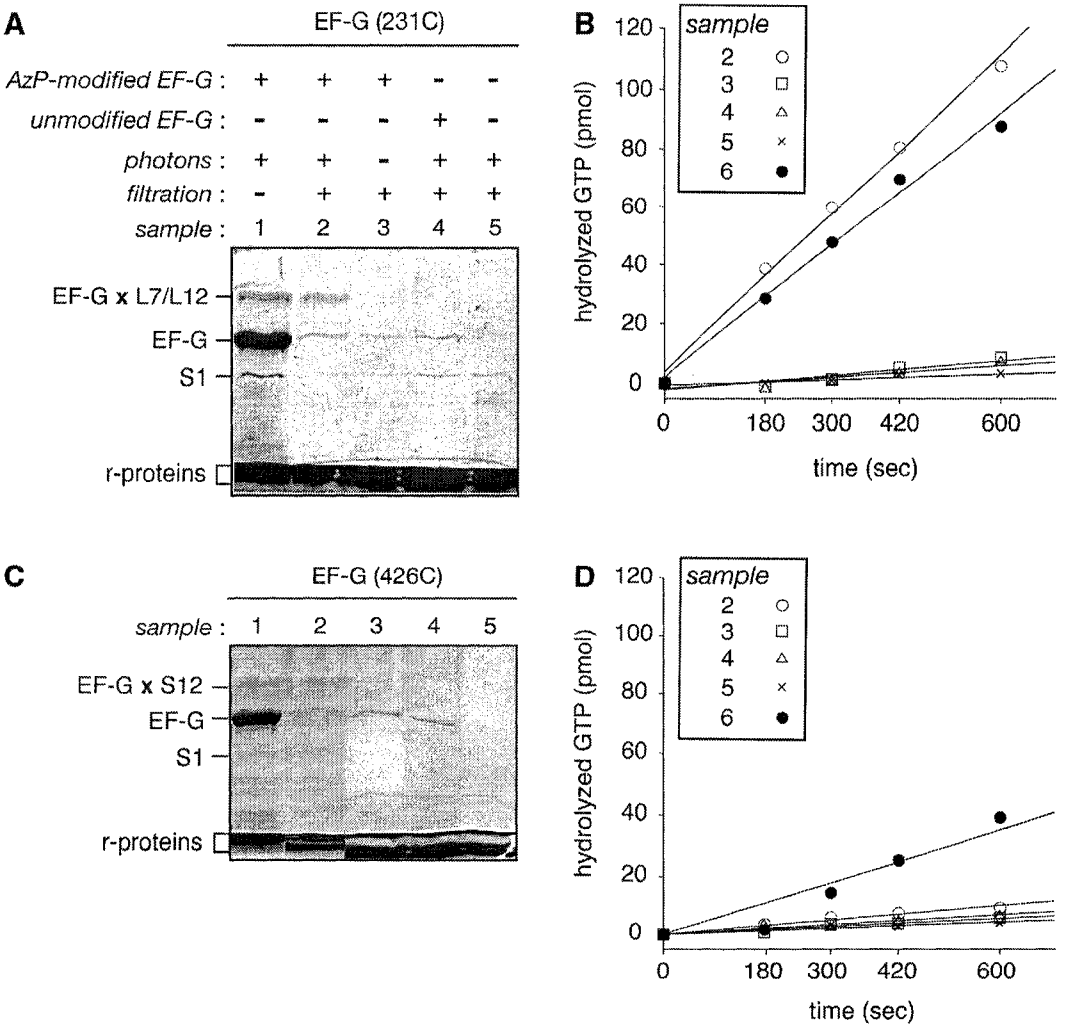


**Fig. III.10 - GTP hydrolysis activity of EF-G crosslinked to the ribosome via L7/L12 or S12. (A, C)** Crosslinking reactions analyzed by SDS-PAGE, stained with Coomassie. **(B, D)** Initial kinetics of GTP hydrolysis (10µl samples; 50µM GTP at t = 0). In samples 1-4, EF-G was bound to the ribosome in the fus state. Fusidic acid and the GDP product were removed from these samples during filtration. Sample 5 contained ribosomes lacking EF-G. Sample 6 contained AzP-modified EF-G, and ribosomes, without crosslinking (no photons) and filtration. Approximately the same amount of EF-G was present in samples 2 and 6, as estimated from densitometry calibrated to a known EF-G titration on a separate gel (not shown): ~2 pmol EFG(231C-AzP) and ~0.5 pmol EF-G(426C-AzP). Reproduced from (Nechifor and Wilson, 2007).

## III.3. DISCUSSION

### III.3.1. Structural studies on the interaction between EF-G and L7/L12

All the experiments presented in this chapter have tried to explore further the interaction between the G' subdomain of EF-G and the r-protein L7/L12.

Initially, by using a cysteine residue probing technique (NTCB cleavage reactions), we tried to assess if the initial crosslinking results we obtained were due to close proximity between residues 209 and 231 and the r-protein L7/L12 or if these residues are actually part of the interaction surface. The NTCB cleavage technique has revealed that neither of these residues is protected by the ribosome when EF-G is bound to the ribosome in either the GDPNP or the fus complex. These probing experiments suggested that although both of these residues are in close proximity to the r-protein L7/L12, it is unlikely that they are part of the interaction surface. This was surprising, especially for residue 231 which had a relatively high crosslinking efficiency, and was expected to interact with L7/L12. The functional experiments in the next chapter will confirm though this initial conclusion in the case of position 231.

Interestingly, there is a three fold difference in the NTCB cleavage of residue 209C between the GDPNP and the fus ribosomal complexes. This observation suggests that although residue 209 is also mostly solvent accessible and not directly interacting with the ribosome, there is a slight change in the position of this residue, being more protected in the fus state than in the GDPNP state. More importantly, this observed protection seems to be due to the r-protein L7/L12 presence because it disappears when we used ribosomes depleted of L7/L12. This result is concurred by a cryo-EM study, which observes the same movement of the residue 209 towards the CTD of the r-protein L7/L12 in the fus complex compared to the GDPNP comples (Datta et al., 2005).

The next step consisted in designing and constructing seven additional cysteine residues in order to test what other elements of the G' subdomain are in close proximity to L7/L12. Four out of the seven new cysteine residue provided positive crosslinking results with the r-protein L7/L12, raising the number of the residues which crosslink to L7/L12 to six and adding additional elements from the structure of the G' subdomain to the possible interaction surface between EF-G and L7/L12.

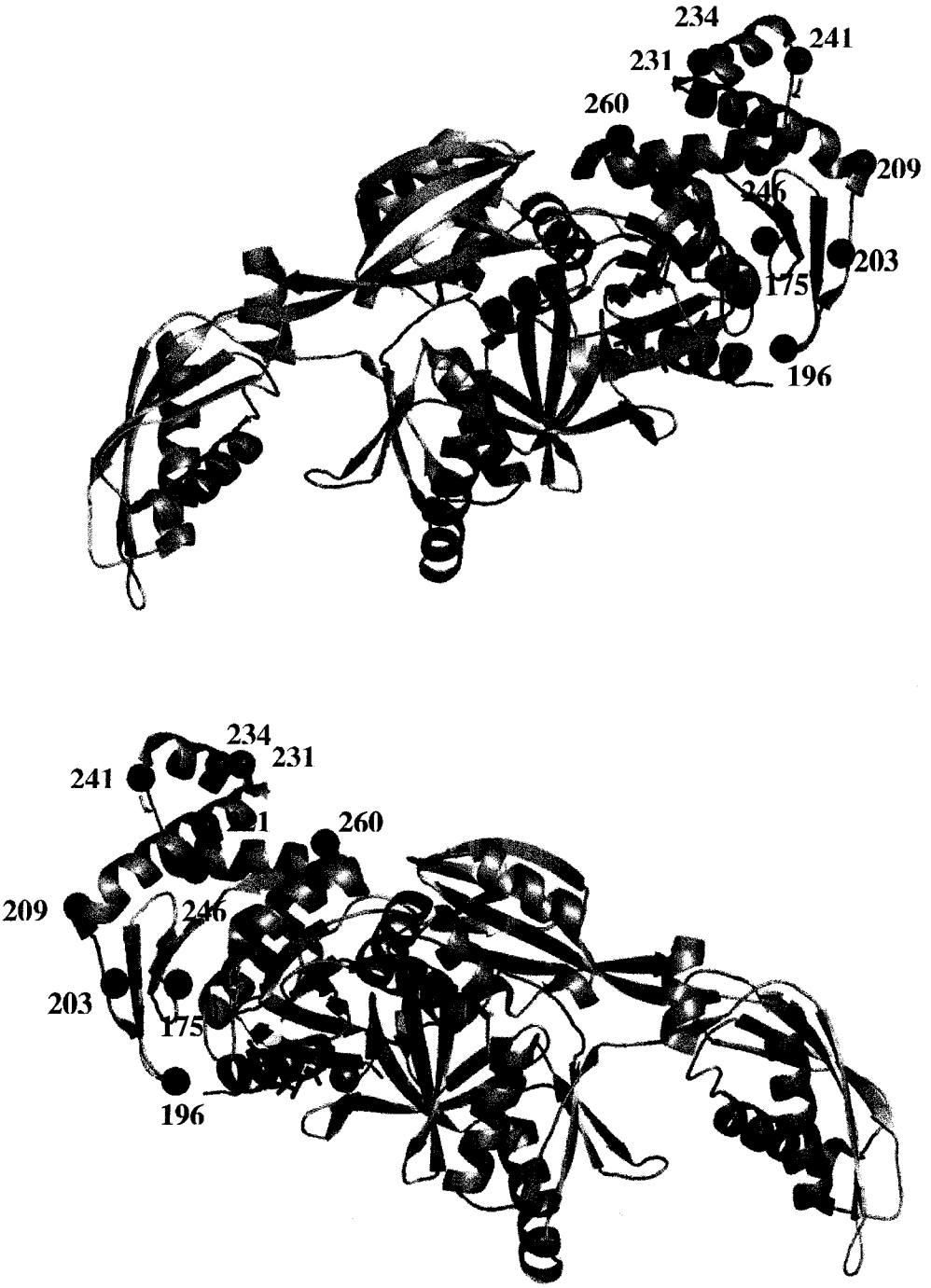


**Fig. III.11 – Structure of EF-G highlighting the constructed cysteine residues in the G' subdomain**. The cysteine mutants which crosslinked to L7/L12 are represented in red spheres, while the cysteines that did not provide a positive crosslinking result are in dark blue. The picture was constructed using PyMOL software (http://pymol.sourceforge.net/) and the pdb file 1FNM (Laurberg et al., 2000).

The results of the new crosslinking experiments showed that helices A and B, as well as the N terminal of helix C are in crosslinking range to L7/L12. All the crosslinking results taken together gave us a better understanding of the region in the G' subdomain of EF-G, which is next to the r-protein L7/L12. Fig. III.11. summarizes the results of our crosslinking experiments, showing the residues that gave us positive and negative crosslinking results.

The efficiency of the crosslinking is also slightly different between different cysteine mutants, most likely due to their position and/or orientation. Based on this observation, it is possible that the N-terminal ends of helices A and C are further apart from the interaction with L7/L12 compared to the C-terminal end of helix A and helix B.

The new crosslinking results did not yield any significant quantitative or qualitative differences between the GDPNP and fus complexes, similar to the previous crosslinking study involving residues 209C and 231C, so they cannot provide additional information regarding conformational changes of this region during translocation (if any exist). Residue 246C provided a crosslinked product which migrated slightly slower in the SDS-PAGE than the other crosslinking products, suggesting potentially that a different region of L7/L12 participates in this particular crosslink.

Trying to identify the interaction surface from the perspective of L7/L12 was unfortunately not successful. In spite of numerous biochemical and mass spectrometry techniques attempted, the interaction surface belonging to L7/L12 has remained elusive and further studies are still needed to address this question.

In the case of EF-Tu, mutagenesis studies have shown that residues in helix D are important for the interaction with L7/L12, forming probably salt bridges and hydrophobic interactions with residues from helices 4 and 5 of CTD of L7/L12 (Kothe et al., 2004). The working model inferred from these mutagenesis experiments was that the interaction surface between EF-Tu and L7/L12 is formed by helix D of EF-Tu, interacting on each side with helices 4 and 5 of the CTD of L7/L12.

The same mutants in helices 4 and 5 of L7/L12 were tested in the case of EF-G, and it was found that only mutants in helix 4 inhibit the functions of EF-G, while mutations in helix 5 had no effect (Savelsbergh et al., 2005). So, in the case of EF-G, the

interaction surface with L7/L12 might be formed by helix 4 of the CTD of L7/L12, which has on either side helices A and B of the G' subdomain.

### III.3.2. GTP hydrolysis of the crosslinked product

The GTP hydrolysis abilities of the crosslinking product between EF-G(231C)-AzP and L7/L12 open up interesting hypothesis. On one hand, this shows that our crosslinking complexes represent a functional state of EF-G in complex with 70S and not a seldom, rarely occurring event. More importantly, GTP is hydrolyzed by EF-G even in the presence of a covalent bond between position 231 of EF-G and L7/L12. One possibility would be that EF-G may not be able to dissociate from the ribosome because of this covalent bond to L7/L12, but it is still able to hydrolyze GTP and exchange GDP for GTP in spite of the fact that it is blocked between the two ribosomal subunits. This hypothesis receives support from the possibility that the ribosome may act as a GDP/GTP exchange for EF-G (Zavialov et al., 2005). Although theoretically possible, the model proposed by these authors has been contested by others in the field (Wilden et al., 2006). However, it seems unlikely that EF-G can exchange the nucleotides and continue its cycle while being trapped in the ribosome cavity because this would lead to vast energy expenditure *in vivo* that could not be tolerated by the cell. Another possibility is that EF-G may still be able to dissociate from the ribosomal cavity in spite of its covalent link to L7/L12. This would be possible because of the hinge region in the structure of L7/L12, which can adopt an extended or closed configuration (Bocharov et al., 2004). The extended structure reaches away from the ribosome (Diaconu et al., 2005), maybe allowing EF-G to dissociate from the ribosomal complex.

In order to explore further this line of experiments, we purified the crosslinking product between EF-G(426C-AzP) and S12, a r-protein relatively fixed on the 30S subunit, and tested its GTP hydrolysis. This crosslinking product does not show a GTP hydrolysis activity above that of the controls, seemingly indicating that EF-G is not able to hydrolyze GTP while being covalently linked to S12. The interpretation of this experiment, which was meant to be a negative control for the L7/L12 crosslinking product, is unfortunately not as straight forward as it may seem. Firstly, the efficiency of the crosslinking between EF-G(426C) and S12 is weaker than in the case of Ef-G(231C)-

AzP-L7/L12, hence resulting in lower quantities of crosslinked product. This probably makes its GTP hydrolysis harder to detect from the background. Secondly, further tests have revealed that some of the L7/L12 is lost during our high salt washes of the ribosomal complexes, which, in theory, could lower further the results of the GTP hydrolysis.

It is plausible that in the case of the crosslinked product between EF-G and L7/L12, EF-G can exchange the nucleotide in solution after the classical model and re-enter the same ribosome cavity in order to hydrolyze another molecule of GTP. These movements are possible because of the unusual mobility of L7/L12 and are unlikely to take place in the case of the r-protein S12. EF-G seems to be able to dissociate from the ribosomal cavity even while being covalently linked with L7/L12, signifying that a break in the interaction between the G' subdomain of EF-G and L7/L12 is not necessary for EF-G to hydrolyze GTP, release $P_i$, dissociate from the ribosome and exchange nucleotides in solution.

## III.4. MATERIALS AND METHODS

### III.4.1. Reagents and buffers

EF-G, 70S and mRNA were purified as previously described in chapter II. AzP, fusidic acid, GTP, GDPNP, and *E. coli* $tRNA^{fMet}$ and $tRNA^{Phe}$ were purchased from Sigma-Aldrich, as were trypsin, trypsin inhibitor, NTCB and iodoacetamide. Polyclonal IgG antibodies (Stoffler and Wittmann, 1971) against *E. coli* r-protein L7/L12 were a generous gift from Dr. R. Brimacombe (Max Planck Institute). *Buffer 1*: 50 mM Tris-HCl pH 8.8, 100 mM $NH_4Cl$, 20 mM $MgCl_2$; *Buffer 2*: 50 mM Tris-HCl pH 7.5, 100 mM $NH_4Cl$, 20 mM $MgCl_2$; *Buffer 3*: 80mM Hepes pH 7.7, 50 mM $NH_4Cl$, 10 mM $MgCl_2$, 1 mM DTT.

AzP modification of cysteine mutants, EF-G•70S complex formation, UV induced crosslinking, as well as L7/L12 depletion of ribosomes were performed as described in chapter II.

### III.4.2. IA/NTCB probing of EF-G

For the probing of EF-G in solution, EF-Gwt or its cysteineless mutant (1μM) was incubated in buffer 1 in the presence of either no nucleotide or GTP (500μM) for 15 min. at 37°C, followed by cooling of the reactions on ice for 5 min. 10mM iodoacetamide was added to the indicated reactions, the modification proceeded for 30 sec. on ice and it was stopped by the addition of 20mM β-mercaptoethanol. Each reaction then received 7M guanidium chloride, 100mM NTCB, and 50mM Tris pH 8.8, and they were incubated at room temperature for 15 min. The reaction products were precipitated using sodium deoxycholate (0.1%) and TCA (8%) for 15 min. at room temperature, and collected by centrifugation 14,000rpm, 30 min. (Eppendorf table top centrifuge). The precipitate was washed in 100μl ice cooled acetone and precipitated again for 90 min. at -20°C in order to remove the remaining TCA. The reactions were again centrifuged 14,000rpm, 30 min. (Eppendorf table top centrifuge), the pellets were dried under vacuum for 10 min., followed by resuspension in 10μl of 8M urea and 112mM $NH_4OH$ and incubation at room temperature for 1h, in the dark. Next, 15μl SDS-PAGE sample buffer was added to each reaction, reactions were denatured at 90°C for 10 min, and separated by 7.5% SDS-PAGE.

Full ribosomal complexes (1μM) were formed in buffer 1 with ribosomes (1μM), mRNA (phage T4 gene 32 – 1.5μM), uncharged $tRNA^{fMet}$ in the P site (1.5μM) and uncharged $tRNA^{Phe}$ in the A site (1.5μM). To these pre-translocation ribosomal complexes, we added either EF-G(209C) or EF-G(231C) (1μM) and GDPNP (500μM) for the GDPNP complex or GTP (500μM) and fusidic acid (500μM) for the fus complex. The EF-G•ribosome complexes, as well as their controls containing EF-G (1μM), GTP (500μM) and fusidic acid (500μM), were cooled on ice for 10 min and probed with iodoacetamide (10mM) for 30 sec. The reactions were stopped with β-mercaptoethanol (20mM), followed by denaturation with 3% SDS and heating at 90°C for 5min. After denaturation, the reactions were let to cool to room temperature and probed with NTCB (100mM) in 50mM Tris pH 8.8 for 1h at room temperature in the dark. The reaction products were precipitated using sodium deoxycholate (0.1%) and TCA (8%) for 15 min. at room temperature, and collected by centrifugation 14,000rpm, 30 min. (Eppendorf table top centrifuge). The precipitate was washed in 100μl ice cooled acetone and

precipitated again for 90 min. at -20°C in order to remove the remaining TCA. The reactions were again centrifuged 14,000rpm, 30 min. (Eppendorf table top centrifuge), the pellets were dried under vacuum for 10 min., followed by resuspension in 10µl of 8M urea and 112mM $NH_4OH$ and incubation at room temperature overnight, in the dark. The next day, 15µl SDS-PAGE sample buffer was added to each reaction, followed by incubation at 90°C for 10 min, and separation by 10% SDS-PAGE.

### III.4.3. Trypsin digestion of EF-G

For the partial trypsin cleavage of EF-G in solution (Fig. III.8A), EF-G (18µM) was pre-incubated in buffer 2 for 10 min at 37°C in the presence of either no nucleotide, GTP (1mM) or GDP (1mM), followed by trypsin addition (4.3µg/ml) and cleavage at 37°C for 15 min. The trypsin digestion was stopped with an equal volume of SDS-PAGE, and the reactions were denatured at 90°C for 10 min, followed by SDS-PAGE separation and Coomassie blue staining.

The ribosomal complexes for Fig. III.8B were assembled in buffer 2 by mixing 2µM 70S and 4.5µM EF-G with either 1mM GDPNP or a combination of 1mM GTP and 1mM fusidic acid, followed by incubation at 37°C for 10 min and on ice for 5 min. The formed complexes are then diluted to 500µl of buffer 2 and ultrafiltrated through YM-100 in order to purify the EF-G•70S complexes from the free EF-G. The EF-G•70S recovered from the solution retained on top of the Microcon filters were mixed with trypsin solution (17µg/ml), incubated at 37°C for 5 min, and the protease cleavage was stopped by addition of an equal volume of SDS-PAGE sample buffer and denaturation at 90°C for 10 min. The samples were separated by SDS-PAGE and stained with Coomassie Blue.

For Edman degradation, the SDS-PAGE containing multiple trypsin digested reactions was transferred to PVDF membranes in a buffer containing 25mM Tris base and 192mM glycine. The membranes were subsequently stained with Coomassie Blue, the bands of interest were cut and send to University of Victoria - Genome British Columbia (UVic-GBC) Proteomics Centre for Edman degradation.

### III.4.4. Purification of the crosslinked product

The crosslinked samples were prepared as described in chapter II with AzP-modified EF-G(231C) in a fus complex, at an UV wavelength of 365nm. After UV irradiation, the samples were diluted to 500µl of 1M $NH_4Cl$ pH 7.0 and ultrafiltrated through Microcons YM-100. This procedure was repeated one more time with 1M $NH_4Cl$ and two more times with buffer 3. The recovered sample was mixed with an equal volume of SDS-sample buffer, denaturated (90°C, 10 min) and analyzed by SDS-PAGE (6% polyacrylamide in the resolving gel).

### III.4.5. GTP hydrolysis

GTP hydrolysis reactions were performed in buffer 3 at 37°C. The reactions contained 50µM GTP, 0.0166µM $\gamma^{32}$P-GTP (Perkin Elmer) and 1/10 of the reaction volumes presented in Fig. III.9A and C. The reactions were stopped at the indicated time points by the addition of an equal volume of 30% solution of formic acid. The $P_i$ was separated from un-hydrolyzed GTP by TLC plates (Sigma Aldridch Ltd.) in 3.5M formic acid buffer at pH 4.0. The TLC plates were dried, exposed to a Phosphoraimager plate overnight, and quantified using a Typhoon scanner and ImageQuant software.

## III.5. CONCLUSION

Our crosslinking results showed that both helices A and B, as well as the N-terminal domain of helix C of the G' subdomain are in close proximity to the r-protein L7/L12 in both the pre- and post-translocational complexes and may be part of the interaction surface between these two proteins when EF-G is bound to the ribosome. From a functional perspective, multiple rounds of GTP hydrolysis are possible even when EF-G and L7/L12 is are covalently linked, but the same type of bond with S12 abolishes its activity.

## III.6. FUTURE DIRECTIONS

Our attempts to analyze the crosslinking product by different mass spectrometry techniques have failed. Some of the technical problems which we were constantly confronted with were the purification of the crosslinked product in large enough

quantities for analysis, and the losses/modifications in the polypeptide chains due to the SDS-PAGE separation and electroelution. Another long debated possibility is that the lack of success in detecting the crosslinked peptide was due to the potential different ionization properties of the crosslinked peptide based on their branched structure compared to the linear structure of the regular protease digestion peptides.

Future experiments could avoid some of these problems by taking advantage of a different crosslinking agent: *N*-((2-pyridyldithio)ethyl)-4-azidosalicylamide (PEAS) (Chen et al., 1994). This crosslinker (Fig. III.12.) belongs to the same class of aryl azides as AzP, so it will probably crosslink to the r-protein L7/L12 in a similar fashion upon UV light activation. It is possible that there will be more crosslinking products, since its arm length is slightly larger (14Å compared to 11Å) than that of AzP (Ebright et al., 1996). The major difference between PEAS and AzP consists in the way PEAS reacts with the cysteine residues, by undergoing a disulfide–thiol interchange of its pyridyldisulfide groups, resulting in the formation of mixed disulfides. These disulfides are stable in the absence of reducing agents, so EF-G cysteine mutants can be modified with PEAS, basically using the identical protocol as for AzP modification, followed by assembling them into ribosomal complexes and activation of the crosslinker by UV light. After crosslinking, the covalent bond between EF-G and L7/L12 can be severed by the addition of reducing agents (e.g. DTT), leaving the vast majority of the crosslinker agent still attached to L7/L12. The next step would be the stripping of the L7/L12 from these ribosomal complexes according to our already established protocol, which would result into a mixture of native and PEAS-modified L7/L12. This mixture could be then digested with different proteases and analyzed by mass spectrometry, comparing it to a control which had no crosslinker added to it. By this method, the material necessary for analysis could be obtained using a more direct approach, would be in larger quantities and hopefully, the labeled peptide from L7/L12 could be easier to identify by mass spectrometry. The crosslinked peptide would have a smaller mass in this case than the previous two crosslinked peptides resulting from AzP crosslinking, which can only help its ionization properties.

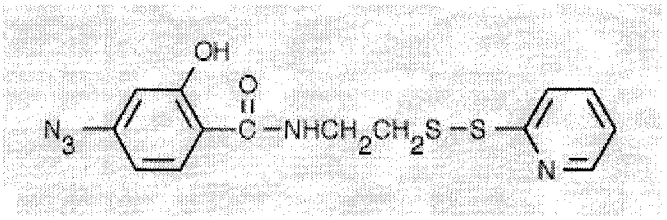


**Fig. III.12. Structure of the PEAS crosslinker** (Molecular Probes, a division of Invitrogen – reproduced from www.invitrogen.com)

Another interesting aspect of this crosslinking agent is its ability to be radiodinated to position 2 of the aromatic ring using $^{125}I$ (Ebright et al., 1996), which can ease a lot the identification of the fraction containing the labeled peptide upon the HPLC separation of the protease digested fragments.

Different cysteine mutants constructed in the elements of the G' subdomain have the possibility to crosslink differently with L7/L12, potentially to neighboring peptides (especially 246C, whose crosslink has different gel migration properties). If this proves to be true, these crosslinking experiments could provide a more complete picture of the interactions between the G' subdomain and L7/L12, with the possibility of modeling the interaction surface based on the points obtained from the mass spectrometry analysis and using the known crystal structure of these regions.

The trypsin cleavage experiments initially suggested a different accessibility of EF-G between the GDPNP and fus complexes. Cryo-EM studies have modeled the structure of EF-G in their densities, suggesting changes in conformation of the G' subdomain between the GDPNP and the fus complexes, due to the interaction with L7/L12 (Agrawal et al., 1999). We soon realized that our trypsin cleavage site probably did not involve the G' subdomain, since there was no difference in the cleavage pattern in the complexes assembled with ribosomes lacking L7/L12. The results of the sequencing confirmed our suspicion, localizing the cleavage site to switch 1. This region is protected from trypsin attack when EF-G is bound to the ribosome in complex with GDPNP, but it becomes exposed in the fus complex. This could be due to either a conformational change in switch 1 or in the ribosomal complex.

Switch 1 has been hypothesized for a long time to be able to change conformations upon GTP hydrolysis based on the structural similarities between the G domains of EF-G and EF-Tu and the drastic conformational changes observed in switch I of EF-Tu (Berchtold et al., 1993). Although there is some sequence conservation between the switches 1 of EF-G and EF-Tu, they are not interchangeable, a constructed mutant of EF-G containing the switch 1 of EF-Tu had decreased activity in GTP hydrolysis and was inactive in translocation (Kolesnikov and Gudkov, 2002). The results we obtained would be in line with the hypothesis that switch 1 of EF-G changes its conformation between the GDPNP and fus complexes. The place of the trypsin cleavage site also corresponds to the point which moves the furthest, according to our modeling of the structure of the switch 1 region in EF-G based on the EF-Tu model.

The 30S subunit of the ribosome has also been described by cryo-EM studies to change conformations between the GDPNP and the fus complex (Agrawal et al., 1999), the 30S subunit undergoing a rotation movement compared to the 50S subunit upon EF-G binding, movement which is reversed in the fus complex. These movements could also explain the difference in trypsin accessibility.

In order to explore further the conformational changes of switch 1 of EF-G, three cysteine residues were constructed and purified: 37C (at the N-terminal), 58C (next to the trypsin cleavage site), and 65C (at the C-terminal) (Fig. III.13.). Their position in regards to different ribosomal elements is difficult to detect directly, none of them yielding any positive crosslinking results (data not shown), and being also relatively distant from rRNA, as assessed by previous hydroxyl radical cleavages (Wilson and Noller, 1998).

Our initial attempts to determine IA accessibility for these cysteine mutants using the IA/NTCB probing protocol have failed to demonstrate any differences between the GDPNP and fus complexes (data not shown). In order to continue this line of experiments, other techniques need to be used (e.g. fluorescent probes).

**Fig. III.13. – The structure of switch 1 of EF-G highlighting the position of the three cysteine residues.** Switch 1 is depicted in yellow, the red spheres represent the position of the cysteine residues, $Mg^{2+}$ is the purple sphere, while the GDP is in dark blue sticks. The figure was created with PyMOL using the structure of EF-G2 - pdb 1WDT (Connell et al., 2007).

## III.7. REFERENCES

Agrawal, R. K., Heagle, A. B., Penczek, P., Grassucci, R. A., and Frank, J. (1999). EF-G-dependent GTP hydrolysis induces translocation accompanied by large conformational changes in the 70S ribosome. Nat Struct Biol *6*, 643-647.

Berchtold, H., Reshetnikova, L., Reiser, C. O., Schirmer, N. K., Sprinzl, M., and Hilgenfeld, R. (1993). Crystal structure of active elongation factor Tu reveals major domain rearrangements. Nature *365*, 126-132.

Bocharov, E. V., Sobol, A. G., Pavlov, K. V., Korzhnev, D. M., Jaravine, V. A., Gudkov, A. T., and Arseniev, A. S. (2004). From structure and dynamics of protein L7/L12 to molecular switching in ribosome. J Biol Chem *279*, 17697-17706.

Chen, Y., Ebright, Y. W., and Ebright, R. H. (1994). Identification of the target of a transcription activator protein by protein-protein photocrosslinking. Science *265*, 90-92.

Connell, S. R., Takemoto, C., Wilson, D. N., Wang, H., Murayama, K., Terada, T., Shirouzu, M., Rost, M., Schuler, M., Giesebrecht, J., *et al.* (2007). Structural basis for interaction of the ribosome with the switch regions of GTP-bound elongation factors. Mol Cell *25*, 751-764.

Datta, P. P., Sharma, M. R., Qi, L., Frank, J., and Agrawal, R. K. (2005). Interaction of the G' domain of elongation factor G and the C-terminal domain of ribosomal protein L7/L12 during translocation as revealed by cryo-EM. Mol Cell *20*, 723-731.

Degani, Y., and Patchornik, A. (1974). Cyanylation of sulfhydryl groups by 2-nitro-5-thiocyanobenzoic acid. High-yield modification and cleavage of peptides at cysteine residues. Biochemistry *13*, 1-11.

Deusser, E., and Wittmann, H. G. (1972). Ribosomal proteins: variation of the protein composition in *Escherichia coli* ribosomes as function of growth rate. Nature *238*, 269-270.

Dey, D., Oleinikov, A. V., and Traut, R. R. (1995). The hinge region of *Escherichia coli* ribosomal protein L7/L12 is required for factor binding and GTP hydrolysis. Biochimie *77*, 925-930.

Diaconu, M., Kothe, U., Schlunzen, F., Fischer, N., Harms, J. M., Tonevitsky, A. G., Stark, H., Rodnina, M. V., and Wahl, M. C. (2005). Structural basis for the function of the ribosomal L7/12 stalk in factor binding and GTPase activation. Cell *121*, 991-1004.

Ebright, Y. W., Chen, Y., Kim, Y., and Ebright, R. H. (1996). S-[2-(4-azidosalicylamido)ethylthio]-2-thiopyridine: radioiodinatable, cleavable, photoactivatible cross-linking agent. Bioconjug Chem *7*, 380-384.

Gudkov, A. T., and Gongadze, G. M. (1984). The L7/L12 proteins change their conformation upon interaction of EF-G with ribosomes. FEBS Lett *176*, 32-36.

Hamel, E., Koka, M., and Nakamoto, T. (1972). Requirement of an *Escherichia coli* 50 S ribosomal protein component for effective interaction of the ribosome with T and G factors and with guanosine triphosphate. J Biol Chem *247*, 805-814.

Jacobson, G. R., Schaffer, M. H., Stark, G. R., and Vanaman, T. C. (1973). Specific chemical cleavage in high yield at the amino peptide bonds of cysteine and cystine residues. J Biol Chem *248*, 6583-6591.

Kolesnikov, A., and Gudkov, A. (2002). Elongation factor G with effector loop from elongation factor Tu is inactive in translocation. FEBS Lett *514*, 67-69.

Kothe, U., Wieden, H. J., Mohr, D., and Rodnina, M. V. (2004). Interaction of helix D of elongation factor Tu with helices 4 and 5 of protein L7/12 on the ribosome. J Mol Biol *336*, 1011-1021.

Laurberg, M., Kristensen, O., Martemyanov, K., Gudkov, A. T., Nagaev, I., Hughes, D., and Liljas, A. (2000). Structure of a mutant EF-G reveals domain III and possibly the fusidic acid binding site. J Mol Biol *303*, 593-603.

Liljas, A., and Gudkov, A. T. (1987). The structure and dynamics of ribosomal protein L12. Biochimie *69*, 1043-1047.

Marsh, R. C., Chinali, G., and Parmeggiani, A. (1975). Function of sulfhydryl groups in ribosome-elongation factor G reactions. Assignment of guanine nucleotide binding site to elongation factor G. J Biol Chem *250*, 8344-8352.

Miyake, R., Murakami, K., Owens, J. T., Greiner, D. P., Ozoline, O. N., Ishihama, A., and Meares, C. F. (1998). Dimeric association of *Escherichia coli* RNA polymerase alpha subunits, studied by cleavage of single-cysteine alpha subunits conjugated to iron-(S)-1-[p-(bromoacetamido)benzyl]ethylenediaminetetraacetate. Biochemistry *37*, 1344-1349.

Moller, W., Groene, A., Terhorst, C., and Amons, R. (1972). 50-S ribosomal proteins. Purification and partial characterization of two acidic proteins, A 1 and A 2, isolated from 50-S ribosomes of *Escherichia coli*. Eur J Biochem *25*, 5-12.

Nechifor, R., and Wilson, K. S. (2007). Crosslinking of translation factor EF-G to proteins of the bacterial ribosome before and after translocation. J Mol Biol *368*, 1412-1425.

Oleinikov, A. V., Jokhadze, G. G., and Traut, R. R. (1993a). *Escherichia coli* ribosomal protein L7/L12 dimers remain fully active after interchain crosslinking of the C-terminal domains in two orientations. Proc Natl Acad Sci U S A *90*, 9828-9831.

Oleinikov, A. V., Jokhadze, G. G., and Traut, R. R. (1998). A single-headed dimer of *Escherichia coli* ribosomal protein L7/L12 supports protein synthesis. Proc Natl Acad Sci U S A *95*, 4215-4218.

Oleinikov, A. V., Perroud, B., Wang, B., and Traut, R. R. (1993b). Structural and functional domains of *Escherichia coli* ribosomal protein L7/L12. The hinge region is required for activity. J Biol Chem *268*, 917-922.

Ramagopal, S., and Subramanian, A. R. (1974). Alteration in the acetylation level of ribosomal protein L12 during growth cycle of *Escherichia coli*. Proc Natl Acad Sci U S A *71*, 2136-2140.

Savelsbergh, A., Mohr, D., Kothe, U., Wintermeyer, W., and Rodnina, M. V. (2005). Control of phosphate release from elongation factor G by ribosomal protein L7/12. EMBO J *24*, 4316-4323.

Silverman, J. A., and Harbury, P. B. (2002). Rapid mapping of protein structure, interactions, and ligand binding by misincorporation proton-alkyl exchange. J Biol Chem *277*, 30968-30975.

Stoffler, G., and Wittmann, H. G. (1971). Ribosomal proteins. XXV. Immunological studies on *Escherichia coli* ribosomal proteins. J Mol Biol *62*, 407-409.

Traut, R. R., Dey, D., Bochkariov, D. E., Oleinikov, A. V., Jokhadze, G. G., Hamman, B., and Jameson, D. (1995). Location and domain structure of *Escherichia coli* ribosomal protein L7/L12: site specific cysteine crosslinking and attachment of fluorescent probes. Biochem Cell Biol *73*, 949-958.

Wilden, B., Savelsbergh, A., Rodnina, M. V., and Wintermeyer, W. (2006). Role and timing of GTP binding and hydrolysis during EF-G-dependent tRNA translocation on the ribosome. Proc Natl Acad Sci U S A *103*, 13670-13675.

Wilson, K. S., and Nechifor, R. (2004). Interactions of translational factor EF-G with the bacterial ribosome before and after mRNA translocation. J Mol Biol *337*, 15-30.

Wilson, K. S., and Noller, H. F. (1998). Mapping the position of translational elongation factor EF-G in the ribosome by directed hydroxyl radical probing. Cell *92*, 131-139.

Zavialov, A. V., Hauryliuk, V. V., and Ehrenberg, M. (2005). Guanine-nucleotide exchange on ribosome-bound elongation factor G initiates the translocation of tRNAs. J Biol *4*, 9.

# IV. FUNCTIONAL CONSEQUENCES OF MUTATIONS IN HELIX A OF THE G' SUBDOMAIN OF EF-G

A version of this chapter has appeared in Nechifor R., Murataliev M., Wilson K.S., "Functional interactions between the G' subdomain of bacterial translation factor EF-G and ribosomal protein L7/L12", J. Biol. Chem. 2007 Dec 21;282(51):36998-7005.

## IV.1. INTRODUCTION

The chapters II and III have focused on the structural aspects of the interaction between the G' subdomain and the r-protein L7/L12. In contrast, the experiments presented in this chapter are centered on the functional implications of this interaction.

L7/L12, through its CTD, was demonstrated to be essential for activation of GTP hydrolysis in EF-G (Traut et al., 1995), but the mechanism of this activation has remained elusive for a long time. This is partly due to lack of detailed structural information regarding the conformation of EF-G bound to the ribosomal complex, as well as the absence of L7/L12 from all the ribosomal crystal structures published so far (Ban et al., 2000; Schuwirth et al., 2005; Selmer et al., 2006; Yusupov et al., 2001). Newer cryo-EM studies have revealed an interesting structure of the stalk region of the 50S subunit, with the C-terminus of L7/L12 reaching far in solution and potentially recruiting the appropriate translation factor for the state of the ribosomal complex (Diaconu et al., 2005). Further mutational studies of conserved residues in L7/L12 have indicated that the activation of GTP hydrolysis may be due to a combination of two different effects: (i) increase in the rate of recruitment of EF-G to the ribosomal complex, and (ii) activation of Pi release from EF-G after GTP hydrolysis (Diaconu et al., 2005; Savelsbergh et al., 2005).

According to our crosslinking experiments (chapters II and III), the interacting partner of L7/L12 is the G' subdomain, an insertion into the G domain, which is not present in EF-Tu. Originally, when this insertion was identified in the crystal structure of EF-G, it was hypothesized that this subdomain could work as an internal GEF, since there is no external GEF identified for EF-G (AEvarsson et al., 1994). The authors argumented their hypothesis by the fact that the G' subdomain makes extensive interactions with the G domain, some of them being similar with the interactions between EF-Tu and its GEF, EF-Ts (AEvarsson et al., 1994). In spite of this original hypothesis, no functional studies have ever tried to address the function of the G' subdomain.

Our previous crosslinking results (chapters II and III) place helices A, B, and the N-terminal of helix C of the G' subdomain in close proximity to L7/L12, suggesting that these helices form or are close to the interaction surface between EF-G and L7/L12. The G' subdomain shows poor conservation in general, and its surface is negatively charged,

as is the majority of the solvent exposed surface of EF-G. Its interacting partner, the C-terminus of L7/L12, is, in contrast, very well conserved, but also generally negatively charged, with the exception of a positively charged patch formed by helices 4 and 5. Mutation studies have assigned these two helices in the C terminal domain of L7/L12 to be the interaction surface with helix $D_G$ of EF-Tu (Kothe et al., 2004). The hypothesized mechanism of interaction involves a hydrophobic surface stabilized by two salt bridges between negatively charged residues of EF-Tu and positively charged residues from helices 4 and 5 of L7/L12 (Kothe et al., 2004). It seems likely that the interaction of L7/L12 with EF-G is similar to the one with EF-Tu, involving hydrophobic, as well as charge-charge interactions.

In order to understand better the role of the G' subdomain and its function in the interaction with L7/L12, we have constructed four different mutants by replacing conserved, negatively charged residues of the G' subdomain with lysines. The present study describes the activity of these proteins in different EF-G functional assays, providing insights into the consequences of disrupting the interaction between EF-G and L7/L12.

## IV.2. RESULTS

Our exploration into the function of the G' subdomain was started by the construction of a deletion mutant, which lacks this entire region of EF-G (amino acids 166-261). Since the two ends are very close in space in the structure of the *T. thermophilus* EF-G (Laurberg et al., 2000), we believed that the entire G' subdomain can be substituted by a glycine residue, without disrupting the structure of the polypeptide chain. This deletion mutant was constructed in the plasmid coding for *E. coli* His tagged EF-Gwt, overexpressed in *E. coli* and tested for activity in different functional assays. During purification, it became obvious that this entire protein was aggregated into inclusion bodies, situation that did not change by varying the IPTG concentration or the growing conditions (temperatures as low as 20°C and/or the use of minimal media). This mutant was finally purified from inclusion bodies under denaturing conditions, using a previously described protocol designed for non-soluble deletion EF-G mutants (Savelsbergh et al., 2000a). Although at first it appeared to be a soluble protein, this

deletion mutant did not hydrolyze GTP either in the presence or absence of ribosomes, did not bind mant-GTP, nor was it active in translocation (data not shown). By diluting the initial stock and filtering it through a 0.22μM pore membrane, we realized that the protein forms large aggregates, which explained completely its lack of activity in any of the assays.

Due to the solubility problems encountered with the deletion mutant, we decided to construct more conservative, point mutations, with the role to disrupt the hypothesized salt bridges between the G' subdomain of EF-G and L7/L12. To that end, we constructed three single lysine mutants, as well as a triple lysine mutant by replacing the glutamic acids at position 224, 228 and 231 in EF-G. The selection criteria were as follows: (i) negatively charged residues, (ii) amino acids situated in the proximity of position 231, and (iii) conserved residues, as gathered from our sequence alignment of G' subdomain primary sequences from different bacteria and mitochondrial phyla (Fig. IV.1.). Residues 224 and 231 are conserved as negatively charged residues (aspartic or glutamic acid, depending on the bacterial specie), while 228, although mostly conserved as a negatively charged residue, is replaced by polar amino acids in certain species (Fig. IV.1.). The triple mutant (TK) has all the three glutamic acids at positions 224, 228 and 231 replaced by lysines.

All four lysine mutants were constructed in the plasmid coding for EF-Gwt and purified under native conditions. None of them displayed any solubility problems, their behavior during purification being similar to EF-Gwt, as were the concentrations of the final stock solutions.

The first functional property of these proteins to be tested was their GTP hydrolysis activity, under multiple turnover GTP hydrolysis conditions, using a small, catalytical amount of EF-G and excess ribosomes. The initial experiments quickly showed that all the lysine mutants were inhibited in multiple rounds of GTP hydrolysis in the presence of ribosomes as compared to the EF-Gwt, with E224K, E228K, and TK having very low GTP hydrolysis activity, barely distinguishable from background. In contrast, EF-G E231K was the most active of all the lysine mutants, with GTP hydrolysis rates relatively close to EF-Gwt (data not shown). To further explore the observed enzymatic defect of these mutants, the $K_M$ for 70S ribosomes and $k_{cat}$ values for ribosome

activated GTP hydrolysis were measured for each EF-G protein. The initial velocity ($v_0$) of the GTP hydrolysis increased with increasing ribosome concentrations, followed by a

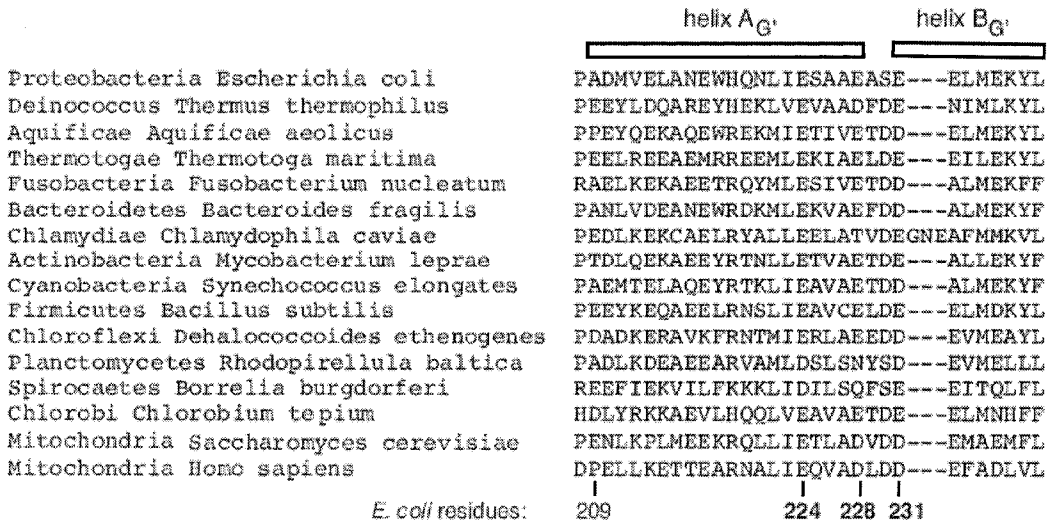


**Fig. IV.1. – Sequence alignment of a portion of the amino acid sequence of the G' subdomain.** Several amino acid sequences from different bacteria and eukaryotic mitochondrial phyla were aligned using PROBCONS (http://probcons.stanford.edu). The composition of helices A and B of the G' subdomain is based on the structure of the *T. Thermophilus* EF-G (Czworkowski et al., 1994). Reproduced from (Nechifor et al., 2007)

decrease when the ribosome concentration increases beyond 2μM, consistent with previous reports describing inhibition of the turnover rate of the EF-G catalyzed GTP hydrolysis by high concentrations of ribosomes (Rohrback and Bodley, 1976). We fitted the data obtained up to the ribosomal concentration of 2μM to the Michaelis-Menton equation. Interestingly, E231K ($K_M$=1.5μM, $k_{cat}$=7.7$s^{-1}$) has similar turnover rate ($k_{cat}$) and apparent ribosome binding constant ($K_M$) with EF-Gwt ($K_M$=0.91μM, $k_{cat}$=9.9$s^{-1}$). In the case of the other lysine mutants (E224K, E228K, and TK), it was not possible to determine $K_M$ and $k_{cat}$ constants due to their very low levels of GTP hydrolysis, which made it impossible to clearly differentiate their activity from the negative controls at ribosome concentrations below 2μM (Fig. IV.2A).

This demonstrated defect in multiple rounds GTP hydrolysis can be due in principle to one or multiple steps in the kinetic pathway (Rohrback and Bodley, 1976). One simple possibility is a defect in GTP binding. We used a fluorescent GTP analog, mant-GTP, to measure the affinity of all the EF-G mutants for GTP. Mant-GTP has been extensively used as a fluorescent GTP analog in the study of different G proteins based on its fluorescence emission increase upon binding to G proteins. We also confirmed the same property for mant-GTP binding to free EF-Gwt in solution, in line with previous reports (Savelsbergh et al., 2000b).

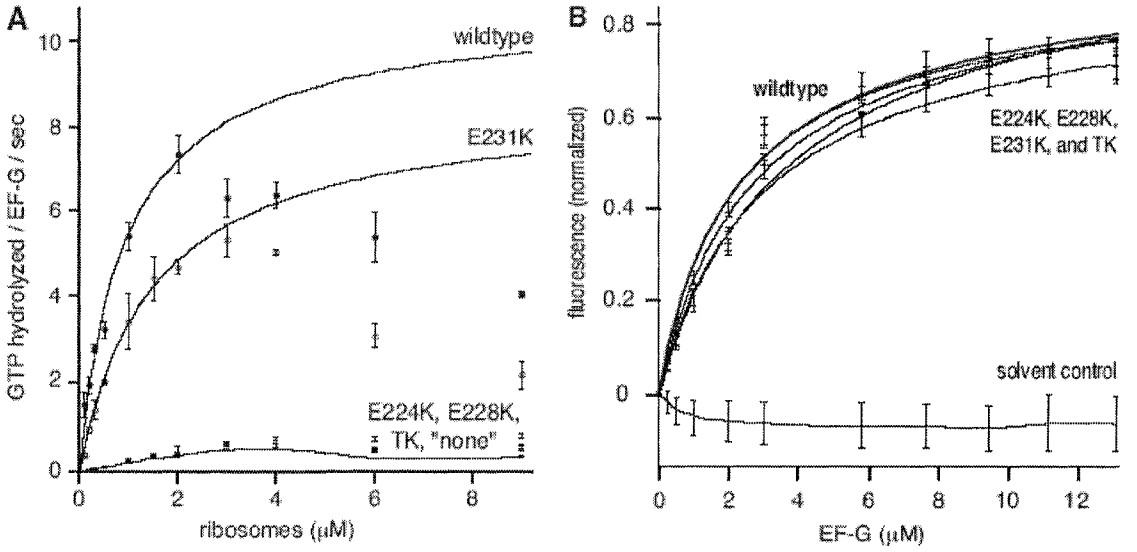


**Fig. IV.2 – The lysine mutants are inhibited in the multiple turnover GTP hydrolysis, but not in GTP binding.** *A.* Multiple turnover GTP hydrolysis catalyzed by EF-G proteins in the presence of vacant ribosomes. Data for EF-Gwt and E231K up to 2 μM ribosome were fitted to the equation: $v_0 = k_{cat}$ x [EF-G] x [R]/($K_M^R$ + [R]). Data for other reactions were fitted to interpolated curves. Reaction "none" contained only ribosomes and GTP. *B.* Binding of mant-GTP to EF-G proteins in the absence of ribosomes. Data were fitted to the equation: $F = F_0 + \Delta F_{max}$ x [EF-G]/($K_d$ + [EF-G]), and normalized with respect to EF-Gwt. In both panels, error bars are centered on the averages ± standard deviations of three independent reactions. Reproduced from (Nechifor et al., 2007)

For measuring the affinity of these proteins for mant-GTP, each EF-G mutant was titrated into a mant-GTP solution. The changes in fluorescence of mant-GTP were calculated and plotted as a function of the EF-G concentration, the $K_d$ for each mutant being obtained from fitting of the data. The lysine mutants had $K_d$ values between 2.2 and 3.7μM, which were practically identical to the one obtained for the wildtype protein (Fig. IV.2B).

In the absence of ribosomes, all the lysine mutants showed a weak, but measurable GTP hydrolysis activity (rates between $3x10^{-4}$ and $3x10^{-3}$ pmols of GTP hydrolyzed/s/pmol of EF-G), somewhat faster than the wildtype protein ($4x10^{-4}$) at similar concentrations of GTP and EF-G protein (Fig. IV.3.).

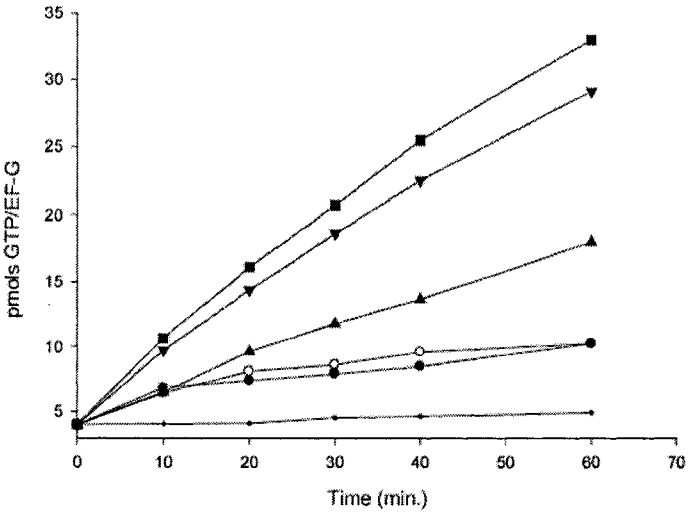


**Fig. IV.3. – Intrinsic GTP hydrolyzing activity of the lysine mutants.** The small dark dots (.) represent the negative control reaction (no EF-G added), the black circles (●) are for TK, the empty circles (○) are for WT, the triangles (▲) are for EF-GE224K, the upside down triangles (▼) are for EF-GE228K, and the diamonds (♦) are for EF-GE231K.

During the mant-GTP binding experiments, we noticed that the addition of 70S to a reaction containing EF-G and mant-GTP determined a gradual decrease in fluorescence which was dependent on the presence of both EF-G and 70S (Fig. IV.4.). This decrease in fluorescence reached a plateau after variable time, the slope being dependent on the concentration of 70S and EF-G (data not shown). Mant-GDP also increased its fluorescence upon binding to EF-G, but this change in fluorescence is approximately three fold lower than the one observed for mant-GTP (Fig. IV.4.), in agreement with previous reports (Savelsbergh et al., 2000b).

Interestingly, we noticed that the increase of mant-GDP fluorescence induced by EF-G reached the same level as the plateau seen in the reaction containing EF-G, 70S, and mant-GTP (data not shown), suggesting that mant-GTP is being hydrolyzed to mant-GDP by EF-G bound to ribosomes. In order to test this hypothesis, we monitored the fluorescence of mant-GTP during the addition of EF-Gwt, followed by extraction of the first sample, addition of ribosomes, and extraction of the second and third samples from the cuvette (Fig. IV.4A). The extracted samples were quenched by acid precipitation and separated by TLC (Fig. IV.4B). According to the TLC separation, the first sample taken after EF-G addition contains just mant-GTP, while the second sample, extracted after addition of ribosomes and during the fluorescence decrease, shows a majority of mant-GDP, with a small amount of mant-GTP left.

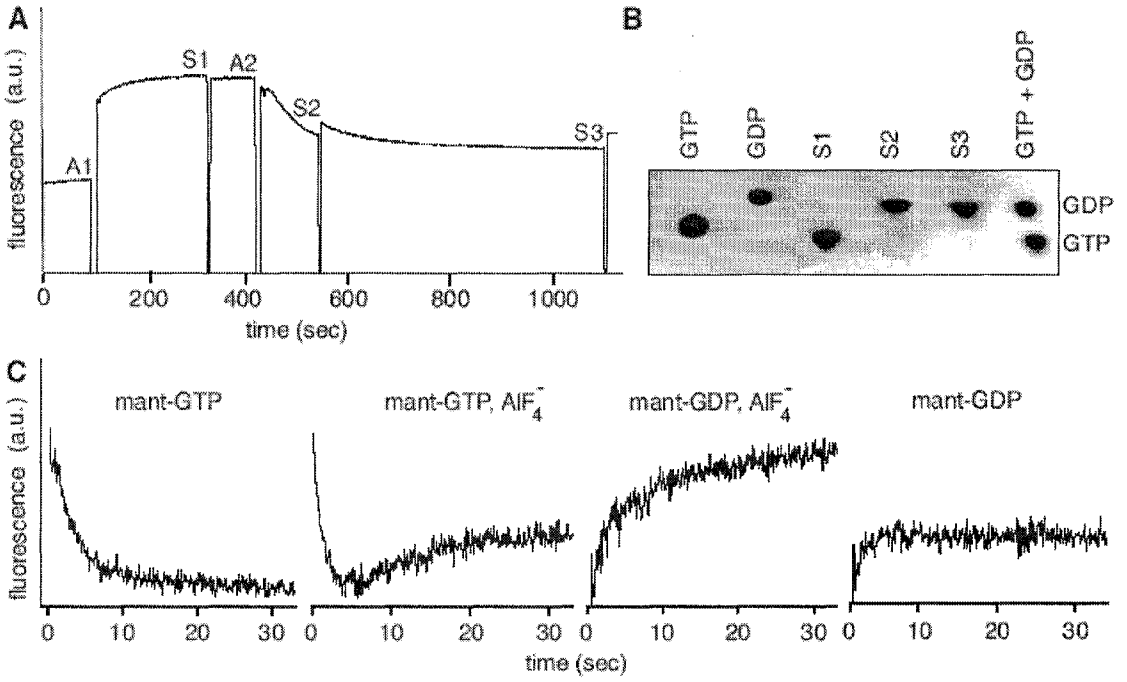


**Fig. IV.4. - Fluorescence changes of mant-GTP associated with its binding and hydrolysis.** *A.* Multiple turnover hydrolysis of mant-GTP (120μM). Additions: *A1*, EF-G (25μM); *A2*, ribosomes (0.7μM). *B.* TLC of samples (*S1-S3*; 20μl), taken from panel A, and controls. *C.* Effects of $AlF_4^-$ on mant nucleotides fluorescence in complex with EF-Gwt and ribosomes. Reproduced from (Nechifor et al., 2007)

The final sample, taken in the fluorescence plateau, contains only mant-GDP, with no detectable traces of mant-GTP. The analysis of these samples clearly shows that the decrease in fluorescence is associated with the hydrolysis of mant-GTP to mant-GDP (Fig. IV.4A and B).

The change in fluorescence between mant-GTP and mant-GDP states suggests that it is due to a conformational change in EF-G, potentially lowering the hydrophobic environment of the mant group in the GDP state. The next question we tried to address was the timing of this event, whether it happens during the cleavage of the phosphoanhydride bond or during the subsequent release of Pi from EF-G.

In order to characterize further this mechanism, we took advantage of the properties of $AlF_4^-$, an analog of the planar transition state structure of the γ-phosphate leaving group, which is known to form tight complexes with many G proteins in the GDP state (Wittinghofer, 1997). We assembled several complexes under single turnover conditions of mant-GTP hydrolysis using a stopped flow device, which rapidly mixed stoechiometric amounts of EF-G•mant-GTP and ribosomes, in the presence or absence of $AlF_4^-$ (Fig. IV.4C).

Under the single turnover conditions, in the absence of $AlF_4^-$, the fluorescence of mant-GTP decreased rapidly, reaching a plateau after approximately 10 sec. In contrast, in the presence of $AlF_4^-$, the rapid decrease in fluorescence is followed by a slow increase. In the case of mant-GDP, there is a small increase in fluorescence upon the addition of ribosomes to the EF-G•mant-GDP complex, probably due to binding to the ribosomes. In the presence of $AlF_4^-$, the addition of ribosomes determines a slow increase in fluorescence signal, resulting in a final large increase in fluorescence (Fig. IV.4C). All these results together indicate that the change in fluorescence of mant-GTP in the presence of both EF-G and ribosomes corresponds to both the hydrolysis and the Pi release steps.

Taking advantage of this finding, we used the fluorescence change of mant-GTP as another GTP hydrolysis assay in order to further explore the properties of these mutant proteins. The initial reactions contained an excess of mant-GTP and EF-G over ribosomes (multiple turnover conditions for ribosomes), and the mutants were found to have the same order of activity as observed in the radioactive GTP hydrolysis assay (data

not shown). More importantly, mant-GTP has allowed us to measure the rates of single round GTP hydrolysis for EF-Gwt and the mutants, under conditions where EF-G was in two fold excess over mant-GTP, and the ribosomes were in slight excess over EF-G. The obtained results clearly show that the mutants are also inhibited in the single round GTP hydrolysis when compared to the wildtype protein, displaying also the same order of activity as the one observed for the multiple turnover GTP hydrolysis assay (Fig. IV.5.). The TK mutant was again the most inhibited of all the lysine mutants, its $k_{obs}$ being 200 fold lower than the one measured for EF-Gwt. E224K and E228K are also severely defective in catalysis of single round GTP hydrolysis, being 65 fold slower than the wildtype protein. As seen before, EF-G E231K is the most active of all the lysine mutants, with a $k_{obs}$ only 2 fold lower than EF-Gwt (Table IV.1.).

Worth noticing was the fact that EF-Gwt hydrolyzed mant-GTP at an observed rate of 1.8 $s^{-1}$, which is approximately 10 fold slower than the reported Pi release rate (20 $s^{-1}$), and 40 fold slower than the previously measured rate of GTP hydrolysis (80 $s^{-1}$) (Savelsbergh et al., 2003). These results suggest that the observed decrease in mant group fluorescence could be due to a conformational change that follows the release of Pi, and it has slower rate than the process of Pi release. Another possibility is that the mant group could partially interfere with the GTP hydrolysis, decreasing the observed reaction rate.

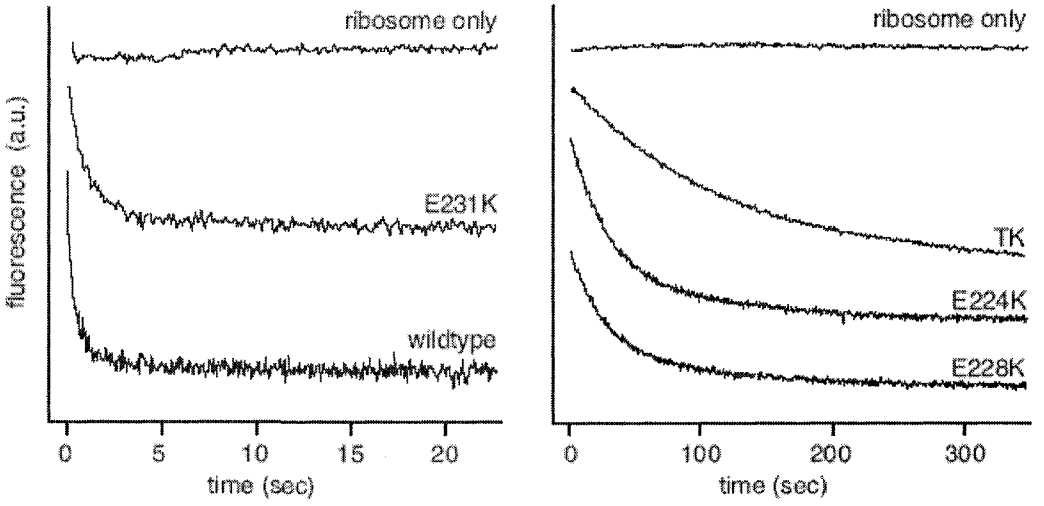


**Fig. IV.5. – The single turnover hydrolysis of mant-GTP catalyzed by EF-G in the presence of ribosomes.** For clarity, the fluorescent traces were mathematically offset on the vertical axis. Note the difference in time scale between the two graphs. Reproduced from (Nechifor et al., 2007)

Since the major role of EF-G is to translocate the tRNAs and mRNA connected to them, our next step was to test the activity in these mutants in translocation assays. The hydrolysis of GTP by EF-G bound to a pre-translocation complex is believed to induce complex conformational changes of the complex, which determine Pi release and the translocation of tRNAs and mRNA (Katunin et al., 2002; Savelsbergh et al., 2003). Since our lysine mutants are defective in GTP hydrolysis, their ability to catalyze translocation could also be affected due to the tight connection between these two processes.

We initially used the toe-printing assay to qualitatively assess if these mutant proteins are able to translocate the mRNA in regard to the 30S subunit. The first experiment attempted contained an equal amount of EF-G (wildtype or mutant) and pre-translocation ribosomal complex, the results showing that all the proteins were able to complete the translocation reaction, without any detectable differences between them (Fig. IV.6.).

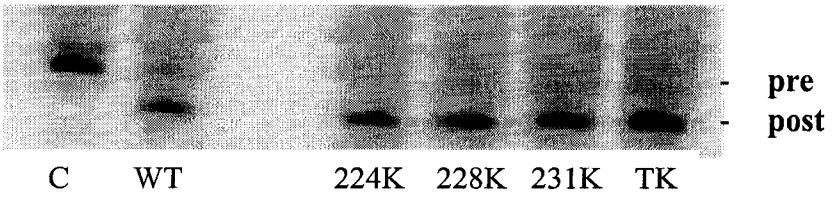


**Fig. IV.6. – Toe-printing assay showing the translocation abilities of the G' mutants under single turnover conditions.** The first reaction (C) is the negative control, which had no EF-G added to it.

In order to detect differences between these mutants and wildtype, we decreased the concentrations of the EF-G proteins to one tenth of that of the ribosomal complexes, causing all the reactions to go through multiple turnovers. In this case, the toe-printing gels clearly showed that mutants take a longer time to reach complete translocation than the wildtype protein, with TK being the slowest one. E231K was still the fastest of our lysine mutants, while E224K and E228K had activities between that of TK and that of 231K (Fig. IV.7.).

The toe-printing gels showed another interesting feature of the translocation reactions. The pre-translocation complex is composed of two distinct conformations,

which map at positions +16 and +17 of the mRNA, in agreement with previous studies (Joseph and Noller, 1998). In the case of EF-Gwt, the complex corresponding to position +17 quickly translocated to position +19, while the one mapping at position +16 was translocated slower. In the case of the lysine mutants, both complexes were translocated slower.

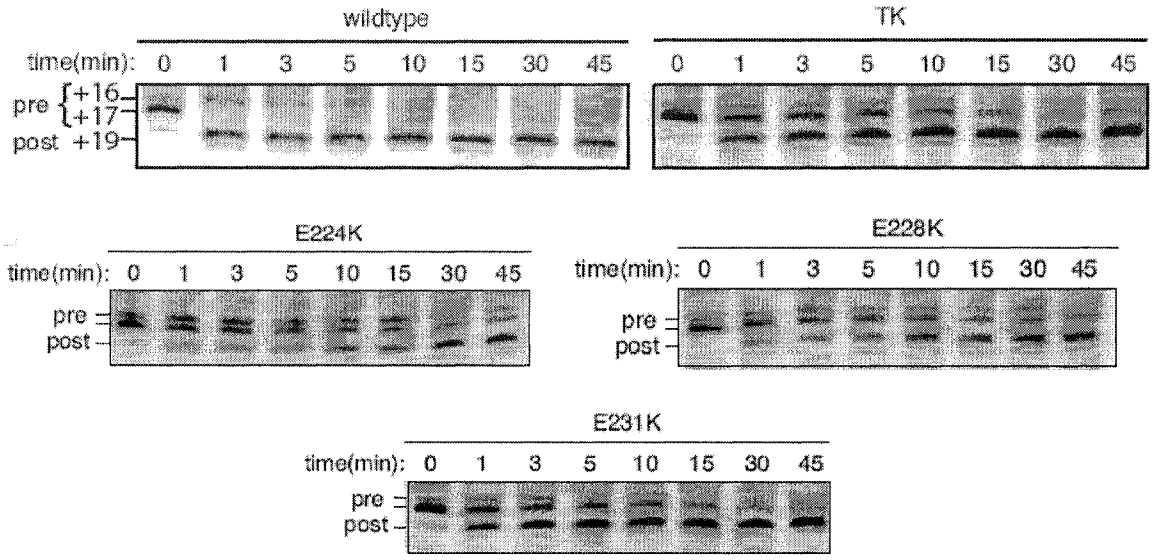


**Fig. IV.7. – Toe-printing assay showing the effects of the G' mutations on mRNA translocation under multiple turnover conditions.** Note the effects on both kinetics and pattern. Reproduced from (Nechifor et al., 2007)

In order to be able to accurately measure the rates of single round translocation, we used a previously developed fluorescent assay (Studer et al., 2003). The pre-translocation ribosomal complex is assembled using a pyrene labeled RNA oligonucleotide, which drastically increases its fluorescence upon binding to ribosomes. Translocation of the RNA oligonucleotide in the ribosomal 30S subunit is associated with a decrease in the pyrene fluorescence, which can be used to measure the rate of translocation. This decrease in fluorescence is not present when the pre-translocation complex is mixed with 1mM GTP (final concentration), showing that there is no translocation in the absence of EF-G (Fig. IV.8.).

Upon addition of EF-G, the decay in fluorescence is clearly biphasic, EF-Gwt having a $k_{obs}$ of 0.58 $s^{-1}$ for the fast phase, and $k_{obs}$ of 0.056 $s^{-1}$ for the slower phase. The rate of the fast phase is similar to the one previously reported for this assay (Studer et al., 2003), but slower than the rate measured in other studies (Feinberg and Joseph, 2006; Savelsbergh et al., 2003). This difference was recently attributed to the C-terminal 6 histidine tag attached to our EF-G construct, as well as other smaller factors (Feinberg and Joseph, 2006).

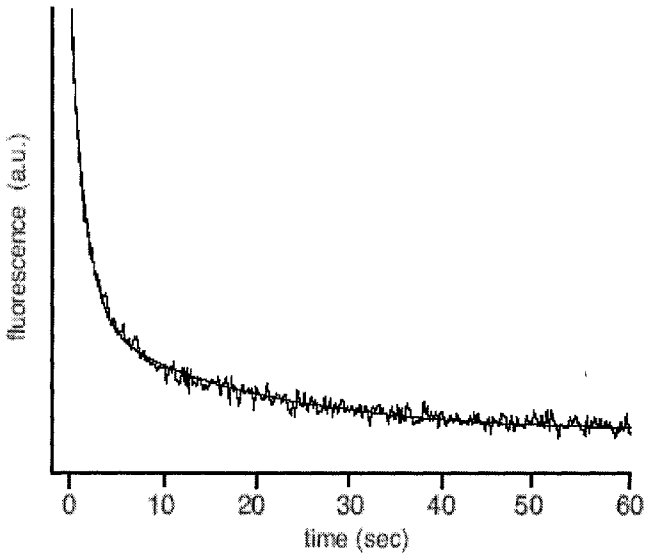


**Fig. IV.8. – Fluorescence decrease of the pyrene labeled mRNA during translocation by EF-Gwt.** Its biphasic kinetic was fitted using a double exponential equation (see Materials and Methods). Reproduced from (Nechifor et al., 2007)

All the lysine mutants showed a slower rate of translocation when compared to EF-Gwt, preserving also the same order of activity as in the GTP hydrolysis reactions. In the case of this translocation assay, E231K was also the most active of all the mutants, showing only approximately 25% inhibition as compared to wildtype. The other single lysine mutants, E224K and E228K, were more inhibited, displaying a translocation rate approximately five fold lower than wildtype, while in the case of the triple lysine mutant we measured a ten fold inhibition (Fig. IV.9. and Table IV.1). The differences between EF-Gwt and mutants are lower than the ones observed in the case of single turnover GTP

hydrolysis and they are attributed mostly to the fast phase of the fluorescence decay, the slower phase being only slightly affected.

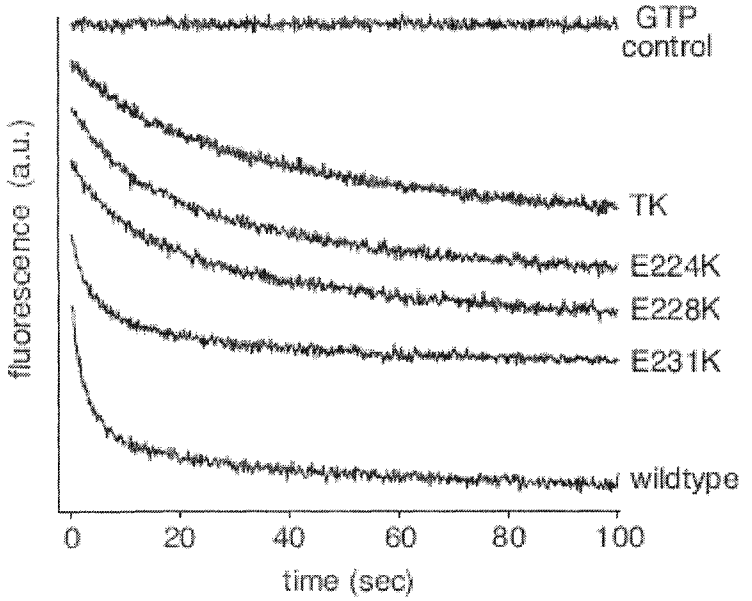


**Fig. IV.9. – Monitoring the single round translocation by the decrease in fluorescence of the pyrene-labeled mRNA.** The fluorescent traces were mathematically offset along the vertical axes for clarity purposes. The trace labeled GTP control contained just the pre-translocation complex and GTP, while the other reactions contained pre-translocation complex, GTP, and EF-G. Reproduced from (Nechifor et al., 2007)

In order to dissect further the defects demonstrated by the lysine mutants in translocation, we measured the rates of translocation for EF-Gwt and mutants at different concentrations of EF-G. The concentrations chosen for these titration experiments were always in great excess over the pre-translocation ribosomal complex (i.e. pseudo-unimolecular conditions).

In the case of EF-Gwt, the translocation rate has increased with increases in EF-G concentration, the fast phase of the translocation reaction being directly dependent on EF-G concentration, while the slow phase was only marginally affected. By contrast, all four of the lysine mutants increased relatively little their translocation rates as compared to the increase observed in the case of wildtype, hence the differences between their translocation rates is even greater at the higher concentration rates (Fig. IV.10.).

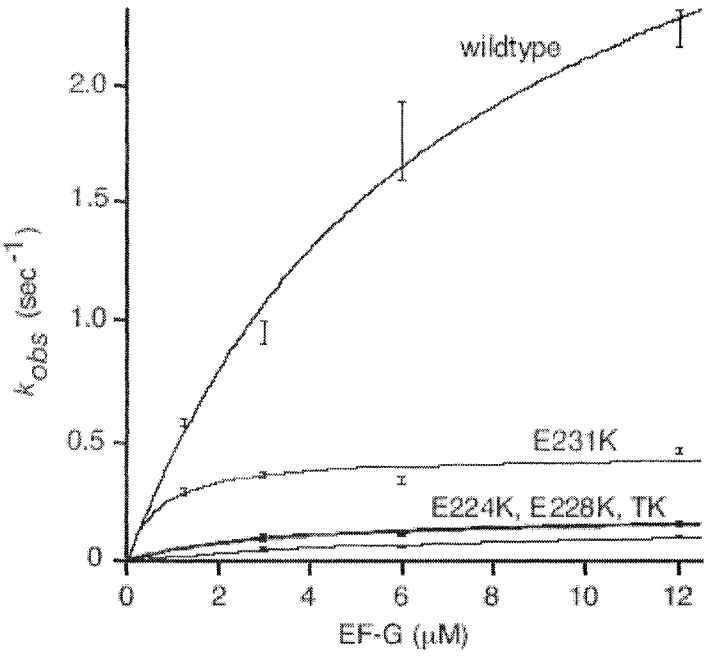


**Fig. IV.10. - Dependence of translocation kinetics on the concentrations of G' mutants and wildtype EF-G.** Values of $k_{obs}$ correspond to the first phase of single-turnover translocation. Data were fitted to the reaction mechanism shown below.

$$A1 + B1 \underset{k_{-1}}{\overset{k_1[A1]}{\rightleftharpoons}} A1 \bullet B1 \xrightarrow{k_2} A2 \bullet B1 \xrightarrow{k_3} A2 \bullet B2$$

where: A1 = EF-G•GTP; A2 = EF-G•GDP; B1 = pre-translocational complex; B2 = post-translocational complex; $k_{obs}$ = A1/(C1xA1 + C2); C1 = (*k2* + *k3*)/*k2*x*k3*; and C2 = (*k-1* + *k2*)/*k1*x*k2*. Error bars are centered on the averages ± standard deviations of three independent reactions. Reproduced from (Nechifor et al., 2007)

The defects detected in the G' mutants are believed to be due to their impaired interaction with the r-protein L7/L12. For further exploration of this association, we repeated our assays using ribosomes that have been depleted of L7/L12 by the $NH_4Cl$/ethanol method (see Materials and Methods). The extent of L7/L12 stripping was quantified by immuno-blotting, which showed that more than 95% of the L7/L12 had been removed (Fig. IV.11.).

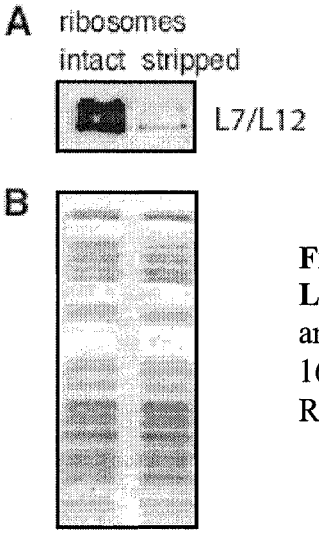


**Fig. IV.11. – Specific removal of the r-protein L7/L12 from the ribosome.** *A.* immunoblot using anti-L7/L12 antibodies. *B.* Commassie blue stained 16.5% SDS-PAGE showing the separated r-proteins. Reproduced from (Nechifor et al., 2007)

When using L7/L12 depleted ribosomes, the multiple turnover rates of GTP hydrolysis drastically decreased for EF-Gwt, measuring an approximate 140 fold difference (9.9 compared to 0.07 $s^{-1}$) between the control and L7/L12 stripped ribosomes (Fig. IV.12.).

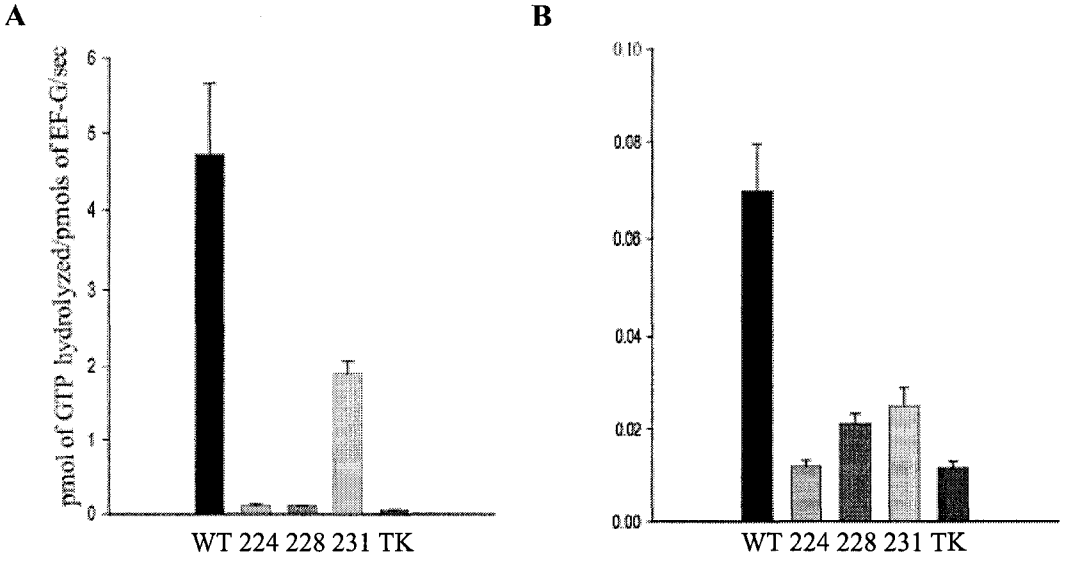


**Fig. IV.12. – GTP hydrolysis rates of EF-G lysine mutants.** *A.* In the presence of control ribosomes. *B.* In the presence of L7/L12 stripped ribosomes. Note the difference in scale between the two graphs.

In the case of mant-GTP hydrolysis, the impact of stripping L7/L12 is not as great, showing a difference of only 12 fold, which suggests that the mant group interferes with the rate of GTP hydrolysis. In contrast, the most defective of the lysine mutants (E224K, E228K, and TK) demonstrated no difference between the rates of mant-GTP hydrolysis in the presence and absence of L7/L12. E231K had a behavior between that of EF-Gwt and the defective lysine mutants. Also, interestingly, in the absence of L7/L12, the rates of mant-GTP hydrolysis are closer between EF-Gwt and the lysine mutants, the small difference remaining being probably due to the residual L7/L12 present on the ribosomes. (Table IV.1)

**Table IV.1. – Functional effects of stripping L7/L12 from the ribosomes**

| | mant-GTP hydrolysis, $k_{obs}$ ($s^{-1}$) [1] | | mRNA translocation, $k_{obs}$ ($s^{-1}$) [2] | |
|---|---|---|---|---|
| *+EF-G* | *+L7/L12* | *- L7/L12* | *+L7/L12* | *- L7/L12* |
| wildtype | 1.8 ± 0.1 | 0.149 ± 0.007 | 0.58 ± 0.02 | 0.067 ± 0.004 |
| E224K | 0.028 ± 0.001 | 0.027 ± 0.001 | 0.055 ± 0.003 | 0.051 ± 0.006 |
| E228K | 0.027 ± 0.001 | 0.024 ± 0.001 | 0.059 ± 0.002 | 0.050 ± 0.005 |
| E231K | 0.8 ± 0.1 | 0.088 ± 0.003 | 0.27 ± 0.01 | 0.057 ± 0.006 |
| TK | 0.009 ± 0.001 | 0.022 ± 0.001 | 0.029 ± 0.001 | 0.029 ± 0.001 |

Single-turnover reactions contained vacant ribosomes[1] or pre-translocation complexes[2], which were intact (+L7/L12) or stripped (-L7/L12). Values represent the averages ± standard deviations of three or four independent reactions (stopped flow injections). Reproduced from (Nechifor et al., 2007)

We have also measured the single round translocation rates using L7/L12 stripped ribosomes to assemble the pre-translocation complexes. Similar to the mant-GTP hydrolysis, in the case of EF-Gwt, there is an approximately 9 fold difference between the control and L7/L12 stripped ribosomes, while the defective lysine mutants showed no clear differences. The rates for both EF-Gwt and mutants are very similar in the absence of L7/L12. (Table IV.1)

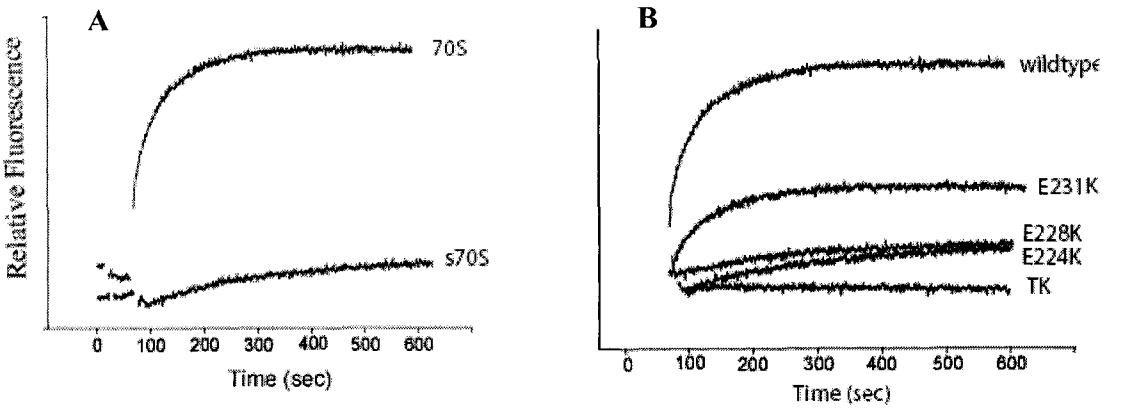


**Fig. IV.13. Binding of mant-GDPNP to the EF-G•70S complex.** *A.* Comparison between binding of mant-GDPNP to EF-Gwt in complex with either control ribosomes (70S) or L7/L12 stripped 70S (s70S). *B.* Comparison between binding of mant-GDPNP to different EF-G proteins in complex with control 70S.

In order to understand better the differences in pre-hydrolysis complex assembly of ribosomes with different lysine mutants, we tested their binding to mant-GDPNP, a non-hydrolyzable GTP analog. Similar to mant-GTP, mant-GDPNP also shows a strong increase in fluorescence upon binding to EF-G, but the $K_d$ for binding in solution is high, being measured at 120μM (Savelsbergh et al., 2000b). In the presence of ribosomes, the $k_d$ decreased by 240 fold, to 0.5μM (Savelsbergh et al., 2000b). We used dilute concentrations of mant-GDPNP, so that the binding, monitored by the increase in fluorescence, can be observed only in the presence of ribosomes. Under these conditions, when EF-Gwt is incubated with mant-GDPNP, there is little to no increase in fluorescence. Upon addition of ribosomes, there is a fast, exponential increase in fluorescence, which stabilizes in a plateau at approximately 50% increase from the initial value. Interestingly, the behavior is very different in the presence of L7/L12 stripped ribosomes, the rise in fluorescence being small (around 5%) and linear rather than exponential (Fig. IV.13A). Identical experiments were repeated for all the lysine mutants in the presence of normal ribosomes. In the case of E231K, there is an exponential rise in the fluorescence of mant-GDPNP with a 2.5 fold lower rate than in the case of wildtype. Interestingly, E231K produces only a 20% increase in the fluorescence of mant-GDPNP, as compared to the 50% increase produced by EF-Gwt. The remaining lysine mutants show a behavior very similar to the L7/L12 stripped ribosomes, with a very small, linear

increase in fluorescence, which is almost undetectable in the case of the triple lysine mutant (Fig. IV.13B).

## IV.3. DISCUSSIONS

L7/L12 is one of the most studied r-proteins due to its involvement in the activity of ribosomal factors. Our crosslinking studies locate the interaction between EF-G and L7/L12 in the G' subdomain, an insertion in the G domain with an unknown role. In order to understand the role of this subdomain and its interaction with L7/L12, we constructed four mutants (E224K, E228K, E231K, and TK) with the intention of disrupting the interaction of helix $A_{G'}$ and the r-protein L7/L12 (Fig. IV.14.).

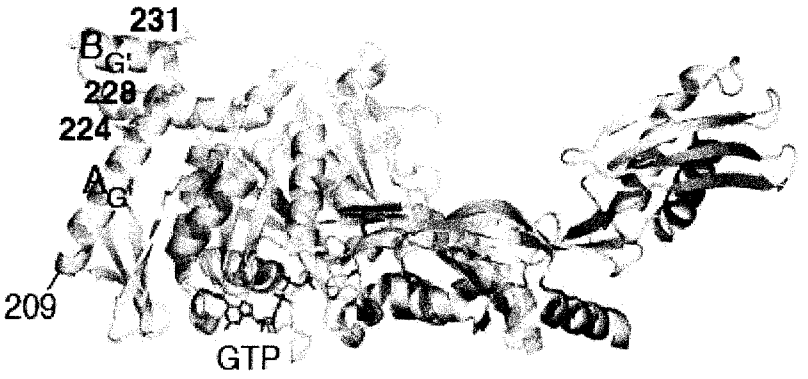


**Fig. IV.14. - Locations of mutated residues in the G' subdomain of EF-G.** Cartoon is based the structure of *T. thermophilus* EF-G-2•GTP, a homologue of EF-G (Connell et al., 2007). *Yellow*, G' subdomain; *orange*, residues equivalent to *E. coli* E224, E228, and E231. Reproduced from (Nechifor et al., 2007)

All the four mutants analyzed in this study have lower activities in multiple turnover GTP hydrolysis, when compared to the wildtype EF-G. The degree of inhibition varies a lot between the constructed mutants, with EF-G E231K being only slightly less active than EF-Gwt, while the remaining three are drastically inhibited in GTP hydrolysis, with TK being the most defective mutant. Importantly, the GTP hydrolysis assay in the absence of ribosomes showed that the mutants are at least as active as the wildtype, when their activity is not stimulated by the presence of ribosomes, indicating that the catalytic defect is not intrinsic to these proteins, but it is caused by their

differential activation by the ribosome. This conclusion also receives support from the fact that these mutants bind mant-GTP similarly to the wildtype protein, demonstrating no defect in nucleotide binding.

Mant-GTP proved to be an excellent tool to dissect further the activity of these mutants by measuring the rates of single round GTP hydrolysis. The presence of a fluorescent change accompanying mant-GTP hydrolysis by EF-G is rare among G proteins, but it is an extremely useful property and it may be used in the future to study in detail the mechanism of GTP hydrolysis in EF-G. A similar fluorescence response was observed for another G protein, $p21^{NRAS}$, and it is believed to be caused by a conformational change corresponding to an activated complex that precedes the hydrolysis step (Neal et al., 1990). A change in fluorescence of mant-GTP was also described for EF-Tu, but the response was biphasic, starting with an increase in fluorescence due to the binding of the ternary complex to the ribosome, and followed by a decrease due to the dissociation of EF-Tu•mant-GDP from the ribosome (Savelsbergh et al., 2005). Upon $AlF_4^-$ studies, it became clear that the change in fluorescence of mant-GTP is due, in the case of EF-G, to a slower conformational change following GTP hydrolysis and Pi release.

The results from the single and multiple rounds GTP hydrolysis show a very similar order of activity for the lysine mutants. The combined results from these experiments lead us to the conclusion that the defects of these mutants do not lie in the turnover step, but on the activation of GTP hydrolysis by the ribosomal complex.

The translocation assays show the mutants to be inhibited in multiple turnovers, as well as in the single round assays. Although the differences between mutants and wildtype are not as large as in the case of GTP hydrolysis, the relative order of activity between the lysine mutants is conserved. In order to dissect further the mechanism of the observed translocation defects, we measured the translocation rates as a function of EF-G concentration. This experiment revealed that the translocation rate of EF-Gwt was directly dependent on concentration, while in the case of the lysine mutants, there were very small, almost insignificant increases. According to these results, the translocation rate of EF-Gwt is limited by its association with the ribosomal complex, while this is not the case for the lysine mutants. The slower translocation rates of all four lysine mutants

(including the most active one, EF-G231K) are not due to defects in productive association with the ribosomal complex, but, in a subsequent step, likely the GTP hydrolysis reaction.

Since the differences observed in GTP hydrolysis assays between EF-G and the lysine mutants are significantly larger than the ones observed in translocation, it is possible that the defects of these mutants directly affect GTP hydrolysis, which in turn affect the translocation rates indirectly. This conclusion is partially in line with a different study which looked at the effects of mutants in the CTD of L7/L12 on EF-G functions and found that the Pi release was affected by these mutations, but surprisingly they did not detect any consequence for translocation rates (Savelsbergh et al., 2005). Another possibility that could explain the lower differences detected in translocation rates is that the 6xHis tag has a more drastic effect on the fast translocation rate of EF-Gwt, while only marginally affecting the already decreased rates of the lysine mutants.

The removal of L7/L12 from ribosomes has decreased the rates of both mant-GTP hydrolysis and translocation for EF-Gwt, as well as for E231K, the most active of all the mutants, bringing them also close to the rates of the defective lysine mutants (E224K, E228K, and TK). Stripping of L7/L12 did not affect the already inhibited rates of the defective lysine mutants. These experiments indicate that the defects detected in the lysine mutants are due to the disrupted interaction with L7/L12.

L7/L12 depleted ribosomes show a very small, linear increase in the fluorescence of mant-GDPNP in the presence of EF-G, as opposed to the one observed with control ribosomes. EF-G E224K, E228K, as well as TK increase very little the fluorescence of mant-GDPNP in the presence of control ribosomes, being similar in behavior to EF-Gwt in the presence of L7/L12 stripped ribosomes. This result highlights again the fact that these lysine mutants disrupt the interaction between EF-G and L7/L12.

The small increase in fluorescence of mant-GDPNP in the presence of the lysine mutants is reminiscent to that observed for an "activated" GTP hydrolysis state formed by addition of mant-GDP and $AlF_4^-$ to EF-G•70S complexes (Mohr et al., 2002), leading to the hypothesis that the binding of mant-GDPNP may also require the formation of an "activated" state. This proposed "activated" state may be determined by an L7/L12 catalyzed conformational change that could decrease the affinity of EF-G for GDPNP

and/or modify the environment of the mant nucleotide, hence increasing the fluorescence of mant-GDPNP.

Positions 224 and 228 in the G' subdomain seem to be extremely important for the interaction between EF-G and L7/L12, their single replacement resulting in drastically defective mutants. TK is the least active of all the mutants due to the replacement of all three glutamic acids with lysines, which probably destabilizes the interaction with L7/L12 more than the individual replacements. The difference between triple and single substitutions is small in the tested assays, suggesting that the individual mutations prevent efficiently the interaction between EF-G and L7/L12 by themselves. In contrast, the replacement of the conserved glutamic acid at position 231 with a lysine has only limited effects, confirming the results of the previous NTCB probing experiments (Chapter III), which indicated that position 231 does not directly interact with L7/L12. The small effects detected for E231K are most likely proximity effects due to its closeness with residues 224 and 228. E224 is very well conserved as a glutamic acid in all the bacterial species, and as a negatively charged residue in mitochondria of eukaryotic organisms (Fig. IV.1.). The hydrophobic residues surrounding position 224 are also conserved, and they may either interact with other hydrophobic residues from L7/L12 and/or stabilize the structure of this region of the G' subdomain. By contrast, E228 is not as well conserved as E224, although its mutation has very similar effects. This residue can be either involved in an *E. coli* specific interaction or it may exert its effects due to the vicinity with position 224.

The interaction between the C terminal of helix $A_{G'}$ and the r-protein L7/L12 promotes probably complex re-arrangements in the G domain, leading to Pi release post GTP hydrolysis, supposingly by the involvement of switches 1 and 2. The specific conformational changes in the G' subdomain and their influence on the potential re-aligning of switches 1 and 2 from the G domain are still unknown and require additional studies to be elucidated.

The combination of results from our previous crosslinking experiments and the new functional study clearly indicate that EF-G interacts with L7/L12 through the C-terminal part of helix A in the G' subdomain, E224 and E228 participating probably in

ion pairs similar with the ones described in the case of helix D of EF-Tu (Kothe et al., 2004).

In addition to EF-Tu and EF-G, whose interaction with the r-protein L7/L12 has been discussed in detail, there are two other G proteins involved in translation: IF2 and RF3. In the case of IF2, earlier crosslinking data (Heimark et al., 1976), confirmed by recent cryo-EM studies (Allen et al., 2005) has shown that IF2 is in close proximity and probably interacts with L7/L12. Its G domain seems to bind in a similar position with the G domains of EF-G and EF-Tu between the two ribosomal subunits. The cryo-EM maps of the initiation complex appear to contain a density corresponding to the CTD of L7/L12, which is seen inserted between the density assigned to the G domain of IF2 and the r-protein L11 (Allen et al., 2005). Due to the proposed drastic conformational changes in the structure of IF2 in the initiation complex, as compared to the crystal structure (free in solution), it was not possible to determine the structural elements which may participate in the interaction with L7/L12. RF3 is also believed to bind with its G domain in the same position between the two ribosomal subunits as the G domains of IF2, EF-Tu and EF-G. Moreover, RF3 and EF-G both contain G' subdomains, while IF2 and EF-Tu do not. Because of similarities in ribosome binding with the other G proteins involved in translation, it is believed that the functional activity of RF3 could also be influenced by L7/L12. For a more detailed review regarding RF3 see (Buckingham et al., 1997).

A new NMR study (Helgstrand et al., 2007) has revealed that all these four translation factors (IF2, EF-Tu, EF-G, and RF3) seem to interact with the same region of L7/L12, namely helices 4 and 5 of the CTD. The authors hypothesize that all these factors interact through their G domains, arguing that this domain is common between all of them. To us, it seems more likely that the region from each factor which interacts with L7/L12 is slightly different (e.g. helix $D_G$ for EF-Tu, and helix $A_{G'}$ for EF-G), contributing probably to the proper factor recognition by the ribosomal complexes.

## IV.4. MATERIALS AND METHODS

### IV.4.1. Materials

RNA oligo (5'-AAGGAGGUAAAAAUGUUUGCUN6-3') was synthesized by Dharmacon. Mant labeled nucleotides were purchased from Invitrogen Inc. (Molecular

Probes). Polyclonal IgG antibodies raised against specific *E. coli* L7/L12 r-protein were a generous gift from R. Brimacombe (Max Planck Institute). The following buffers were used in experiments: *buffer 1*, 50mM Tris-HCl pH 8.0, 100mM KCl, 10mM $MgCl_2$, 0.1mM EDTA, 1mM PMSF, and 10mM β-mercaptoethanol *buffer 2*, 80 mM Hepes (pH 7.7), 50 mM $NH_4Cl$, 10 mM $MgCl_2$, 1 mM DTT, and *buffer 3*, 50 mM Hepes-KOH (pH 7.7), 100 mM $NH_4Cl$, 20 mM $MgCl_2$, 1 mM DTT. *$AlF_4^-$ complex*: 100μM $AlCl_3$ and 10mM NaF in buffer 2.

### IV.4.2. Construction and purification of ΔG' mutant

A deletion mutant of the G' subdomain was constructed by site-directed mutagenesis (Evnin and Craik, 1988) from the EF-G expression plasmid pET24b-fusA using the primer 5'-CGCAGAACCACAGGTTACCAGGATGCCGTTCGCGCCCAGACGGGTTTTGATC-3', which replaces the whole G' subdomain (residues 166-261) with a single glycine residue. The colonies were screened using colony PCR technique and successful mutagenesis was confirmed by plasmid DNA sequencing. This mutant was overexpressed in *E. coli* BL21(DE3) by addition of 1mM IPTG. Protein purification from the soluble fraction obtained after cell lysis did not yield a full length protein, the mutant being present only in inclusion bodies. The full length protein was finally purified from inclusion bodies using a protocol adapted from (Savelsbergh et al., 2000a). Bacterial cells were lysed by sonication in buffer 1, following by centrifugation (Beckman Coulter Optima-90K Ultracentrifuge, Ti50 rotor, 16,500rpm, 20 min, 4°C), resuspension of the pellet in buffer 1 + 7M urea, and a second centrifugation identical to the first one. The supernatant was added to 3ml of Ni-NTA beads (Qiagen), which were previously washed three times with the same buffer, and allowed to bind for 2h at 4°C with shaking. After the binding step, the urea was washed from the Ni-NTA beads by a 30ml gradient between buffer 1 + 7M urea and buffer A (no urea added), followed by 30ml wash with the same buffer 1 + 20mM imidazole, and elution of the protein with buffer 1 + 1M imidazole. The chosen fractions were concentrated using ultrafiltration (Microcons YM-10, 3,000g, 30 min.) and dialyzed against the standard storage buffer.

### IV.4.3. GTP hydrolysis assay

Reactions contained 50μM GTP, 0.05 μCi [$\gamma$-$^{32}$P]GTP, 0.04μM EF-G, and various concentrations of 70S ribosomes (as indicated in the figures) in 10 μl of buffer 2. EF-G and 70S were pre-incubated at 37°C for 10 minutes before addition of GTP, in order to equilibrate the reactions at 37°C and to hydrolyze any potential GTP present in either the EF-G or 70S preparations (Rohrback and Bodley, 1976). The reactions were started by the addition of GTP mix and quenched with an equal volume of 30% (v/v) formic acid after variable time intervals. In general, between 3 and 5 time points were collected. Sample separation using TLC PEI-cellulose plates and quantification of percentage of GTP hydrolysis were done as previously described in Chapter III.

### IV.4.4. Mant-GTP binding and hydrolysis assays

The fluorescence of mant nucleotides was excited at 362±2 nm and detected at 438±4 nm using a PTI QM-6 (Photon Technology International) equipped with a LPS-220B lamp. For the binding experiment, we titrated 1μM mant-GTP solution in 2ml of buffer 2 with EF-G (0-15μM). The solution was continuously mixed with a stir bar and the fluorescence emission was measured after the solution was allowed to reach equilibrium following each EF-G aliquot.

For the experiment in Fig. IV.3., the fluorescence of 120μM MantGTP in buffer 1 (250μl final reaction volume) was measured, followed by the serial additions of 25μM EF-Gwt and 0.7μM 70S, at the times indicated in the figure, and mixed by pippeting. Three different samples (20μl) were extracted from the cuvette at the indicated time points and acid precipitated with 0.2M HCl. The supernatant of these reactions was concentrated to a final volume of approximately 8μl using a Vacufuge (Eppendorf), and 2μl (~ 500pmols) were spotted on a silica TLC plate (silica gel 60 F-254 – EM reagents, Brinkmann Instruments Canada Ltd.) together with controls containing 2500 pmols of mant-GTP, 1200 pmols of mant-GDP, and 500 pmols of 1:1 mixture of mant-GTP and mant-GDP respectively. The TLC plate was separated in a running buffer containing 2-propanol:25%$NH_4OH$(v/v):$H_20$ = 9:5:1(v/v/v) (Savelsbergh et al., 2000b), dried and the mant nucleotides were visualized by UV irradiation at 365nm (UV lamp model UVLS-24, Upland).

Single round mant-GTP hydrolysis was measured using a stopped-flow MiniMixer (KinTek Corporation) attached to the above described fluorimeter. The MiniMixer has two syringes. Syringe A contained 20μM EF-G pre-incubated with 24.4μM 70S in buffer 2 at room temperature, while syringe B contained 10μM mant-GTP in buffer 2. In some experiments, $AlF_4^-$ complex (100μM) was mixed in syringe B. The MiniMixer injects the same volume (200μl) from each syringe, mixing them rapidly with a dead time of 3.5 ms and injecting them into the cuvette. Data points were collected every 50-1000 ms, depending on the activity of the mutant tested, and recorded by Felix32 (analysis mode) software using a timebased method. The reaction rates were calculated by fitting the fluorescent data to a single exponential, three parameter decay curve using SigmaPlot2001 software: $F_t = F_\infty + \Delta F_{max} \times exp(-k_{obs} \times t)$, where $F_0$ is the initial fluorescence at time = 0, $F_t$ is the fluorescence at time t, $\Delta F_{max}$ is the maximum fluorescence change ($F_0 - F_t$), and $k_{obs}$ is the observed reaction rate constant. The standard deviations were calculated from 3-4 stopped-flow injections.

### IV.4.5. Toe-printing assay

Pre-translocation complexes (1 μM) were formed in 90μl of buffer 3 with ribosomes, mRNA (phage T4 gene *32*), uncharged $tRNA^{fMet}$ in the P site and uncharged $tRNA^{Phe}$ in the A site, as previously described (chapter II). EF-G (wildtype or mutants) and GTP were added to a final concentration of 1.0μM or 0.1μM, and 500μM respectively in buffer 3, followed by 10μl sample extractions at the indicated time points, elongation of the attached primer, denaturation and separation on a 6% polyacrylamide-7M urea gel (see chapter II for further details).

### IV.4.6. Fluorescent translocation assay

The RNA oligonucleotide (62.5μM) was incubated with 50mM pyrene butiryl hydroxysuccinimid for 4h at 60°C in a buffer containing 100mM $Na_2HPO_4$ pH 8.0, 0.1mM EDTA, and 50% DMF, followed by ethanol precipitation (overnight, -20°C). The pelleted product was resuspended in TE buffer pH 8.0, denatured in a double volume of loading buffer (7M urea, 0.025% bromphenol blue, and 0.025% xylene cyanol), and separated on a 10% polyacrylamide-7M urea gel. The pyrene-labeled RNA was extracted

overnight from the gel using buffer TE pH 8.0, and 0.1% SDS, followed by precipitation with 0.3M sodium acetate pH 5.2 and three volumes of ethanol. The final pellet was resuspended in $H_2O$, and the concentration was measured by absorbance.

For the fluorescent translocation assay, the same instrument and the same setup was used as in the case of single round mant-GTP hydrolysis assay. The pre-translocation complexes were formed in buffer 3 as described (Studer et al., 2003), with slight modifications of the final component concentrations (0.5μM 70S, 0.4μM pyrene-RNA, 0.6μM uncharged $tRNA^{fMet}$ in the P site, and 0.6μM uncharged $tRNA^{Phe}$ in the A site). The pre-translocation complexes were mixed with an equal volume of 2.5μM EF-G, 2mM GTP in buffer 3 and the fluorescence of pyrene was excited at 332±4 nm, and detected at 377±8 nm. Fluorescence decrease was fitted to a double exponential decay using SigmaPlot2001 and the equation: $F_t = F_\infty + \Delta F_1 \times exp(-k_1 \times t) + \Delta F_2 \times exp(-k_2 \times t)$. Standard deviations were calculated from 3-4 stopped-flow injections.

### IV.4.7. Mant-GDPNP binding

The fluorescence of 2.5μM mant-GDPNP in buffer 1 (200μl) was excited at 362nm and monitored at 438nm during addition (manual mixing) of 1μM EF-G (wildtype or mutants), followed by 1.4μM vacant 70S (control or stripped 70S).

## IV.5. CONCLUSIONS

The interaction of the helix $A_{G'}$ and the r-protein L7/L12 appears to be accomplished by salt bridges and probably a hydrophobic surface, in a manner similar to the one described for helix $D_G$ of EF-Tu (Kothe et al., 2004). The salt bridges are likely formed using residues E224 and E228 at the C terminus of helix $A_{G'}$.

Disrupting this interaction surface has drastic consequences on the GTP hydrolysis rates, likely due to the slowing of a conformational change that is promoted by the interaction with L7/L12. We have also detected smaller effects on translocation, which may be indirect, due to the slower rates of GTP hydrolysis in the defective mutants.

## IV.6. FUTURE DIRECTIONS

A very important question to answer in order to understand better the mechanism of the GTP hydrolysis activation on the ribosome is the connection between the G' subdomain and the conformational changes in the G domain. Two loops of the G' subdomain form interactions with the guanosine binding region of the G domain, potentially influencing the binding of nucleotides. This interaction surface is one of the reasons for the initial hypothesis that the G' subdomain could act an internal GEF (AEvarsson et al., 1994). The problem in testing the function of that these loops is that their primary sequence is not conserved, as is the case with the majority of the G' subdomain. In spite of this, we believe that we found two good candidates to be mutated: E176 and W193. The side chain of E176 stacks on top of residues 147-148 (aa 142-146 provide interactions for guanosine) (Fig. IV.15.). This residue is conserved in bacterial and mitochondrial EF-G and could be mutated to alanine (no charge), lysine (positive side chain) and tryptophan (bulky, hydrophobic side chain). The other residue, W193, is universally conserved as an aromatic residue in both bacterial and mitochondrial EF-G. W193 is part of a hydrophobic pocket between subdomain G' and domain G situated in the proximity of the GTP binding site (Fig. IV.15.), and could be mutated to alanine, lysine and glutamic acid. The functional assays of these new mutants could provide important clues regarding the role of this interaction. It is possible that the main role of W193 is a structural one, while its mutation to a charged residue may disrupt the local structure. Because of this, the most important mutant to be tested will be W193A, which although cannot accomplish all the interactions of the tryptopahn residue, should not have a major disrupting effect on the hydrophobic pocket.

L7/L12 is involved in the rapid association of the ternary complex with the ribosomal complex (Diaconu et al., 2005). A similar association role of L7/L12 has also been hypothesized for EF-G although the data is not as conclusive as in the case of EF-Tu (Diaconu et al., 2005; Savelsbergh et al., 2005). One of the problems encountered by researchers is the lack of a kinetic EF-G binding assay, the majority of the information regarding EF-G binding to the ribosomal complex being obtained indirectly from functional assays. The easiest way to accomplish that would be to use a fluorescent probe attached to EF-G in such a way not to affect its activity. The first step for this approach is

the construction of a single cysteine mutant, so that there is a single target for the fluorescent probe, and all the future functional mutants would have to be constructed in this new mutant.

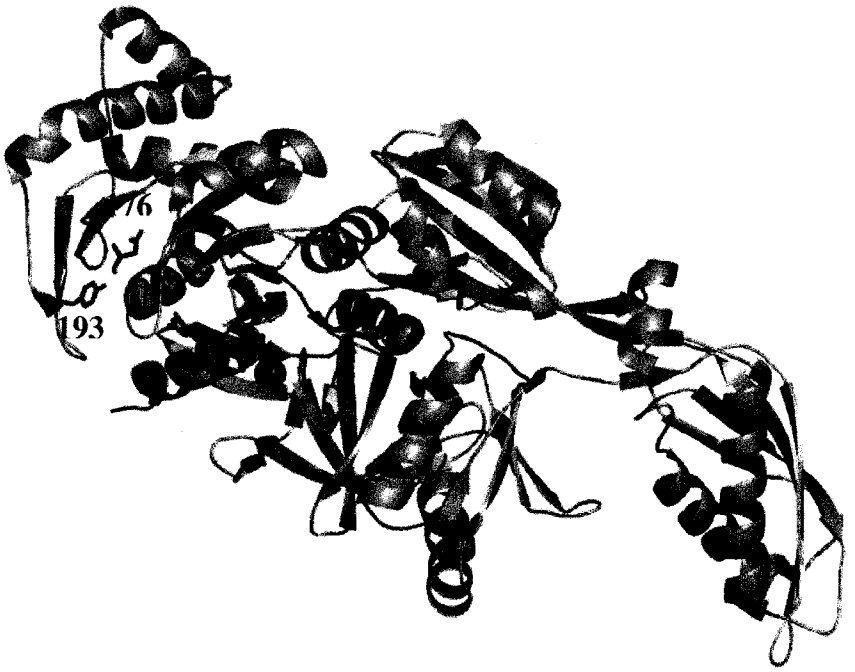


**Fig. IV.15. – Position of the proposed functional mutants in the G' subdomain.** The cartoon was created using PyMOL (http://pymol.sourceforge.net) and it is based on the structure of EF-G from *T. thermophilus* - pdb 1FNM (Laurberg et al., 2000). The side chains correspond to the sequence of *T. Thermophilus*, while the numbers are from *E. coli*. The purple sphere represents the $Mg^{2+}$ ion, while the GDP is in blue sticks.

Another interesting hypothesis is that the conformation of this region is really important for the proper geometry of the binding. Studying the sequence alignments, we found that *Chlamydia spp.* has a three amino acids insertion between helixes A and B of the G' subdomain in EF-G, as compared to the rest of the bacteria. Interestingly, this is mirrored by a one amino acid insertion in helix 4 of the CTD of L7/L12, which could have the role to re-align the interaction surfaces. It would be interesting to introduce this mutation in *E. coli* EF-G and functionally test the mutant in order to identify the consequences of this small insertion.

## IV.7. REFERENCES

AEvarsson, A., Brazhnikov, E., Garber, M., Zheltonosova, J., Chirgadze, Y., al-Karadaghi, S., Svensson, L. A., and Liljas, A. (1994). Three-dimensional structure of the ribosomal translocase: elongation factor G from *Thermus thermophilus*. EMBO J *13*, 3669-3677.

Allen, G. S., Zavialov, A., Gursky, R., Ehrenberg, M., and Frank, J. (2005). The cryo-EM structure of a translation initiation complex from *Escherichia coli*. Cell *121*, 703-712.

Ban, N., Nissen, P., Hansen, J., Moore, P. B., and Steitz, T. A. (2000). The complete atomic structure of the large ribosomal subunit at 2.4Å resolution. Science *289*, 905-920.
Buckingham, R. H., Grentzmann, G., and Kisselev, L. (1997). Polypeptide chain release factors. Mol Microbiol *24*, 449-456.

Connell, S. R., Takemoto, C., Wilson, D. N., Wang, H., Murayama, K., Terada, T., Shirouzu, M., Rost, M., Schuler, M., Giesebrecht, J., *et al.* (2007). Structural basis for interaction of the ribosome with the switch regions of GTP-bound elongation factors. Mol Cell *25*, 751-764.

Czworkowski, J., Wang, J., Steitz, T. A., and Moore, P. B. (1994). The crystal structure of elongation factor G complexed with GDP, at 2.7Å resolution. EMBO J *13*, 3661-3668.

Diaconu, M., Kothe, U., Schlunzen, F., Fischer, N., Harms, J. M., Tonevitsky, A. G., Stark, H., Rodnina, M. V., and Wahl, M. C. (2005). Structural basis for the function of the ribosomal L7/12 stalk in factor binding and GTPase activation. Cell *121*, 991-1004.

Evnin, L. B., and Craik, C. S. (1988). Development of an efficient method for generating and screening active trypsin and trypsin variants. Ann N Y Acad Sci *542*, 61-74.

Feinberg, J. S., and Joseph, S. (2006). Ribose 2'-hydroxyl groups in the 5' strand of the acceptor arm of P-site tRNA are not essential for EF-G catalyzed translocation. Rna *12*, 580-588.

Heimark, R. L., Hersehy, J. W., and Traut, R. R. (1976). Cross-linking of initiation factor IF2 to proteins L7/L12 in 70 S ribosomes of *Escherichia coli*. J Biol Chem *251*, 779-784.

Helgstrand, M., Mandava, C. S., Mulder, F. A., Liljas, A., Sanyal, S., and Akke, M. (2007). The ribosomal stalk binds to translation factors IF2, EF-Tu, EF-G and RF3 via a conserved region of the L12 C-terminal domain. J Mol Biol *365*, 468-479.

Joseph, S., and Noller, H. F. (1998). EF-G-catalyzed translocation of anticodon stem-loop analogs of transfer RNA in the ribosome. Embo J *17*, 3478-3483.

Katunin, V. I., Savelsbergh, A., Rodnina, M. V., and Wintermeyer, W. (2002). Coupling of GTP hydrolysis by elongation factor G to translocation and factor recycling on the ribosome. Biochemistry *41*, 12806-12812.

Kothe, U., Wieden, H. J., Mohr, D., and Rodnina, M. V. (2004). Interaction of helix D of elongation factor Tu with helices 4 and 5 of protein L7/12 on the ribosome. J Mol Biol *336*, 1011-1021.

Laurberg, M., Kristensen, O., Martemyanov, K., Gudkov, A. T., Nagaev, I., Hughes, D., and Liljas, A. (2000). Structure of a mutant EF-G reveals domain III and possibly the fusidic acid binding site. J Mol Biol *303*, 593-603.

Mohr, D., Wintermeyer, W., and Rodnina, M. V. (2002). GTPase activation of elongation factors Tu and G on the ribosome. Biochemistry *41*, 12520-12528.

Neal, S. E., Eccleston, J. F., and Webb, M. R. (1990). Hydrolysis of GTP by p21NRAS, the NRAS protooncogene product, is accompanied by a conformational change in the wild-type protein: use of a single fluorescent probe at the catalytic site. Proc Natl Acad Sci U S A *87*, 3562-3565.

Nechifor, R., Murataliev, M., and Wilson, K. S. (2007). Functional interactions between the G' subdomain of bacterial translation factor EF-G and ribosomal protein L7/L12. J Biol Chem.

Rohrback, M. S., and Bodley, J. W. (1976). Steady state kinetic analysis of the mechanism of guanosine triphosphate hydrolysis catalyzed by *Escherichia coli* elongation factor G and the ribosome. Biochemistry *15*, 4565-4569.

Savelsbergh, A., Katunin, V. I., Mohr, D., Peske, F., Rodnina, M. V., and Wintermeyer, W. (2003). An elongation factor G-induced ribosome rearrangement precedes tRNA-mRNA translocation. Mol Cell *11*, 1517-1523.

Savelsbergh, A., Matassova, N. B., Rodnina, M. V., and Wintermeyer, W. (2000a). Role of domains 4 and 5 in elongation factor G functions on the ribosome. J Mol Biol *300*, 951-961.

Savelsbergh, A., Mohr, D., Kothe, U., Wintermeyer, W., and Rodnina, M. V. (2005). Control of phosphate release from elongation factor G by ribosomal protein L7/12. EMBO J *24*, 4316-4323.

Savelsbergh, A., Mohr, D., Wilden, B., Wintermeyer, W., and Rodnina, M. V. (2000b). Stimulation of the GTPase activity of translation elongation factor G by ribosomal protein L7/12. J Biol Chem *275*, 890-894.

Schuwirth, B. S., Borovinskaya, M. A., Hau, C. W., Zhang, W., Vila-Sanjurjo, A., Holton, J. M., and Cate, J. H. (2005). Structures of the bacterial ribosome at 3.5Å resolution. Science *310*, 827-834.

Selmer, M., Dunham, C. M., Murphy, F. V. t., Weixlbaumer, A., Petry, S., Kelley, A. C., Weir, J. R., and Ramakrishnan, V. (2006). Structure of the 70S ribosome complexed with mRNA and tRNA. Science *313*, 1935-1942.

Studer, S. M., Feinberg, J. S., and Joseph, S. (2003). Rapid kinetic analysis of EF-G-dependent mRNA translocation in the ribosome. J Mol Biol *327*, 369-381.

Traut, R. R., Dey, D., Bochkariov, D. E., Oleinikov, A. V., Jokhadze, G. G., Hamman, B., and Jameson, D. (1995). Location and domain structure of *Escherichia coli* ribosomal protein L7/L12: site specific cysteine crosslinking and attachment of fluorescent probes. Biochem Cell Biol *73*, 949-958.

Wittinghofer, A. (1997). Signaling mechanistics: aluminum fluoride for molecule of the year. Curr Biol *7*, R682-685.

Yusupov, M. M., Yusupova, G. Z., Baucom, A., Lieberman, K., Earnest, T. N., Cate, J. H., and Noller, H. F. (2001). Crystal structure of the ribosome at 5.5Å resolution. Science *292*, 883-896.

# V. FINAL CONCLUSIONS AND DISCUSSION

## V.1. Translocation model

The individual projects presented in the previous chapters have all contributed to broaden our knowledge of the interactions between EF-G and elements of the bacterial ribosome, especially the r-protein L7/L12. Summarizing our crosslinking results, EF-G is in close proximity and likely interacting with at least four r-proteins (S12, L6, L7/L12, and L14), each of them being close to particular domains of EF-G. While the r-protein S12 was detected in previous cryo-EM maps to be next to domain III of EF-G (Valle et al., 2003), the proximity between helix A of domain V and the r-protein L6 is novel and interesting, hinting towards another r-protein which could contribute to the conformational changes undergone by EF-G and the ribosomal complex during translocation.

L7/L12 has the most clearly defined functional role, among all the r-proteins identified in our crosslinking study and our following experiments were concentrated on this particular partnership. The interaction surface between the EF-G and L7/L12 seems to be represented by the C-terminal portion of helix A of the G' subdomain (as gathered from the combination of crosslinking and mutagenesis studies), but helix B and the N-terminal of helix C of the G' subdomain are also close to L7/L12. The interaction between EF-G and L7/L12 appears to activate a step after the hydrolysis of the phosphoanhydride bond in GTP, which could be represented by the Pi release or a subsequent conformational change, and seems to affect the translocation kinetics, as well. Most importantly, our results reveal the role of the G' subdomain as the interaction site with the r-protein L7/L12 and the likely partner to transmit the conformational changes due to ribosome binding towards domain G. Hence, we shed some light on the previously unknown role of this insertion into the G domain of EF-G. This discovery does not exclude the possibility that the G' subdomain has additional roles, through its interactions with the G domain. Moreover, it is possible that this insertion could act as a recognition element for the ribosomal complex to differentiate between the elongation factors (EF-Tu and EF-G).

Since the first high resolution crystal structures of the ribosomal subunits were revealed in 2000 (Ban et al., 2000; Wimberly et al., 2000), multiple ribosomal structures were published, containing either ribosomal subunits in complex with small compounds,

as well as both ribosomal subunits with or without tRNAs and mRNA. In the future it seems likely that high resolution structures of ribosomes in complex with different translation factors will be resolved, which will hopefully supply a wealth of information regarding details of the interactions between these factors and the ribosomal elements. Although the structural data will not directly solve the mechanisms of action, it will likely provide important clues and interesting hypotheses, which could be tested using additional functional studies.

The mechanism of translocation has been elusive for some time now, many studies trying to address various elements involved (see Chapter I for details). In late years, the pieces of the puzzle started to connect, broadening our understanding of the EF-G functions. Our own studies have provided insights into some of the structural and functional aspects, revealing the role of the G' subdomain as the interaction partner of the r-protein L7/L12.

So, after all these studies, how does translocation really work? The answer is not clear yet, but we have an emerging picture. EF-Tu and EF-G are recruited to the proper ribosomal complex, being specifically recognized by the ribosome at the proper step during elongation. Although EF-G and the ternary complex seem to interact with the ribosomal complex in a very similar way, small differences (distance and/or angle) between the positions of ribosomal elements could favor the binding of one factor over the other. These factors seem to provide a different binding partner for the r-protein L7/L12: helix D of the G domain in the case of EF-Tu (Kothe et al., 2004) and helix A of the G' subdomain for EF-G. It is difficult at this moment to predict exactly the position of these helixes upon binding to the ribosomal complex, but it is possible that their orientation is slightly different, so that it allows their differential recognition by L7/L12. Due to its unusual mobility and extensibility, this r-protein could help recruit the factors to the ribosomal complex, theory which was confirmed in the case of the ternary complex and believed also to hold true for EF-G (Diaconu et al., 2005). The simple binding of EF-G•GTP to the ribosomal complex determines conformational changes, which result in the translocation of the tRNAs in regard to the 50S subunit (Valle et al., 2003). Upon binding to the ribosome, GTP is also hydrolyzed quickly by EF-G, followed by Pi release and a series of conformational changes, processes in which L7/L2 appears to play a key role

(Savelsbergh et al., 2005). After this step, the story becomes less clear. It is believed that the conformational changes in EF-G induce also conformational changes in the ribosomal complex, which result in translocation of the tRNAs and the mRNA in regard to the 30S subunit, followed by the dissociation of EF-G•GDP from the ribosomal complex. The interaction between domain III of EF-G and the r-protein S12 appears to be playing an important role in translocation, potentially triggering conformational changes in the 30S subunit which allow the release of tRNAs from the A and P sites and their binding to the next tRNA binding sites. These conformational changes could be transmitted to domain III of EF-G from switches 1 and 2 of the G domain and be the consequence of GTP hydrolysis. On the other hand, the role of the r-protein L6 and its interaction with domain V of EF-G is unclear. It was proven that a certain distance between domains I and V of EF-G is essential for EF-G dissociation from the ribosomal complex (Peske et al., 2000), so the interaction with L6 may stabilize a certain EF-G conformation. Further structural and functional studies are needed to address the remaining questions and decipher the remaining details in the intricate mechanism of translocation.

### V.2. *In vitro* versus *in vivo* functional studies

The recent use of fluorescent techniques and improved ways of assembling ribosomal complexes have led to measuring reaction rates *in vitro* which are relatively close to the presumed *in vivo* rates (Rodnina et al., 1997). There are still some questions regarding the relevance of the *in vitro* experiments as compared to the *in vivo* reality, especially for the quantitative type of experiments. First of all, the concentrations used *in vitro* are very dilute as compared to the *in vivo* situation, and although we could extrapolate the numbers to the presumed *in vivo* concentrations, it is not the same as accurately measuring them.

Secondly, another question is if all the components of the bacterial translation system have really been identified. Some researchers would argue that the translation system containing the canonical factors (IF1, IF2, IF3, EF-Tu, EF-Ts, EF-G, RF1, RF2, RF3, and RRF) is not complete. Additional translation factors (EF-P and W) have also been identified, but they are not generally accepted in the field. **EF-P** is believed to be another elongation factor, with a role in increasing the rate of peptide bond formation (for

a detailed review see (Ganoza et al., 2002)). This factor is supposed to increase the affinity of the aminoacylated tRNA for the A site, potentially by facilitating the accommodation of the amino acid in the 50S subunit binding site. This factor may not be needed for all amino acids, some of them (e.g. phenylalanine) having a high affinity for the binding site to the 50S subunit and not needing further help. This observation could also explain why the concentration of this factor is only 10-20% of that of the ribosomes *in vivo*. Interestingly, the gene coding for this factor (*efp*) is conserved in all bacteria, even the smallest bacterial genome (*Mycoplasma genitalium*) still containing a copy of this gene. Additional studies revealed that this gene is essential for bacterial cells viability, the absence of EF-P stopping protein synthesis (Aoki et al., 1997).

The structure of EF-P was recently published and it revealed a three domain protein, which resembles the three dimensional L shaped structure of a tRNA (Hanawa-Suetsugu et al., 2004). This type of structure might entice hypothesis in which EF-P could occupy one of the tRNA binding sites between the two ribosomal subunits. At the moment, the binding site and the action mechanism of this factor are unknown.

Interestingly, both archae and eukaryotes have homologues of EF-P, called aIF5A and eIF5A. eIF5A was initially believed to be an initiation factor, because it was observed to help the formation of the first peptide bond, but did not affect the following peptide bonds. Although real, the effect on protein synthesis observed *in vivo* is very small, as compared to other initiation factors. Subsequent studies have revealed that eIF5A seems to be associated with elongating ribosome complexes, raising the question if the assignment of this protein as an initiation factor was potentially premature and it may belong actually to elongation factors. Consistent with earlier studies, the effects on protein synthesis remain small (approximately two fold effects). To complicate the story further, additional studies have reported significant roles of this protein in several other cellular processes: mRNA binding and degradation, HIV infection (Rev-1 nucleocytoplasmatic transport), and cell cycle progression. The element essential for these functions is a unique posttranslational modification of this protein: hypusination of a lysine residue. For a more detailed review on eIF5A and its functions see (Zanelli and Valentini, 2007). The crystal structure of aIF5A was published, revealing a two domain structure, which are basically similar to domains I and II of EF-P, but lacking domain III

(Kim et al., 1998). Although clearly important factors, it is unknown at this time if EF-P and eIF5A truly share a function or if their functions are different.

Another presumed elongation factor, the protein named **W**, is believed to also act on protein synthesis by facilitating binding of certain aminoacylated tRNAs and stimulating the dissociation of the deacylated tRNA from the elongating ribosomal complex. This protein is reported to exhibit its effects on formation of oligopeptides and has no effect on synthesis of dipeptides. It also seems to work cooperatively with both EF-G and EF-P. (Ganoza et al., 1995)

Thirdly, there have been some hypotheses regarding a higher organization of translation system *in vivo*. In eukaryotes, it is known that the majority of the cystosolic ribosomes are associated with the cytoplasmic membrane of the endoplasmic reticulum through their 60S subunit, injecting the nascent protein directly inside the endoplasmic reticulum for later secretion. There are also ribosomes spread in the cytoplasm, which translate water soluble proteins. In bacteria, the ribosomes can be associated with the cytoplasmatic face of the cellular membrane in order to synthesize the proteins belonging to the structure of the membrane. These proteins are folded in the exterior space (Gram positive bacteria) or in the periplasmic space (Gram-negative bacteria). (Spirin, 1999)

Even early ribosomal studies have noted that the ribosomes can associate in larger complexes called polysomes. It was later understood that the polysomes are multiple ribosomes linked by one mRNA and are due to their subsequent initiation of protein synthesis on the same mRNA. Interestingly, electron microscopy studies have revealed that the polysomes can have different forms: oval/circular for the ribosomes bound to membranes and straight or zig-zag lines for the ribosomes in the cytoplasm. The distance between ribosomes in these polysome complexes is dependent on the intensity of protein synthesis in that cell, at that particular time. (Spirin, 1999)

Crystals of full ribosomal complexes have shown an organization of ribosomes in tetramers (Yusupova et al., 2001), in such a way that one mRNA can be simultaneously bound to each ribosome of the tetramer and the A and E sites of neighborhood ribosomes are next to one another. This observation has raised the question if this conformation is also present *in vivo*. The advantage of such an organization would be that the ribosomes could be passing tRNAs and translation factors from one to the next, increasing the speed

and efficiency of protein synthesis. The only problem with this hypothesis is that the tRNA leaving the E site is deacylated and it would have to be charged in order to be able to participate in peptide synthesis. This problem would be resolved by the presence of the synthesases in the proximity of these complexes. (Yusupova et al., 2001)

The idea of this type of organization in which the ribosomes, mRNA, tRNAs, elongation factors and tRNA synthesases are associated in a "super-complex" is very intriguing. For this system to work, all the individual pieces have to be held in place and maybe organized by a matrix, which was hypothesized by some studies to be represented by cytoskeleton components. Bacteria also contain elements of the cytoskeleton, which have certain similarities to the eukaryotic counterparts: FtsZ is the bacterial tubulin, MreB belongs to the actin family, while other proteins are similar to intermediate filaments. These proteins play important roles in adoption and maintenance of the specific cell shape, cell division, chromosome and plasmid segregation. The above mentioned proteins and their functions are described in detail in (Graumann, 2007). In support of this hypothesis, EF1α was detected to be localized together with actin and tubulin in certain cytoplasmatic fractions (Wu et al., 1998). The major problem associated with this type of studies is the high concentration of both EF1α and cytoskeletal elements inside the cell, which could easily lead to a false identification of an interaction between these proteins. Although very interesting, this hypothesis lacks solid experimental support at this point. If proven to be correct, this further organization of the translation system could open an entirely new chapter in the study of protein synthesis.

### V.3. The usefulness of studying translation systems

Slowly, but surely, it seems that most of the questions regarding the bacterial translation systems are being answered by different experimental approaches, some structural, others functional. So what is the purpose of this immense amount of work that goes into deciphering all the details of the protein synthesis in bacteria? Apart from the intrinsic beauty in understanding biological mechanisms for their own sake, we also hope to understand the mechanism of action of antibiotics involved in inhibition of protein synthesis, as well as the methods by which bacteria develop resistance against these

drugs. It is hoped that understanding all the structural and functional details of the translation system in bacteria would lead to intelligent drug design of new antibiotics. Also useful for this type of studies would be the detailing of similarities and differences between the eukaryotic and the bacterial protein synthesis systems, in the hope that the newly designed drugs would inhibit specifically translation in bacteria, but have little or no effect on their eukaryotic counterparts.

Small molecules inhibiting protein synthesis in eukaryotes have been tested for additional therapeutic uses. Different studies have looked at using antibiotics for the treatment of:

- genetic diseases (e.g. cystic fibrosis, Duchenne muscular dystrophy), in order to promote readthrough of nonsense mutations and increase the quantity of the necessary protein;
- viral infections (e.g. HIV), inhibiting the frameshift required for synthesis of important viral proteins;
- cancer, by blocking a key step in protein synthesis of cancerous cells, which is particular to the tumors, and not to the healthy cells. (Pelletier and Peltz, 2007)

Due to the multiple therapeutic possibilities resulting from the studies on the translation system in bacteria and eukaryotes, we can anticipate that all the detailed structural and functional information gathered over more than 50 years of research will find quickly its use in various drug designs.

## V.4. REFERENCES

Aoki, H., Dekany, K., Adams, S. L., and Ganoza, M. C. (1997). The gene encoding the elongation factor P protein is essential for viability and is required for protein synthesis. J Biol Chem *272*, 32254-32259.

Ban, N., Nissen, P., Hansen, J., Moore, P. B., and Steitz, T. A. (2000). The complete atomic structure of the large ribosomal subunit at 2.4Å resolution. Science *289*, 905-920.

Diaconu, M., Kothe, U., Schlunzen, F., Fischer, N., Harms, J. M., Tonevitsky, A. G., Stark, H., Rodnina, M. V., and Wahl, M. C. (2005). Structural basis for the function of the ribosomal L7/12 stalk in factor binding and GTPase activation. Cell *121*, 991-1004.

Ganoza, M. C., Cunningham, C., and Green, R. M. (1995). A new factor from *Escherichia coli* affects translocation of mRNA. J Biol Chem *270*, 26377-26381.

Ganoza, M. C., Kiel, M. C., and Aoki, H. (2002). Evolutionary conservation of reactions in translation. Microbiol Mol Biol Rev *66*, 460-485, table of contents.

Graumann, P. L. (2007). Cytoskeletal elements in bacteria. Annu Rev Microbiol *61*, 589-618.

Hanawa-Suetsugu, K., Sekine, S., Sakai, H., Hori-Takemoto, C., Terada, T., Unzai, S., Tame, J. R., Kuramitsu, S., Shirouzu, M., and Yokoyama, S. (2004). Crystal structure of elongation factor P from *Thermus thermophilus* HB8. Proc Natl Acad Sci U S A *101*, 9595-9600.

Kim, K. K., Hung, L. W., Yokota, H., Kim, R., and Kim, S. H. (1998). Crystal structures of eukaryotic translation initiation factor 5A from *Methanococcus jannaschii* at 1.8Å resolution. Proc Natl Acad Sci U S A *95*, 10419-10424.

Kothe, U., Wieden, H. J., Mohr, D., and Rodnina, M. V. (2004). Interaction of helix D of elongation factor Tu with helices 4 and 5 of protein L7/12 on the ribosome. J Mol Biol *336*, 1011-1021.

Pelletier, J., and Peltz, S. W. (2007). Therapeutic Opportunities in Translation, In Translational Control in Biology and Medicine, M. B. Mathews, N. Sonenberg, and J. W. B. Hershey, eds. (New York: John Inglis), pp. 934.

Peske, F., Matassova, N. B., Savelsbergh, A., Rodnina, M. V., and Wintermeyer, W. (2000). Conformationally restricted elongation factor G retains GTPase activity but is inactive in translocation on the ribosome. Mol Cell *6*, 501-505.

Rodnina, M. V., Savelsbergh, A., Katunin, V. I., and Wintermeyer, W. (1997). Hydrolysis of GTP by elongation factor G drives tRNA movement on the ribosome. Nature *385*, 37-41.

Savelsbergh, A., Mohr, D., Kothe, U., Wintermeyer, W., and Rodnina, M. V. (2005). Control of phosphate release from elongation factor G by ribosomal protein L7/12. EMBO J *24*, 4316-4323.

Spirin, A. (1999). Ribosomes (New York: Kluwer Academic/Plenum).

Valle, M., Zavialov, A., Sengupta, J., Rawat, U., Ehrenberg, M., and Frank, J. (2003). Locking and unlocking of ribosomal motions. Cell *114*, 123-134.

Wimberly, B. T., Brodersen, D. E., Clemons, W. M., Jr., Morgan-Warren, R. J., Carter, A. P., Vonrhein, C., Hartsch, T., and Ramakrishnan, V. (2000). Structure of the 30S ribosomal subunit. Nature *407*, 327-339.

Wu, Y., Muench, D. G., Kim, Y. T., Hwang, Y. S., and Okita, T. W. (1998). Identification of polypeptides associated with an enriched cytoskeleton-protein body fraction from developing rice endosperm. Plant Cell Physiol *39*, 1251-1257.

Yusupova, G. Z., Yusupov, M. M., Cate, J. H., and Noller, H. F. (2001). The path of messenger RNA through the ribosome. Cell *106*, 233-241.

Zanelli, C. F., and Valentini, S. R. (2007). Is there a role for eIF5A in translation? Amino Acids *33*, 351-358.